AD-A151 449 ATMOSPHERIC AND PRESSURIZED LOW SPEED WIND TUNNEL PERFORMANCE AND COST COMPARISONS(U) AERONAUTICAL RESEARCH LABS MELBOURNE (AUSTRALIA) N MATHESON MAY 84 1/1

UNCLASSIFIED ARL/AERO-R-160 F/G 14/2 NL

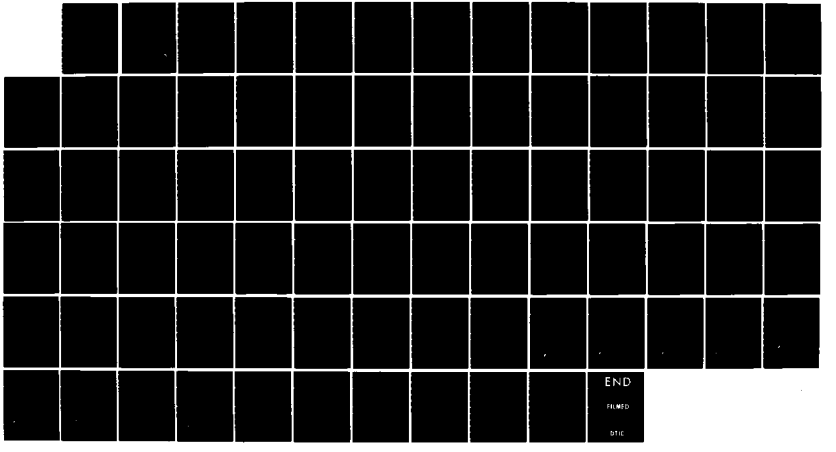

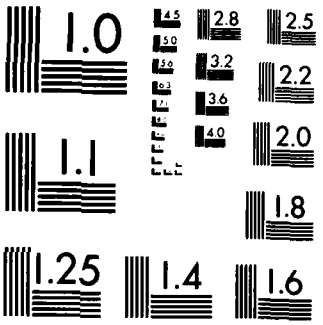

ARL-AERO-R-160

AR-003-027

AUSTRALIA

# DEPARTMENT OF DEFENCE

## DEFENCE SCIENCE AND TECHNOLOGY ORGANISATION

## AERONAUTICAL RESEARCH LABORATORIES

**MELBOURNE, VICTORIA**

AERODYNAMICS REPORT 160

# ATMOSPHERIC AND PRESSURIZED LOW SPEED WIND TUNNEL PERFORMANCE AND COST COMPARISONS

by

N. MATHESON



MAY 1984

COPY No

AR-003-027

DEPARTMENT OF DEFENCE
DEFENCE SCIENCE AND TECHNOLOGY ORGANISATION
AERONAUTICAL RESEARCH LABORATORIES

AERODYNAMICS REPORT 160

# ATMOSPHERIC AND PRESSURIZED LOW SPEED WIND TUNNEL PERFORMANCE AND COST COMPARISONS

by

N. MATHESON

*SUMMARY*

*The performance of a series of low-speed wind tunnels designed to operate at various maximum pressures ranging from 2 to 5 atmospheres is estimated and compared with the performance of a similar atmospheric tunnel on the basis of capital cost and power input. The choice of the design of a new tunnel is usually influenced by cost and power considerations and it is important to provide the most capable design and to maximize performance within given limits of these variables.*

*Pressurization offers a major advantage in allowing $R_N$ and $M_N$ effects to be investigated separately. This can be particularly important for tests of modern aircraft configurations at high lift. For the same capital cost and power consumption pressurization allows the maximum $R_N$ and $M_N$ to be increased substantially, but the working section is much smaller. This may make it difficult to satisfy some test requirements particularly for V/STOL aircraft. Models for a pressurized tunnel are also more complex and may be more costly because they must withstand much higher aerodynamic loads.*

*To illustrate the effects of tunnel pressurization the analysis is applied to a tandem section low-speed tunnel previously suggested as suitable for future Australian test requirements.*[1,2]



POSTAL ADDRESS: Director, Aeronautical Research Laboratories,
Box 4331, P.O., Melbourne, Victoria, 3001, Australia

## CONTENTS

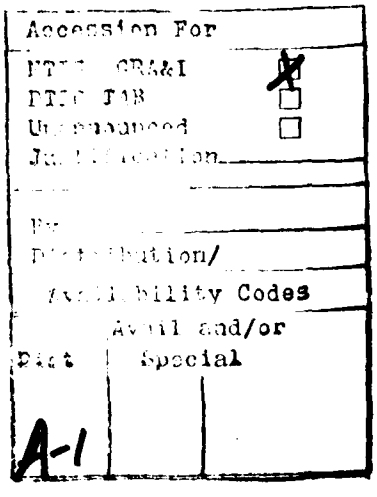


## NOTATION

| | |
|---|---|
| $A$ | cross section area of the working section of the Wind Tunnel |
| $A_1$ | characteristic surface area on which lift coefficient is based |
| $A_d$ | surface area of cooling pipes |
| $A_\sigma$ | cross sectional area based on normal tensile or compressive stress |
| $A_\tau$ | cross sectional area based on shear stress |
| $b$ | cost factor |
| $C$ | capital cost |
| $C_L$ | lift coefficient $= L/(\frac{1}{2}\rho V^2 A_1)$ |
| $C_{dc}$ | capital cost of main drive and cooling system |
| $C_f$ | skin friction coefficient |
| $c$ | wing chord |
| $c_p$ | specific heat at constant pressure |
| $D$ | drag force |
| $d$ | diameter of sting |
| $d_c$ | diameter of cooling pipes |
| $E$ | modulus of elasticity |
| $e$ | cost factor |
| $F_x$ | force along $x$ axis |
| $F_y$ | force along $y$ axis |
| $F_z$ | force along $z$ axis |
| $f$ | $C_{dc}/C =$ main drive and cooling system cost factor |
| $f_c$ | $m_p/m_a =$ cost factor |
| $G$ | modulus of elasticity in shear |
| $g$ | pressurization cost factor |
| $h$ | heat transfer coefficient |
| $I_x$ | moment of inertia about $x$ axis |
| $J_{Mz}$ | polar moment of inertia about $z$ axis |
| $K$ | $(N_p/N_a)\,(\eta_p/\eta_a)\,(1-k_{1p}-k_{2p})/(1-k_{2a})$ |
| $K_f$ | friction loss coefficient |
| $K_1$ | pressure loss coefficient |
| $K_o$ | total loss coefficient for a given component of the tunnel circuit |
| $K_s$ | mass of stored air/(mass of air in tunnel) |

| | |
|---|---|
| $K_v$ | volume of air in tunnel/(tunnel length scale)$^3$ |
| $k$ | thermal conductivity |
| $k_1$ | $N_p/N$ = pressurization power ratio |
| $k_2$ | $N_c/N$ = cooling power ratio |
| $L$ | lift force |
| $l$ | tunnel length scale |
| $l_m$ | model length scale |
| $l_s$ | sting length scale |
| $M_N$ | Mach number |
| $M_x$ | Moment about $x$ axis |
| $M_y$ | Moment about $y$ axis |
| $M_z$ | Moment about $z$ axis |
| $m$ | cost factor |
| $m_f$ | compressor air mass flow rate |
| $N$ | total power input |
| $Nc$ | power required for cooling system |
| $Np$ | power required for pressurization system |
| $Nt$ | power required to move the air around the tunnel circuit |
| $N_u$ | Nusselt number = $hd_c/k$ |
| $n$ | cost factor |
| $P$ | pressure |
| $P_n$ | Prandtl number = $c_p\mu/k$ |
| $P_r$ | pressure ratio across compressor stage |
| $P_s$ | pressure of stored air above tunnel design pressure |
| $Q$ | total heat transfer |
| $q$ | dynamic pressure |
| $R$ | characteristic gas constant |
| $R_d$ | Reynolds number based on diameter of cylinder |
| $R_N$ | Reynolds number |
| $r$ | Reynolds number length scale factor |
| $S$ | number of stages in compressor (integer) |
| $S_c$ | cost of air storage as a proportion of total cost excluding the cost of the drive and cooling systems |
| $T$ | temperature (° absolute) |
| $T_i$ | air temperature at entrance to compressor (° absolute) |
| $V$ | freestream velocity in working section |
| $V_1$ | local freestream velocity |
| $v$ | polytropic index of compression |

| | |
|---|---|
| $x$ | $x$ axis of cartesion coordinate system |
| $y$ | $y$ axis of cartesion coordinate system |
| $Z_{Mz}$ | polar 'section modulus' about $z$ axis (polar moment of inertia/distance to fibre considered) |
| $Z_x$ | section modulus about $x$ axis |
| $Z_y$ | section modulus about $y$ axis |
| $z$ | $z$ axis of cartesion coordinate system |
| $\alpha$ | angle of attack |
| $\delta$ | small increment in variable |
| $\eta$ | tunnel efficiency (or energy ratio) |
| $\eta_s$ | compressor and compressor drive efficiency |
| $\theta_m$ | mean temperature difference |
| $\theta_s$ | sting deflection |
| $\theta_y$ | deflection in the $y$ axis direction |
| $\lambda$ | time to fill air storage containers |
| $\mu$ | dynamic viscosity of air |
| $\rho$ | density of air |
| $\sigma$ | normal tensile or compressive stress |
| $\sigma_{Fz}$ | normal stress due to force along $z$ axis |
| $\sigma_{Mx}$ | normal stress due to moment along $x$ axis |
| $\sigma_{My}$ | normal stress due to moment along $y$ a xis |
| $\tau$ | shear stress |
| $\tau_{Fx}$ | shear stress due to force along $x$ axis |
| $\tau_{Fy}$ | shear stress due to force along $y$ axis |
| $\tau_{Mz}$ | shear stress due to moment about $z$ axis |
| $\phi_z$ | angle of twist about $z$ axis |

*Subscripts*

| | |
|---|---|
| $a$ | atmospheric tunnel |
| $D$ | design condition |
| $E$ | extracted from tunnel circuit |
| $I$ | input to tunnel circuit |
| $m$ | model |
| $p$ | pressurized tunnel |
| $x$ | $x$ axis |
| $y$ | $y$ axis |
| $z$ | $z$ axis |

## 1. INTRODUCTION

One of the main advantages of pressurizing a low-speed wind tunnel is that it enables the effects of scale and compressibility to be investigated separately. Compressibility effects have become more significant in modern high performance aircraft operating at low free-stream Mach numbers (less than $\approx 0{\cdot}4$, refs 3, 4) and it is important to take these effects into account when predicting performance. For example, in tests of rotor tip profiles and high lift wings, very high local velocities (approaching Mach 1) can develop and lead to local shocks and separations which reduce the performance substantially.[3,5] The effect of $M_N$ and $R_N$ on the maximum lift coefficient of a typical high lift wing are shown in Figure 1 (ref. 3). If the tests had been carried out in an atmospheric tunnel only the results along the line marked 'atmospheric' would have been obtained. As well as influencing the lift coefficient compressibility can also significantly affect other performance parameters such as drag, pitching moment and stall. In addition, a pressurized tunnel may also have the advantage of a higher test $R_N$ than an atmospheric tunnel and this can be particularly important in tests of high lift wings and V/STOL aircraft.

However, pressurized low-speed tunnels have disadvantages. Both tunnel and model design are more complicated, and capital, operating and model costs would be higher for a working section of the same size. Pressurized tunnels are also less convenient to operate and are usually less suitable for acoustic testing.[6] Slotted working sections can still be used to alleviate wall effects, but they require a fully enclosed outer shell.

In Europe, two pressurized low-speed tunnels, the RAE 5 m tunnel[3] and the ONERA F1 tunnel,[7] have been built in the last decade. These tunnels can be pressurized up to 3 and 4 atmospheres respectively, and their specifications are briefly summarized in Table 1. In both cases it was considered essential to be able to investigate Reynolds number and Mach number effects separately, particularly for aircraft in the high lift landing configuration, and it was this requirement which led to the tunnels being pressurized. This indicates that, at least as far as some European testing is concerned, the benefits of pressurization outweigh the drawbacks. On the other hand, The Netherlands and the Federal Republic of Germany have recently combined their resources and constructed a new low-speed tunnel which cannot be pressurized, but which has interchangeable working sections;[8] details are given in Table 1.

Any major new low-speed wind tunnel will cost many millions of dollars and there will probably be a limit on the funds available for its construction. It is therefore very important to ensure that the most versatile tunnel with the 'best' performance is provided within a given cost constraint. Economy of operation is also very important. Currently, owing to the high-cost of energy, power costs are a significant part of the overall running expense and it is therefore necessary to minimize the power requirement. For example, since power varies directly with pressure, the square of the linear scale, and the cube of the air speed, less power would be used in obtaining a specified Reynolds number by increasing the pressure in the circuit than by increasing either the linear dimensions or the air speed.

In the following sections the performance of a low-speed wind tunnel designed to operate at various maximum pressures ranging from 2 to 5 atmospheres is estimated and compared with the performance of a similar atmospheric tunnel on the basis of capital cost and power input. Additional factors to allow for some non-similarity in the design can be incorporated in the analysis if necessary. For example, it may be cheaper to build an atmospheric tunnel with rectangular sections throughout the circuit, but circular sections may be structurally preferable for a pressurized tunnel.

**TABLE 1**

**Recently Constructed Large Overseas Wind Tunnels**

| Establishment and Country | Tunnel | Test Section Size | Type of Tunnel | Maximum Air Speed | Maximum Reynolds Number* | Mach No. | Static Pressure | Main Drive Power | Turbulence Level |
|---|---|---|---|---|---|---|---|---|---|
| RAE, Farnborough, England | 5 m | 5·0 m × 4·2 m × 12 m | Closed circuit, closed working section | 110 $ms^{-1}$ at 2¼ atm., 94 $ms^{-1}$ at 3 atm. | $9{\cdot}0 \times 10^6$ | 0·33 | 1 to 3 atm. | 11 MW | 0·10–0·15% |
| ONERA, Le Fauga, France | F1 | 4·5 m × 3·5 m × 11 m (cart length = 8 m) | Closed circuit, closed working section | 120 $ms^{-1}$, 80 $ms^{-1}$ at 4 atm. | $8{\cdot}8 \times 10^6$ | 0·36 | 1 to 4 atm. | 9·5 MW | |
| DNW Noordoostpolder, The Netherlands | DNW | 9·5 m × 9·5 m | Closed circuit, closed working section, slotted wall | 62 $ms^{-1}$ | $4{\cdot}1 \times 10^6$ | 0·18 | atm. | 12·7 MW | |
| | | 8·0 m × 6·0 m | Closed circuit, closed or open section, slotted wall | 110 $ms^{-1}$ | $5{\cdot}3 \times 10^6$ | 0·33 | atm. | | |
| | | 6·0 m × 6·0 m | Closed circuit, closed section, slotted wall | 145 $ms^{-1}$ | $6{\cdot}0 \times 10^6$ | 0·43 | atm. | | |

* Based on length scale of $0{\cdot}1\sqrt{A}$ and an air temperature of 15°C.

## 2. CAPITAL COST AND RELATIVE PERFORMANCE OF SIMILAR PRESSURIZED AND ATMOSPHERIC TUNNELS

### 2.1 Capital Cost

The capital cost of a wind tunnel that can be pressurized above about 2 bar will be significantly greater than an atmospheric tunnel of the same size. This extra cost arises because:

1. the shell must be built from steel[3] or relatively thick reinforced concrete,[7] whereas timber, concrete, or thin steel, will suffice for an atmospheric tunnel;

2. maximum productivity and convenience of operation require a pressure shell to be placed around the entire working area with doors opening to the tunnel circuit and to atmosphere to enable access for both models and personnel by depressurizing only the working section part of the circuit, (in the RAE 5 m tunnel this enables repressurization to 3 atmospheres in eleven minutes compared with forty-five minutes for the whole circuit);

3. compressors, air-storage, air-driers, piping and connectors are required to improve productivity and avoid prohibitively high pumping capacity and pumping power;

4. the shell must be pressure tested.

As an indication of relative costs, Spence and Spee[9] estimated that the total capital cost of a major tunnel designed to be pressurized to three atmospheres would be nearly four times the cost of an atmospheric tunnel of the same size. Capital cost includes the cost of the shell and its components, the working section and pressure isolation chamber, cooling system, compressors, air storage, drive system, balances, stings and control and electrical systems, as well as pressure testing the circuit. However, the cost of the air supply may be partly offset if it can be used as an auxiliary air supply for model tests, such as in jet simulation work. The cost of the site, site preparation and any buildings or offices associated with the tunnels is not included.

If the tunnel is only pressurized to 2 bar or less the cost of the shell will not increase greatly (provided it is steel or concrete) because it can normally withstand pressures up to around 2 bar without a significant increase in thickness, but there will be additional costs for the air supply, piping, compressors and the working section. If significantly lower productivity can be accepted then the elaborate pressure shell around the working section may be deleted. In addition, if a supply of air at the required pressure is already available at the tunnel site then a significant portion of this extra cost may also be eliminated.

In the following analysis the overall capital cost is considered in broad terms (not on the basis of the cost of each individual component) in order to estimate the relative performance of similar atmospheric and pressurized tunnels. Costing data indicate that the capital cost of an atmospheric tunnel of a given design can be expressed as proportional to the cross-sectional area of the working section (or the smaller section of a tandem design) plus the cost of the main drive and cooling systems as:

$$C_a = n_a A_a^{m_a} + C_{dc,a} \tag{1}$$

The cost of the main drive and cooling systems are treated separately because their cost depends on the power input to the tunnel circuit. For a similar pressurized tunnel with a maximum design pressure ranging from 2 to 5 atmospheres the capital cost can be written as:

$$C_p = n_p A_p^{m_p} + C_{dc,p} \tag{2}$$

The cost of the pressurization system is included in the term $n_p A_p^{m_p}$, and the subscripts $p$ and $a$ refer to the pressurized and atmospheric tunnel respectively. Expressing the cost of the main

drive and cooling systems as $C_{dc,a} = f_a C_a$ and $C_{dc,p} = f_p C_p$, then the relative sectional area of the tunnels is obtained from:

$$A_a = g A_p^{f_c} [C_a/C_p]^{1/m_a} [(1-f_a)/(1-f_p)]^{1/m_a} \tag{3}$$

where

$$g = (n_p/n_a)^{1/m_a} \text{ and } f_c = m_p/m_a. \tag{4}$$

### 2.2 Power Input

In addition to capital cost, the other major expense is the cost of the power, and this is considered on a relative power input basis. Owing to the current high cost of energy the cost of the power consumed can be a very large proportion of the overall running costs so it is important to minimize the power input. All other expenses, such as personnel, data gathering and analysis, and maintenance, are not considered, or alternatively they may be considered to be the same for each type of tunnel.

The power required to move the air around the tunnel circuit is taken as $Nt = \frac{1}{2}\rho V^3 A/\eta$, where $\eta$ is ratio of energy of the air in the working section to the input energy and is a measure of the tunnel efficiency. This approach is satisfactory for estimating relative performance of similar atmospheric and pressurized tunnels when their detailed design is not finalized, but the more rigorous approach of summing the predicted losses of individual components should be adopted to determine actual performance when the designs are in their final stages.

Expressing the total power input as the sum of the power to move the air around the tunnel, the power necessary for providing compressed air to pressurize the circuit, and the power for cooling (if a separate power supply is needed) then

$$N_a = Nt_a + Nc_a \tag{5}$$

$$N_p = Nt_p + Nc_p + Np_p \tag{6}$$

Letting

$$k_{1p} = Np_p/N_p,$$

$$k_{2p} = Nc_p/Np_p,$$

$$k_{2a} = Nc_a/N_a,$$

and taking

$$Nt = \tfrac{1}{2}\rho V^3 A/\eta$$

for an atmospheric and a pressurized tunnel respectively, then the relative velocity in the working sections is given by

$$V_p/V_a = K^{1/3}(A_p/A_a)^{-1/3}(\rho_p/\rho_a)^{-1/3} \tag{7}$$

where

$$K = [(N_p/N_a)(\eta_p/\eta_a)(1 - k_{1p} - k_{2p})/(1 - k_{2a})].$$

A pressurized tunnel will probably have a lower utilization rate because of the time taken to change the pressure or in repressurization after access. In addition, more tests of a particular model must be undertaken in a pressurized tunnel to separate scale and compressibility effects.

The extra costs involved must be assessed against the additional information gained, and the advantage of separating Reynolds and Mach number effects can have a significant cost penalty.

### 2.3 Relative Performance

In the following assessment of relative performance air is assumed to be incompressible and the relative density is given by

$$\rho_a/\rho_p = (P_a/P_p)(T_p/T_a). \tag{8}$$

With a Reynolds number based on the length scale

$$l_m = r(A)^{1/2} \tag{9}$$

commonly accepted in assessing tunnel performance[10] then the Reynolds number, Mach number, velocity and dynamic pressure ratios for similar models tested in similar atmospheric and pressurized tunnels are given by:

$$R_{Np}/R_{Na} = K^{1/3}(P_p/P_a)^{2/3}(A_p/A_a)^{1/6}(T_p/T_a)^{-2/3}(\mu_p/\mu_a)^{-1} \tag{10}$$

$$M_{Np}/M_{Na} = V_p/V_a = K^{1/3}(P_p/P_a)^{-1/3}(A_p/A_a)^{-1/3}(T_p/T_a)^{-1/6} \tag{11}$$

$$q_p/q_a = K^{2/3}(P_p/P_a)^{1/3}(A_p/A_a)^{-2/3}(T_p/T_a)^{-1/3} \tag{12}$$

and the model and tunnel size ratios are given by:

$$l_p/l_a = l_{m,p}/l_{m,a} = (A_p/A_a)^{1/2} \tag{13}$$

The relative performance of comparable atmospheric and pressurized tunnels can be estimated from equations 3, 4, 10, 11, 12 and 13 after the relevant constants have been determined. Depending on the actual Mach numbers involved, the assumption that air is incompressible can lead to a slightly optimistic estimate of performance. For example, if $M_N = 0{\cdot}2$ compressibility has a negligible effect on $R_N$, but at $M_N = 0{\cdot}4$ and $M_N = 0{\cdot}6$ compressibility effects reduce the $R_N$ by the order of 5% and 15% respectively.

### 2.4 Cost Factors

The cost factors $f_c$, $g$, $m_a$, $f_a$ and $f_p$ must now be determined. Cost estimates, and Spence and Spee's data[9] indicate that the cost of the materials for the shell varies directly with the volume of material used (length scale cubed). Manufacturing and construction costs, and the cost of the auxiliaries vary at a much lower rate, so that overall the capital cost (excluding main drive and cooling system costs) varies approximately with the cross sectional area of the working section, and thus $m_a \approx 1{\cdot}0$ and $f_c \approx 1{\cdot}0$.

Although accurate cost data for pressurized tunnels is very difficult to obtain the data available indicates that $g$, given by equation (4), depends on the additional equipment necessary for pressurizing the tunnel, as well as the design pressure, and that for design pressures between 2 and 5 atmospheres $g$ can be expressed by:

$$g = b + e[(P_p/P_a)_D - 1] \tag{14}$$

The factor, $b$, takes into account the cost of the extra items of equipment necessary to pressurize the tunnel, such as the compressors, air storage and the pressure isolation chamber; and the factor, $e$, allows for the increase in cost as the tunnel design pressure increases above atmospheric pressure. For relatively large facilities necessary for aircraft development it is estimated that $b \approx 2{\cdot}0$ and $e \approx 0{\cdot}7$. These values are applicable to pressurized tunnels with air storage tanks capable of holding $1{\cdot}5$ times the mass of air in the tunnel circuit ($K_s = 1{\cdot}5$) at a pressure of 10

of $\approx 1 \cdot 6$ m to be tested down to 10 ms$^{-1}$ (ref. 16). However, since the size of the model is primarily determined by the minimum test velocity, larger models could be tested at higher minimum speeds[13,16] For example V/STOL models with rotor diameters or wing spans of $2 \cdot 0$ m could be tested in the $3 \cdot 3$ m $\times$ $3 \cdot 3$ m section down to a speed of about 15 ms$^{-1}$. Although this size and speed limit is usually not adequate for commercial development work, it can be satisfactory in other applications, such as research, provision of data for mathematical models, and some investigations of operational problems.[16]

It may be possible to undertake limited investigations in the very low speed range of $\approx 10$ to 20 ms$^{-1}$ by testing models in the settling chamber.[13] The flow quality will not be as good and additional test time will be required because all of the circuit must be repressurized after access. Unfortunately poor flow quality can cause serious errors in predicted full scale performance, particularly when the performance is being optimized by making relatively small changes to the model configuration.[19,20] Therefore, there is some risk in using the settling chamber as a test section. The size of the settling chamber for the pressurized tunnel, corresponding to the atmospheric tunnel in Figure 20, is $\approx 8 \cdot 3$m $\times$ $8 \cdot 3$ m and the maximum air speed is $\approx 14$ ms$^{-1}$ (at 1 atmosphere). This would allow a $2 \cdot 0$ m model to be tested from $\approx 14$ ms$^{-1}$ down to about 8 ms$^{-1}$ without excessive interference. However, it would not be possible to test larger rotors at such low speeds, and there would also be an intermediate speed range for larger rotors which could not be covered. For example, a $2 \cdot 6$ m model could only be tested above $\approx 20$ ms$^{-1}$ in the $3 \cdot 3$ m $\times$ $3 \cdot 3$ m section and between $\approx 11$ and 14 ms$^{-1}$ in the settling chamber without excessive wall interference, leaving a speed range between 14 ms$^{-1}$ and 20 ms$^{-1}$ which could not be covered. Active control of the flow through the walls by blowing or suction can reduce interference, so it may be possible to cover the low-speed range using a slightly larger model.[21] However, since size limits prevent a $2 \cdot 6$ m model from being tested in the smaller section, then the maximum test speed is the top speed in the $3 \cdot 3$ m $\times$ $3 \cdot 3$ m section which is 95 ms$^{-1}$. This is well below the test speed of 130 ms$^{-1}$ currently considered necessary for helicopters and other V/STOL aircraft.[13] It therefore seems that a pressurized tunnel of the size and type considered could not cope with commercial V/STOL development test requirements, although it would be suitable for many other types of V/STOL work.

For the development of large transport CTOL aircraft, spans of the order of 3 m are again necessary to allow models with sufficient detail to be tested, although slightly smaller models are adequate for smaller utility and general purpose CTOL aircraft. In the pressurized tunnel, spans of the order of only $2 \cdot 3$ m and $1 \cdot 9$ m could be accommodated in the larger and smaller sections respectively without excessive wall effects. A pressurized tunnel of the same capital cost as an atmospheric tunnel would therefore not be large enough to cope with the model size requirements for commercial development of large CTOL aircraft, but as in the V/STOL case, it would be suitable for other CTOL aircraft test requirements.

In the particular case considered here, it seems that a tunnel pressurized to approximately 3 atmosphere and costing the same as the projected atmospheric tunnel[1] would not allow large enough models to be tested for adequate commercial development of V/STOL or large CTOL aircraft, although it may be satisfactory for the development of smaller V/STOL, utility and transport aircraft. However, it would meet the model size and other test requirements for many other investigations, and it would have the advantage of enabling $R_N$ and $M_N$ effects to be investigated separately over at least a part of the test range, as well as allowing significantly higher test Reynolds numbers to be achieved.

### 5.3 Alternative Pressurized Tunnel

Since tunnel pressurization offers some real advantages a different arrangement to the tandem section tunnel might be more suitable. One possible alternative is to have only one working section with slotted walls and a cross section of $4 \cdot 8$ m $\times$ $4 \cdot 0$ m which could be pressurized to around 3 atmospheres. The maximum speed would be about 90 ms$^{-1}$ at 3 atmospheres and 130 ms$^{-1}$ at ambient pressure for the same power consumption as the tandem section

Currently, the $R_N$ sensitivity of new aerodynamic designs, particularly at high lift, appears to be increasing and the expanded $R_N$ test range can be very important. However, the advantages of both a higher test $R_N$ and the ability to separate Reynolds and Mach number effects, must be assessed against the disadvantages of reduced model size and increased design complexity discussed in the following sections.

### 5.2 Tunnel and Model Size

In addition to the requirements for high test Reynolds numbers, the models must be large enough so that their full scale geometry can be faithfully reproduced. This is necessary to enable the effects of small changes in detail to be quantified, and is especially important when testing intricate and complex high lift devices where a small change in geometry can lead to a critical change in the flow. Lack of correlation between wind tunnel and full scale results has often been attributed to poor geometric similarity.[14] Obtaining high Reynolds numbers by testing larger models at lower speeds can also aid in extrapolation by minimizing extraneous Mach number effects.

The model must also be free from unwanted surface distortions and mounted in the tunnel so that model support and wall interference effects are minimized. In some cases where $R_N$ effects are known to be important correct geometrical scaling and low interference have been assessed as being equally important.[3] To satisfy these requirements, it is necessary to test larger models in bigger working sections than normally used in the past. Unfortunately, this leads to large facilities which are very expensive to construct and operate. Large detailed models are also very costly, as well as being difficult and time-consuming to make, and hard to manipulate. In most cases a compromise between cost and technical requirements is necessary.

Templin[6] concluded that to obtain a sufficiently high test Reynolds number, and to allow the complex geometrical detail inherent in V/STOL aircraft to be reproduced with sufficient accuracy, models with a wing span or rotor diameter of about 3 m are necessary for industrial development of aircraft, but that 2 m models are adequate for research. In addition, to keep wall constraint effects within acceptable limits and to avoid flow breakdown or recirculation, a solid wall test section should have linear dimensions of at least twice, and preferably three times the model span or rotor diameter to permit testing down to a lower speed limit of 10 to 15 $ms^{-1}$ (refs 3, 13 and 16). This is about the lowest practicable test speed and is needed to investigate performance in the low-speed flight regime where design is difficult. If a higher minimum test speed can be accepted, and if slotted or porous walls can be used to reduce interference,[3,17,18] then the working section can be made smaller relative to the model. Since large wind tunnels are expensive the choice of a minimum size is important.

On the other hand, for investigations of both V/STOL and CTOL aircraft in the higher-speed lower-specific-lift regime where the downwash angle is much smaller, the main requirement is to obtain a sufficiently high Reynolds number using a model which is large enough to enable the full size geometry to be accurately scaled. However, in this case, the size problem is alleviated significantly because wing spans and rotor diameters of the order of two-thirds the tunnel width can normally be used without excessive interference.

In Section 3.1.3 it was indicated that the dimensions of the working section of a tunnel designed to be pressurized to 3 to 4 atmosphere would be of the order of 0·5 to 0·6 of the dimensions of an atmospheric tunnel. Assuming a value of 0·55 is applicable for a tunnel pressurized to 3 atmospheres then the working sections would be 3·3 m × 3·3 m and 2·6 m × 1·9 m in size compared with 6·0 m × 6·0 m and 4·7 m × 3·4 m for the atmospheric tunnel. The model must also be reduced in size in the same proportions and in many cases it would be too small to meet the requirements discussed previously.

The size of the 6 m × 6 m slotted wall section in the atmospheric tunnel[1] will allow commercial development of helicopters and other V/STOL aircraft, including investigations of operational problems, which require testing at speeds down to about 10 $ms^{-1}$. The corresponding 3·3 m × 3·3 m pressurized slotted section will only allow models with a rotor diameter or wing span

Australia has a closed octagonal working section 2·7 m wide, 2·1 m high and 3·6 m long, with a maximum airspeed of 100 $ms^{-1}$. Based on a mean chord (length scale) of $0{\cdot}1\sqrt{A}$ the maximum test Reynolds number is only $1{\cdot}6\times10^6$. Broadly speaking, this tunnel will not enable sufficiently high Reynolds numbers to be achieved, nor will it allow sufficiently large and detailed models to be tested to meet future requirements.[1] In particular, tests of V/STOL models cannot be made satisfactorily in the subsonic high-lift regime where high downwash effects are present, mainly because the working section is not large enough to accommodate models of the required size.

To overcome current deficiencies and satisfy many of the anticipated test requirements over perhaps the next forty years a major new low-speed wind tunnel will be required. After an extensive study of Australian requirements a design for a new tunnel was put forward for discussion amongst potential users and interested parties in accordance with the ASTEC's recommendation.[2] The layout of the tunnel followed traditional lines to minimize technical risk and cost, although the less common arrangement of closed tandem working sections was specified as shown in Figure 20 (refs 1 and 15). The smaller working section had a width of 4·7 m, a height of 3·4 m and a length of 10·0 m, with a maximum airspeed of 135 $ms^{-1}$; and the larger section had a width of 6 m, a height of 6 m and a length of 13·5 m, with a maximum airspeed of 60 $ms^{-1}$. The drive power was estimated to be 5·6 MW. Both sections would be provided with appropriately ventilated walls (slotted or porous) and operate at atmospheric pressure.

Although the proposal[1] called for an atmospheric tunnel it was considered that further investigation into the effects of tunnel pressurization on performance was needed. In the following section the analysis previously given in Section 2 is applied and a comparison is made between similar pressurized and atmospheric tunnels on the basis that the capital cost and the power input of both tunnels are the same. If required, the performance for other conditions can be estimated using the relevant equations given earlier in this report.

### 5.1 Reynolds and Mach Number Test Envelope

The Reynolds and Mach number test envelope, calculated from the equations in Section 2, for each of the tandem working sections with $(P_p/P_a)_D = 5$, 4, 3 and 2, and cost factors $b = 2{\cdot}0$, $e = 0{\cdot}7$ and $b = 1{\cdot}5$, $e = 0{\cdot}4$ are shown in Figures 21 and 22 respectively. These figures are based on the compressor and air storage conditions given at the beginning of Section 3, and a tunnel air temperature of 40°C. The $R_N - M_N$ operating limit line for the projected atmospheric tunnel is also shown in each figure. The figures show quite a large gain in performance at high design pressure ratios, but decreasing the cost factors from $b = 2{\cdot}0$, $e = 0{\cdot}7$ to $b = 1{\cdot}5$, $e = 0{\cdot}4$ results in only a very small increase in $R_N$.

In the smaller working section, with $b = 2{\cdot}0$ and $e = 0{\cdot}7$, a design pressure ratio of 5 gives a maximum Reynolds number of $7{\cdot}0\times10^6$ which is more than twice the value of $3{\cdot}2\times10^6$ in the $4{\cdot}7\text{ m}\times3{\cdot}4\text{ m}$ atmospheric tunnel, and a design pressure ratio of 3 gives a maximum Reynolds number of $5{\cdot}3\times10^6$ or more than 1½ times its value in the atmospheric tunnel. If $b = 1{\cdot}5$ and $e = 0{\cdot}40$, the maximum $R_N$ is only approximately 4% higher and the $M_N$ about 16% lower than for $b = 2{\cdot}0$ and $e = 0{\cdot}7$. The maximum Reynolds number at a design pressure ratio of between 4 and 5 is in accordance with the range of $(6\text{–}8)\times10^6$ which was found to be technically desirable for predicting the performance of modern 'high lift' aircraft by RAE prior to building their 5 m pressurized tunnel.[3] For example, this $R_N$ range would enable models of the HSA Hawk and the Australian Nomad to be tested near their full scale approach $R_N$, and the European Airbus (A300B) to be tested at about ¼ full scale approach $R_N$.

In the larger working section the maximum Reynolds number for a given design pressure ratio is lower than in the smaller section, and for $b = 2{\cdot}0$ and $e = 0{\cdot}7$ the maximum value of $4{\cdot}6\times10^6$ occurs at a design pressure ratio of 5 and a value of $3{\cdot}5\times10^6$ at a design pressure ratio of 3, as shown in Figure 22.

Figures 21 and 22 both show the very much expanded operating Reynolds and Mach number range that can be achieved from a pressurized tunnel with the same cost as an atmospheric tunnel

require additional distortion of the fuselage. Increased fuselage distortion and sting interference can have a significant effect on the test results and may offset the gains of a higher test Reynolds number in the pressurized tunnel.[10]

### 4.4 Model and Sting Deflection

In the previous sections the model and sting designs were considered on the basis of maximum or design stress. However, the model and sting may also be required to meet certain deflection or rigidity requirements.

Many models must be sufficiently rigid to remain 'undistorted' during testing. In some cases it is necessary to reproduce steady state in-flight deflections because of their effects on aerodynamic performance. In still other cases, for instance in flutter or dynamic stability tests, the models must be made so that their dynamic distortion is similar to the full scale aircraft.

To illustrate the effects of model deflection consider the wing of a simple aircraft mounted on a single sting or strut as shown in Figure 17. The relative twist and deflection at corresponding locations along the span of the wings of similar models tested in a pressurized and an atmosphere tunnel are given by equations (3) and (4) in Appendix III.

If the proportions of the wings, or structural members in the wings, are constant then the relative deflections are given by:

$$(\phi_{z,p}/\phi_{z,a}) = (q_p/q_a)(G_a/G_p) \tag{35}$$

and

$$(\theta_{y,p}/l_{m,p})/(\theta_{y,a}/l_{m,a}) = (q_p/q_a)(E_a/E_p) \tag{36}$$

If $E$ and $G$ are constant then the deflections increase in proportion to the dynamic pressure. Substituting for the dynamic pressure from equation (12) gives the deflections as a function of capital cost, power input and design pressure for given cost factors $b$ and $e$. Figure 18 shows the relative deflection for the cost and power input variations previously discussed when $b = 2{\cdot}0$ and $e = 0{\cdot}7$. For some models the increased deflection in the pressurized tunnel may not be troublesome, but when the models are 'flexible' interpretation of the test results can be very difficult. Ideally, the higher strength materials required for models tested in pressurized tunnels should have a modulus of elasticity which increases in the same proportion as the dynamic pressure. This would allow the relative deflections to remain the same and would avoid the problems of increased deflection that can be experienced in a pressurized tunnel.

Sting deflection is also important because it affects the angle of attack of the model. Using a similar analysis to that used for the wing, the relative change in angle of attack of a symmetrical model mounted on a cylindrical sting at an angle of attack $\alpha$ is given by

$$(\theta_{s,p}/l_{s,p})/(\theta_{s,a}/l_{s,a}) = (q_p/q_a)(l_{m,p}{}^4/l_{m,a}{}^4)(d_a{}^4/d_p{}^4)(E_a/E_p) \tag{37}$$

This equation has the same form as equation (4) in Appendix III and similar comments apply for the deflection of the model mount as apply for the deflection of the wing. However, the increased deflection in a pressurized tunnel is of less consequence if the attitude of the model is measured directly.[14]

## 5. PRESSURIZATION CONSIDERATIONS FOR A NEW AUSTRALIAN LOW-SPEED WIND TUNNEL

In a previous report[1] it was concluded that existing low-speed aerodynamic test facilities are barely sufficient for current requirements, and that they would not be adequate for anticipated future needs, especially for military purposes. The most capable aeronautical tunnel available in

function of relative capital cost, power input, and design pressure ratio for given capital cost factors $b$ and $e$. Figure 18 shows the relative section area and modulus for cost factors $b = 2{\cdot}0$ and $e = 0{\cdot}7$ and the various cost and power input conditions considered earlier, assuming the model is designed to withstand the maximum pressure in the tunnel. If $(P_p/P_a)_D = 5$, $C_p = C_a$ and $N_p = N_a$ the section area and modulus must be increased by a factor of $4{\cdot}5$ compared with a model in the atmospheric tunnel. For a lower design pressure ratio of 3 the section area and modulus need to be increased by a factor of $3{\cdot}0$. In many cases, particularly when the model is highly loaded, it may not be possible to accommodate these increases in size within the required model surface geometrical constraints. However, the relative section modulus and area both decrease as the capital cost is increased or the power input is reduced, as shown in Figure 18, enabling the model design requirements to be met more easily.

On the other hand, if the relative area and modulus are constant then the design stress must be increased in the same proportion as the dynamic pressure as shown in Figure 18. For example, if $C_p = C_a$ and $N_p = N_a$, the design stress must be increased by a factor of $4{\cdot}5$ when $(P_p/P_a)_D = 5$, and $3{\cdot}0$ when $(P_p/P_a)_D = 3$. However, if the cost of the pressurized tunnel can be increased by 50% the dynamic pressure will be reduced and the design stress need only be increased by a factor of $3{\cdot}0$ or $2{\cdot}0$ for design pressure ratios of 5 and 3 respectively. High strength steels may not satisfy some of these stress requirements.

### 4.3 Strength of Model Support

Selection of a support system is a decision which calls for considerable compromise and the choice can be more critical in a pressurized tunnel where the dynamic pressure can be high. In most cases the stress in a sting must be low to avoid large deflections. Multiple stings or pylons can assist but they may introduce additional restrictions such as a reduced model attitude range and greater interference.

The relative size of the mounting sting for similar models tested in a pressurized and an atmospheric tunnel can be estimated from equations similar to equations (4) and (7) in Appendix II. Assuming the sting has a circular section then the relative diameter estimated on a design tensile stress or shear stress basis (where shear stress is critical) is

$$(d_p/l_{m,p})/(d_a/l_{m,a}) = [(\sigma_a/\sigma_p)_D(q_p/q_a)]^{1/3} = [(\tau_a/\tau_p)_D(q_p/q_a)]^{1/3} \qquad (34)$$

If the design stress for the stings is the same then the relative diameter must be increased in proportion to the cube root of the dynamic pressure ratio. Substituting for the dynamic pressure ratio from equation (12) into equation (34) gives the relative diameter as a function of capital cost, power input, and design pressure for given cost factors. Figure 19 shows the relative diameter of stings made from the same material as a function of design pressure for the capital cost and power input conditions given earlier and with cost factors $b = 2{\cdot}0$ and $e = 0{\cdot}7$. Compared with an atmospheric tunnel, the increase in diameter of a sting in a pressurized tunnel can be as high as 65% when $(P_p/P_a)_D = 5$, $C_p = C_a$ and $N_p = N_a$. Quite large additional fuselage distortion and sting interference effects can result from this increased sting size. However, increasing the capital cost (which increases the tunnel size) or reducing the power input, results in a lower dynamic pressure and a relatively smaller sting as shown in Figure 19.

If the relative diameter $(d_p/l_{m,p})/(d_a/l_{m,a})$ is unity then the design stress of the sting in the pressurized tunnel must be increased in the same proportion as the dynamic pressure. For example, if $C_p = C_a$, $N_p = N_a$ and $(P_p/P_a)_D = 5$ then the design stress must be $4{\cdot}5$ times higher than for the sting in the atmospheric tunnel. Again, increasing the capital cost or reducing the power input to the pressurized tunnel lowers the dynamic pressure and reduces the design stress. If a high strength material is needed for the sting in the atmospheric tunnel then material with the required strength may not be available for the sting in the pressurized tunnel and it would have to be made comparatively larger in diameter. This will cause greater interference and may

by the compressor motors, but the storage is slightly larger and more costly, and the size of the tunnel is slightly smaller, as shown in Figure 16. As in the previous case for changes in $K_s$, changing $P_s$ by $\pm 50\%$ has a greater effect on performance as the capital cost is increased or the power input is reduced.

## 4. MODEL DESIGN AND MOUNTING FOR TESTS IN PRESSURIZED TUNNELS

### 4.1 Model Size and General Design

As well as giving the relative working section size, Figures 7 and 8 also show the relative size of geometrically similar models tested in similar tunnels. In a tunnel designed to operate at around 3 to 4 atmospheres with $C_p = C_a$, $N_p = N_a$, and realistic cost factors of $b \approx 2{\cdot}0$ and $e \approx 0{\cdot}7$, or slightly less, the model size ratio, $l_{m,p}/l_{m,a}$, varies from about $0{\cdot}50$ to $0{\cdot}60$. However, increasing the cost by 50% permits the model size ratio to be increased to $\approx 0{\cdot}65$ to $0{\cdot}75$, and a 100% increase in capital cost permits the ratio to be $\approx 0{\cdot}75$ to $0{\cdot}85$. The smaller models for the pressurized tunnel may be cheaper but they will also be more difficult to construct with sufficient accuracy and detail, and tests on certain full size and large scale objects may be precluded. The models may need to be more complex to ensure the maximum amount of testing before tunnel depressurization and any extra cost involved must be offset against any cost savings due to the reduced size. In addition, the high dynamic pressures they must withstand will almost certainly require a large part of each model to be constructed from high strength materials which can be expensive and difficult to machine and fabricate. It is therefore not clear, a priori, whether smaller models will be cheaper.

In modern aircraft aeroelastic effects can be as important as Reynolds number effects[11,12,13] and an increasing amount of testing is now necessary on static and dynamic aeroelastic models, for example for flutter testing. Static aeroelastic models are considerably more expensive than 'rigid' models; and dynamic models—where the mass is scaled as well as the stiffness—will be even more complicated, expensive and time-consuming to design and build. In view of the manufacturing difficulties, and the high cost and long lead times associated with making models, particularly large aeroelastic ones, both model size and construction considerations are important factors to be taken into account when assessing wind tunnel designs.

### 4.2 Strength of Model

The strength of a model may limit the maximum dynamic pressure (and hence the circuit static pressure and power input) at which the tunnel can be operated. For fixed wing aircraft the design is often governed by the stress at the wing root, although other areas, such as the tail-plane must also be considered.

To illustrate the problems of model design consider a simple aircraft mounted on a single sting or strut as shown in Figure 17. The relative stresses, forces and moments at corresponding locations in the wings of geometrically similar models tested in a pressurized and an atmospheric tunnel are given in Appendix II. In most cases the stresses and dimensions of the load carrying members of the wing can be compared using equations (4) and (7) in Appendix II.

If the design stress for each model is the same, for instance when the same material is used, then the equations

$$(A_{r,p}/l_{m,p}{}^2)/(A_{r,a}/l_{m,a}{}^2) = q_p/q_a \tag{32}$$

$$(Z_{x,p}/l_{m,p}{}^3)/(Z_{x,a}/l_{m,a}{}^3) = q_p/q_a \tag{33}$$

derived from equations (4) and (7) in Appendix II, show that the relative section area and modulus for a given structural member of a model tested in the pressurized tunnel must be increased in the same ratio as the dynamic pressure. Substituting the dynamic pressure from equation (12) into equations (32) and (33) enables the relative section area and modulus to be calculated as a

11 are obviously excessive and would not be practicable. If $N_p/N_a$ and $K_s$ are constant increasing the capital cost increases the size of the tunnel (see Figure 8) and the time required for pressurization becomes longer because of the increased mass of air to be compressed. Reducing the total power input for a given capital cost leads to an increase in pressurization time both because the mass of air to be stored is increased, since the tunnel is slightly larger, and because the power available for the compressors is reduced in the same proportion as the reduction in the power input since $k_{1p}$ is constant. The pressurization time also decreases slightly as the tunnel design pressure decreases due to the dominant effect of the lower air density in reducing the stored air mass.

The Reynolds and Mach number ratios for tunnels with a design pressure of $(P_p/P_a)_D$ 4 and $k_{1p} = 0{\cdot}10$ are shown in Figure 12 for the capital cost and power input conditions nominated at the beginning of Section 3.2. These results may be compared with those in Figure 9(*b*) where the pressurization time is constant at 4 hours. For $C_p = C_a$ and $N_p = N_a$ there is only a very small improvement in $R_N$ when $k_{1p} = 0{\cdot}10$ compared with the case when $\lambda = 4$ hours, but there is a significant improvement in $R_N$ as the capital cost, $C_p$, is increased. This is due to both the increased size of the tunnel and the increased circuit power since $k_{1p}$ is constant. However, the extra performance is associated with the disadvantage of a much longer pressurization period as shown in Figure 11.

Reducing the relative mass of air to be stored, $K_s$, for a constant filling time, $\lambda$, reduces the power needed by the compressor motors and improves the tunnel performance if $N_p/N_a$ is constant. In addition, for a given capital cost, the size of the tunnel will be increased slightly owing to the reduced cost of the storage containers. This involves small changes in the values of $b$ and $e$, and the tunnel performance can then be estimated by assuming that at constant pressure the air storage costs are proportional in the storage volume which leads to

$$b_2 = b_1[1 + S_c(K_{s,2}/K_{s,1} - 1)] \tag{28}$$

$$e_2 = e_1[1 + S_c(K_{s,2}/K_{s,1} - 1)] \tag{29}$$

where $S_c$ is the cost of the air storage containers as a proportion of the total cost excluding the cost of the drive and cooling systems. When $K_s = 1{\cdot}5$ and $P_s = 10$ atm. it is estimated that $S_c = 0{\cdot}15$.

The effects on performance of changing $K_s$ from $1{\cdot}5$ to $0{\cdot}75$ and $2{\cdot}25$ for a tunnel with $(P_p/P_a)_D = 4$, $P_s = 10$ atm., and $\lambda = 4$ hr are shown in Figure 13. This relatively large change in $K_s$ leads to less than 2% change in $R_N$ and $M_N$ when $C_p = C_a$ and $N_p = N_a$. However, as the capital cost is increased or the power input is reduced the changes in performance become more significant. If $C_p = 2{\cdot}0\,C_a$ and $N_p = 0{\cdot}5\,N_a$ the power input is not sufficient for the compressor motors when $K_s = 2{\cdot}25$ which is obviously not practicable. The effect of changing $K_s$ on the size of the tunnel is quite small, as shown in Figure 14, because the cost of the storage tanks is only of the order of 15% of the cost of the tunnel.

Increasing the design pressure of the air storage for a given mass reduces the volume of the storage container but it must be thicker to withstand the increased pressure. This also leads to a small change in the values of $b$ and $e$ and the tunnel performance can be estimated using

$$b_2 = b_1[1 + \delta b] \tag{30}$$

$$e_2 = e_1[1 + \delta e] \tag{31}$$

where

$$\delta b = S_c \,|\, [(P_{s,1} + (P_p/P_a)_D)/(P_{s,2} + (P_p/P_a)_D) - 1] \,|^{\,2/3}$$

$$\delta e = S_c \,|\, [(P_{s,1} + (P_p/P_a)_D)/(P_{s,2} + (P_p/P_a)_D) - 1] \,|^{\,2/3}$$

and

$\delta e$ and $\delta b$ are +ve for $P_{s,1} > P_{s,2}$

$\delta e$ and $\delta b$ are −ve for $P_{s,1} < P_{s,2}$

The effect of changing $P_s$ by ± 50% from $P_s = 10$ atmosphere for a tunnel with a design pressure of 4 atmosphere, $K_s = 1{\cdot}5$ and $\lambda = 4$ hr is shown in Figure 15. Decreasing the storage pressure for the same mass improves the performance because of the decreased power needed

If the capital cost is increased by 50% from $C_p = C_a$ to $C_p = 1{\cdot}5\,C_a$ and the power input remains constant at $N_p = N_a$, then the maximum $R_N$ ratio is only increased by about 5% and the maximum $M_N$ ratio is decreased by $\approx$20%, as shown in Figure 9. If the power input is reduced by 50% from $N_p = N_a$ to $N_p = 0{\cdot}5\,N_a$ and $C_p = 1{\cdot}5\,C_a$, then the maximum $R_N$ and $M_N$ ratios are decreased by $\approx$30% and $\approx$32% respectively, and at a design pressure ratio of 5 the maximum $R_N$ is about 60% higher and the maximum $M_N$ $\approx$10% less than in the atmospheric tunnel. At a lower design pressure ratio of 3, the maximum $R_N$ is only $\approx$20% higher and the maximum $M_N \approx 20\%$ less than in the atmospheric tunnel.

For the case when $N_p = 0{\cdot}5\,N_a$, an increase in capital cost of 50% permits the size of the tunnel to be increased significantly as indicated earlier and shown in Figure 8. The speed of the air in the working section will then be reduced both because of the increased section area and because a greater proportion of the available power is absorbed by the compressors in providing the increased mass flow required to pressurize the air storage containers in a given time. However, the increased length scale does not compensate for the loss of airspeed and consequently the maximum $R_N$ is reduced by $\approx$4% irrespective of the design pressure.

As shown in Figure 10, if the capital cost is increased by 50%, for a constant power input ratio, then the dynamic pressure in the pressurized tunnel is reduced significantly both because of the increased section area and because of the increased proportion of power absorbed by the compressors.

### 3.2.3 $C_p = 2{\cdot}0\,C_a$, $N_p = N_a$ and $N_p = 0{\cdot}5\,N_a$

If the capital cost of the pressurized tunnels can be increased by 100% compared with the cost of the atmospheric tunnel, then for a constant power input of between $0{\cdot}5\,N_a$ and $1{\cdot}0\,N_a$ the linear dimensions of the tunnel will be $\approx$55% greater than when $C_p = C_a$, as shown in Figure 8. For a design pressure of 3 to 4 atmospheres the size of the working section will now be $\approx 0{\cdot}75$ to $0{\cdot}85$ times the size of the section for the atmospheric tunnel. As for the case when the capital cost was increased by 50%, a 100% increase in cost does not lead to a significant change in $R_N$ when $N_p = N_a$, but when $N_p = 0{\cdot}5\,N_a$ the Reynolds number is reduced substantially. This reflects the dominant effect of increased power necessary for the compressors to pressurize the air storage in a given time. The decrease in $M_N$ and dynamic pressure follow the same trends as the previous case when the cost was increased by 50% as shown in Figures 9 and 10.

Overall, on the basis of $R_N$ and $M_N$ considerations it seems preferable to keep the power input to the pressurized tunnel as high as possible, although to avoid excessive compressibility effects the actual freestream $M_N$ should not be too high. In addition, excessive reductions in the power input to the pressurized tunnel compared with the atmospheric tunnel can lead to impracticable designs. Furthermore, the large increases in capital cost in the examples given could only be justified on the basis of increased test section size and not on the small improvements in the test Reynolds number.

## 3.3 Effect of Changes in Compressor and Air Storage Conditions

The time to pressurize the storage tanks, $\lambda$, the relative mass of air to be stored, $K_s$, and the storage pressure are the main variables governing the power input to the compressors. If the time to pressurize the storage tanks can be increased (at constant storage pressure) then the compressor flow rate will be reduced and the power required by the compressor motor will also be reduced. Similarly if the storage pressure or the relative stored air mass is decreased then the flow rate will also be reduced for a given filling time. In the cases considered previously 4 hours ($\lambda$ = 4 hr) was allowed to compress $1{\cdot}5$ times the mass of air in the tunnel ($K_s = 1{\cdot}5$) to a pressure of 10 atmospheres above the tunnel design pressure ($P_s$ = 10 atm.). Figure 11 shows the time required to compress this same mass of air ($K_s = 1{\cdot}5$) to the same pressure using only 10% of the total power input for the compressor motor ($k_{1p} = 0{\cdot}10$). Some of the times shown in Figure

dimensions of an atmospheric tunnel. This may lead to cheaper models but they will be more difficult to construct with sufficient detail. In addition, tests on some full scale objects or large scale models may be precluded.

### 3.2 Alternative Capital Costs and Power Inputs

The tunnel size, dynamic pressure, Reynolds number and Mach number ratios for five other cost and power input variations, namely:

1. $C_p = C_a$, $N_p = 0{\cdot}5\,N_a$
2. $C_p = 1{\cdot}5\,C_a$, $N_p = N_a$
3. $C_p = 1{\cdot}5\,C_a$, $N_p = 0{\cdot}5\,N_a$
4. $C_p = 2{\cdot}0\,C_a$, $N_p = N_a$
5. $C_p = 2{\cdot}0\,C_a$, $N_p = 0{\cdot}5\,N_a$

are shown in Figures 8, 9 and 10. These figures have all been prepared for cost factors $b = 2{\cdot}0$ and $e = 0{\cdot}7$ which are representative of relatively large facilities, as discussed in Section 2.4, and for the compressor and air storage conditions given at the beginning of Section 3.

#### 3.2.1 $C_p = C_a$ and $N_p = 0{\cdot}5\,N_a$

For a constant capital cost ratio, reducing the cost of the drive system by reducing the power input, allows the cost of the circuit and pressurization system to be increased accordingly so that the tunnel can be made larger. For example, if $C_p = C_a$ and the power input is reduced from $N_p = N_a$ to $N_p = 0{\cdot}5\,N_a$ then the size of the tunnel will be increased by $\approx 5\%$ as shown in Figure 8. However an increase in size of only 5% will not alleviate the problems of model size and fidelity referred to earlier. Figure 9 shows that at design pressure ratios of 5, 4 and 3, the maximum $R_N$ and $M_N$ ratios are all decreased by $\approx 23\%$ and $\approx 27\%$ respectively compared with the case when $C_p = C_a$ and $N_p = N_a$. The maximum $R_N$ is still appreciably greater than in the atmospheric tunnel, but the maximum $M_N$ is only slightly higher.

The maximum dynamic pressure in the pressurized tunnel with $C_p = C_a$ and $N_p = 0{\cdot}5\,N_a$, shown in Figure 10, is now only about half its value for the case when $C_p = C_a$ and $N_p = N_a$ and little difficulty would be expected with the design of the model or its support.

#### 3.2.2 $C_p = 1{\cdot}5\,C_a$, $N_p = N_a$ and $N_p = 0{\cdot}5\,N_a$

If the cost of the pressurized tunnel can be increased by 50% compared with the cost of the atmospheric tunnel for either $N_p = N_a$ or $N_p = 0{\cdot}5\,N_a$, then the linear dimensions of the working section will be 25 to 30% greater than for the corresponding pressurized tunnel with $C_p = C_a$, as shown in Figure 8. Reducing the power input from $N_p = N_a$ to $N_p = 0{\cdot}5\,N_a$ only allows the size of the tunnel to be increased by $\approx 4\%$. For a tunnel with a design pressure of 3 to 4 atmospheres the size of the working section will be $\approx 0{\cdot}65$ to $0{\cdot}75$ of the size of the atmospheric tunnel, and this will alleviate model size problems to some extent.

respectively 2·18 and 1·62 times the capability of an atmospheric tunnel, but if $(P_p/P_a)_D = 3$ the maximum Reynolds number and Mach number decrease respectively to 1·65 and 1·44 times their value in an atmospheric tunnel.

For a constant design pressure ratio, increasing the cost factor $g$ by increasing $b$ or $e$, leads to a reduction in tunnel size, and for the same power input results in a significant increase in the Mach number ratio and a relatively small reduction in the Reynolds number ratio as shown in Figures 3, 4 and 5. At a high design pressure ratio a change in $e$ has a slightly greater effect than a change in $b$, but as the design pressure ratio decreases a change in $b$ has a greater effect. This is because the change in performance associated with a change in $b$, which is related to the cost of the extra equipment needed to pressurize the tunnel, is effectively independent of the design pressure, but the change in performance associated with a change in $e$, which is related to the increased cost as the design pressure is increased, depends on the design pressure.

The maximum Mach number ratio has been taken to occur when operating at atmospheric pressure, but, of course, higher ratios can be obtained by operating below atmospheric pressure if the design permits. In this paper pressures below atmospheric are not considered although they would be feasible in most pressurized designs at little extra cost.

### 3.1.2 Dynamic Pressure

Figure 6 shows the very high dynamic pressure which can occur in a pressured tunnel when operating at a high pressure ratio and when the cost factors are high. For example, when operating at a design pressure ratio of 5 and when $b = 2·5$ and $e = 1·0$ the dynamic pressure is 5·6 times the dynamic pressure in the atmospheric tunnel, but for more realistic cost factors of $b = 2·0$ and $e = 0·7$ the maximum dynamic pressure ratio reduces to 4·5.

The dynamic pressure ratio is also reduced as the operating pressure decreases below the design pressure. For example, with $b = 2·0$ and $e = 0·7$, operation at 3 atmospheres in a tunnel designed for 5 atmospheres leads to a dynamic pressure ratio of 3·8 compared with 4·5 at 5 atmospheres. In addition, reducing the design pressure reduces the dynamic pressure. For example, for the same cost factors, a design pressure of 3 atmospheres gives a maximum dynamic pressure ratio of 3·0 compared with a value of 4·5 in a tunnel with a design pressure ratio of 5·0.

The very high dynamic pressure developed at maximum speed in a tunnel with a high design pressure ratio leads to very large forces and moments on the model which can cause problems in its design and support. This is a limiting factor in selecting the design pressure ratio.

### 3.1.3 Size of Working Section

An atmospheric tunnel will be considerably larger than a pressurized tunnel of the same cost, as indicated by equations (3) and (13). The relative linear size of the pressurized working section is shown in Figure 7 as a function of the design pressure ratio for various cost factors. For $b = 2·0$ and $e = 0·7$, a tunnel with a design pressure ratio of 4 will only be half the size of the atmospheric tunnel, but if the value of $b$ or $e$ is reduced the size of the working section will be increased. For example, if $b = 1·5$ and $e = 0·4$, then the size ratio will be 0·63. At a lower design pressure ratio the sections will be slightly larger provided $b$ and $e$ remain constant as shown in Figure 7.

It therefore seems that for realistic cost factors and design pressures of 3 to 4 atmospheres the linear dimensions of a pressurized tunnel will only be of the order of 0·50 to 0·60 of the linear

but this assumption will most likely involve non-similarity of some of the external parts of the cooling system. However, reasonably large errors in $k_{2p}$ and $k_{2a}$ would not affect the relative performance estimates significantly since both $k_{2p}$ and $k_{2a}$ are quite small with respect to unity.

## 3. RELATIVE REYNOLDS NUMBER, MACH NUMBER, DYNAMIC PRESSURE AND TUNNEL SIZE

In the following, the relative performance of pressurized and atmospheric wind tunnels is evaluated for various capital cost and power input ratios using the equations and constants given in the previous sections. The effect of changing the cost factor $b$ from 2·0 to 1·5 and 2·5, and $e$ from 0·7 to 0·4 and 1·0 are also included. Unless stated otherwise it is assumed that the tunnels are operated at the same temperature, and that the air storage and compressor operating conditions used to determine $k_{1p}$ remain constant as follows:

$$S = 3,\ K_s = 1{\cdot}5,$$
$$T_i = 288^\circ \text{ abs},$$
$$\eta = 0{\cdot}5,$$
$$\lambda = 4 \text{ hours},$$
$$\nu = 1{\cdot}3,$$
$$P_s = 10 \text{ atm}.$$

### 3.1 Constant Capital Cost and Constant Power Input

Since capital expenditure will usually be limited, and as power costs are a major part of the running expense, an important case for comparison is when the capital cost and power input for both tunnels are the same.

#### 3.1.1 Reynolds and Mach Number Capability

The ratio of Reynolds number in the pressurized tunnel to the Reynolds number in the atmospheric tunnel is plotted against the ratio of the Mach number in the pressurized tunnel to the Mach number in the atmospheric tunnel in Figure 2 for tunnels with design pressure ratios of 2, 3, 4 and 5, operating at constant power but at various pressure ratios up to the design maximum. Since the Mach number ratio corresponds to the velocity ratio Figure 2 also shows the increased velocity in the working section of the pressurized tunnel compared with the atmospheric tunnel.

The effect of changing the cost factors from $b = 2{\cdot}0$ and $e = 0{\cdot}7$ used for Figure 2($a$), to $b$ 2·5, $e$ 1·0, and $b$ = 1·5, $e = 0{\cdot}4$, are shown in Figures 2($b$) and 2($c$) respectively. Current brief cost estimates indicate that values of $b = 2{\cdot}0$ and $e = 0{\cdot}7$ are slightly high, but that $b$ 1·5 and $e$ 0·5 are rather low. Values of $b = 2{\cdot}5$ and $e = 1{\cdot}0$ are unrealistically high but are included to show the effect of very high cost factors. The range of values chosen indicate how relatively large variations in the cost factors effect the performance and size of pressurized tunnels.

Figure 2 shows that the Reynolds number and Mach number test capability increases as the design pressure ratio increases, and it would therefore seem advantageous (from a $R_N$ and $M_N$ point of view) to have a tunnel that can operate at a relatively high pressure ratio. For example, for $b$ = 2·0, $e$ = 0·7 and $(P_p/P_a)_D = 5$, the maximum $R_N$ and $M_N$ test capability is

Typically, the ratio of the friction losses to the total losses in a tunnel is of the order of 0·3 (ref. 4) and thus $\Sigma K_{1,a}/\Sigma K_{f,a} \approx 2{\cdot}3$. Table 1 shows values of $\eta_p/\eta_a$ for $2{\cdot}5 \geqslant R_{Np}/R_{Na} \geqslant 0{\cdot}5$ determined by substituting the skin friction ratio from equation (26), together with $\Sigma K_{1,a}/\Sigma K_{f,a} = 2{\cdot}3$, into equation (25). The effect of changing $\Sigma K_{1,a}/\Sigma K_{f,a}$ from 2·3 to 1·0 and to 4·0 corresponding to 50% and 20% friction losses are also shown. Since the $R_N$, $M_N$ and velocity ratios depend on $(\eta_p/\eta_a)^{1/3}$, which changes by less than $\pm 3\%$ within the $R_N$ range considered, then the effect of variations in tunnel efficiency will be small and the tunnel performance will not be significantly affected. The ratio of circuit efficiencies $\eta_p/\eta_a$ can therefore be taken as unity at least within the range $2{\cdot}5 \geqslant R_{Np}/R_{Na} \geqslant 0{\cdot}5$.

**TABLE 1**

**Efficiency Ratios for Various Reynolds Number Ratios**

| $R_{Np}/R_{Na}$ | $\Sigma K_{1,a}/\Sigma K_{f,a} = 1{\cdot}0$ | | $\Sigma K_{1,a}/\Sigma K_{f,a} = 2{\cdot}3$ | | $\Sigma K_{1,a}/\Sigma K_{f,a} = 4{\cdot}0$ | |
|---|---|---|---|---|---|---|
| | $\eta_p/\eta_a$ | $(\eta_p/\eta_a)^{1/3}$ | $\eta_p/\eta_a$ | $(\eta_p/\eta_a)^{1/3}$ | $\eta_p/\eta_a$ | $(\eta_p/\eta_a)^{1/3}$ |
| 2·5 | 1·091 | 1·030 | 1·053 | 1·018 | 1·035 | 1·011 |
| 2·0 | 1·069 | 1·023 | 1·041 | 1·013 | 1·027 | 1·009 |
| 1·5 | 1·041 | 1·013 | 1·024 | 1·008 | 1·016 | 1·005 |
| 1·0 | 1·000 | 1·000 | 1·000 | 1·000 | 1·000 | 1·000 |
| 0·5 | 0·931 | 0·976 | 0·957 | 0·985 | 0·971 | 0·990 |

### 2.7 Tunnel Cooling and Cooling Power Factors

High air temperatures can cause problems with models, parts of the tunnel circuit and the instrumentation; and the Reynolds number drops as the temperature rises (at constant power). To overcome these problems the air in the circuit is usually cooled or an air exchanger is fitted. However, since the use of an air exchanger is precluded for pressurized tunnels it is assumed that both types of tunnel are fitted with an internal heat exchanger.

Relatively high-powered tunnels, such as the ones being considered here, require a very large cooling surface area and special cooling installations are needed which can cause a significant pressure loss in the circuit. They also require a small amount of power to circulate the coolant. The pressure loss across the cooler is taken into account by the tunnel efficiency term and the power to circulate the coolant is allowed for by the terms $k_{2a}N_a$ and $k_{2p}N_p$ for atmospheric and pressurized tunnels respectively.

The heat input, the heat losses, and the heat extracted by the heat exchanger for both the pressurized and atmospheric tunnels are briefly considered in Appendix I. This analysis indicates that is is reasonable to assume that both types of tunnel can be operated with similar air temperatures in their circuits for a reasonable period of time.

The power required to circulate the coolant depends on the detail design of the cooling system but is mainly dependent on the friction in the pipework and the head loss in any external cooling tower. For an atmospheric tunnel operating at a maximum speed of 130 m/s approximately 5% of the power input is required to circulate the coolant and $k_{2a} \approx 0{\cdot}05$. Assuming the power to circulate the coolant is proportional to the power for the tunnel circuit then $k_{2p}$ can be calculated from

$$k_{2p}/k_{2a} = 1 - k_{1p} \tag{27}$$

then the relative power factor for different pressurized tunnels, in relation to a given atmospheric tunnel, is given by:

$$k_{1p,1}/k_{1p,2} = [N_{p,2}/N_a][N_a/N_{p,1}][\lambda_2/\lambda_1][\eta_{s,2}/\eta_{s,1}][T_{i,1}/T_{i,2}]$$
$$[(P_p/P_a)_{D,1}/(P_p/P_a)_{D,2}][K_{s,1}/K_{s,2}][S_1/S_2][\rho_{a,1}/\rho_{a,2}]$$
$$[P_{r,1}{}^{(\nu-1)/\nu}-1]/[P_{r,2}{}^{(\nu-1)/\nu}-1][C_{p,1}/C_a]^{3/(2m_p)}[C_a/C_{p,2}]^{3/(2m_p)}$$
$$[(1-f_a(C_a/C_{p,1})(N_{p,1}/N_a)(1-k_{1p,1}))/(1-f_a(C_a/C_{p,2})(N_{p,2}/N_a)(1-k_{1p,2}))]^{3/(2m_p)}$$
$$[\{b+e[(P_p/P_a)_{D,2}-1]\}/\{b+e[(P_p/P_a)_{D,1}-1]\}]^{(3m_a)/(2m_p)} \quad (21)$$

Subscript 1 denotes a given pressurized tunnel and subscript 2 a pressurized tunnel with different design parameters.

Equation (21) enables alternative values of $k_{1p}$ to be calculated for changes in the design parameters once an initial value of $k_{1p}$ has been determined. For example, if the time available for pressurizing the storage is increased then the flow rate will be smaller and $k_{1p,2}$ will be less than $k_{1p,1}$. It is estimated that $k_{1p} \approx 0{\cdot}10$ for design cost and power conditions $C_p = C_a$ and $N_p = N_a$ when a centrifugal compressor is used to pressurize the storage tanks under the following conditions: $S = 3$ (3 stage compressor), $K_s = 1{\cdot}5$ (mass of air in storage tanks is $1{\cdot}5$ times mass of air in tunnel), $T_i = 288°$ abs. (initial air temperature of 15°C), $(P_p/P_a)_D = 5$ (tunnel design pressure of 5 atmospheres), $P_r = 2{\cdot}47$ (storage air pressure of 10 atmospheres above tunnel design pressure),[7] $\lambda = 4$ (pressurization time of 4 hours), $\eta_s = 0{\cdot}5$ (efficiency of compressor and motor of 50%) and $\nu = 1{\cdot}3$ (polytropic compression index $= 1{\cdot}3$). These values can be used in equation (21) to determine $k_{1p}$ for other design conditions as required.

### 2.6 Relative Efficiency

The tunnel circuit efficiency (energy ratio) can be written as

$$\eta = 1/(\Sigma K_o) \quad (22)$$

where $K_o = \delta P/(\frac{1}{2}\rho V^2)$ is the total loss coefficient for a given component of the circuit referred to the dynamic pressure in the working section. Taking $K_o$ to be the sum of a pressure loss coefficient $K_f$ due to friction, which depends on the Reynolds number, and a pressure loss coefficient $K_l$ due to the remaining pressure loss, which is assumed to be constant and independent of Reynolds number, then the tunnel efficiency is given by:

$$\eta = 1/(\Sigma K_l + \Sigma K_f) \quad (23)$$

For similar pressurized and atmospheric wind tunnels operating at different Reynolds numbers the ratio of the circuit efficiencies can be expressed as:

$$\eta_p/\eta_a = (\Sigma K_{l,a} + \Sigma K_{f,a})/(\Sigma K_{l,p} + \Sigma K_{f,p}) \quad (24)$$

Since $K_{l,a} = K_{l,p}$ and $K_{f,p}/K_{f,a} = C_{f,p}/C_{f,a}$ for similar tunnels then equation (24) can be written as

$$\eta_p/\eta_a = (\Sigma K_{l,a}/\Sigma K_{f,a} + 1)/(\Sigma K_{l,a}/\Sigma K_{f,a} + \Sigma C_{f,p}/\Sigma C_{f,a}) \quad (25)$$

Equation (25) can be evaluated once the ratio of the total skin friction losses to the total pressure losses in the circuit, and the ratio of the total skin friction coefficients, are known. Assuming the ratio of the skin friction coefficients, $\Sigma C_{f,p}/\Sigma C_{f,a}$, can be approximated as the ratio of the skin friction coefficients for a smooth flat plate in a zero pressure gradient by the Prandtl-Von Karman equation then

$$\Sigma C_{f,p}/\Sigma C_{f,a} = (R_{Na}/R_{Np})^{1/5} \quad (26)$$

Substituting the Reynolds number ratio from equation (10) into equation (26) enables the tunnel performance to be estimated iteratively.

atmospheres above the tunnel design pressure ($P_s = 10$ atm.). However, there is some uncertainty in the values because of the lack of availability of cost data of known accuracy, and therefore the effects of relatively large variations in $b$ and $e$ are illustrated in Section 3.

The cost of the drive and cooling system of an atmospheric tunnel depends on the power input to the tunnel circuit, which, in turn, is related to the maximum speed and the allowable air temperature in the working section. For a conventional tunnel with a maximum air speed of 130 m/sec and a maximum air temperature of about 45°C it is estimated that $f_a \approx 0{\cdot}20$ and $k_{2a} \approx 0{\cdot}05$. Since the cost of the drive and cooling system is directly proportional to the maximum power input,[9] then from equations (1) and (5), together with $Nt = \frac{1}{2}\rho V^3 A/\eta$ and $C_{dc,a} = f_a C_a$, the equations

$$f_{a,1}/f_{a,2} = (A_{a,1}/A_{a,2})(\rho_{a,1}/\rho_{a,2})(V_{a,1}/V_{a,2})^3 \\ ((1-k_{2a,2})/(1-k_{2a,1}))(\eta_{a,2}/\eta_{a,1})(C_{a,2}/C_{a,1}) \tag{15}$$

$$(1-f_{a,1})/(1-f_{a,2}) = (C_{a,2}/C_{a,1})(A_{a,1}/A_{a,2})^{m_a} \tag{16}$$

enable the values of $f_{a,2}$ to be calculated for other selected values of maximum velocity and capital cost, area and velocity, or capital cost and area, combined with variations in temperature (provided none of these quantities vary excessively from their original values). Normally, $k_{2a,1}$ and $k_{2a,2}$ are small with respect to unity and $\eta_{a,2}/\eta_{a,1} \approx 1$ (see Section 2.6), and for operation at the same temperature equation (15) can be simplified to:

$$f_{a,1}/f_{a,2} = (A_{a,1}/A_{a,2})(V_{a,1}/V_{a,2})^3(C_{a,2}/C_{a,1}) \tag{17}$$

Thus, for example, if $V_{a,2}$ is chosen to be less than $V_{a,1}$ then for a given tunnel ($A_{a,1} = A_{a,2}$) $f_{a,2} < f_{a,1}$ and $C_{a,2} < C_{a,1}$; or for a given cost ($C_{a,1} = C_{a,2}$) then $f_{a,2} < f_{a,1}$ and $A_{a,2} > A_{a,1}$.

For the pressurized tunnel, again taking the cost of the main drive and cooling systems as proportional to their power inputs, then $f_p$ can be calculated from the equation

$$f_p = f_a(1-k_{1p})(C_a/C_p)(N_p/N_a) \tag{18}$$

### 2.5 Pressurization Power Factor

The proportion of total power required for pressurization, $k_{1p}$, depends mainly on the time allowed to fill the storage, the quantity of air to be stored and the pressure at which it is stored.

In the following analysis it is assumed that multistage centrifugal compressors are operated to supply air to the storage containers at the same time as the main drive. Reciprocating compressors are not suitable because of the difficulties in obtaining the required mass flow, and axial flow compressors cannot give the required pressure rise. If the compressors are not operated at the same time as the main drive then $k_{1p}$ can be taken as zero.

The power required for an electric motor to drive a multistage centrifugal compressor is given by

$$k_{1p}N_p = m_f v/(v-1)RT_i[(P_r)^{(v-1)/v}-1]S/\eta_s \tag{19}$$

where the pressure ratio per stage, $P_r$, is normally not greater than about 3. The mass of air to be stored is assumed to be proportional to the mass of air contained in the tunnel and the average mass flow rate:

$$m_i = K_s[(P_p/P_a)_D\rho_a K_v 1^3]/\lambda \tag{20}$$

is the stored mass divided by the time, $\lambda$, to fill the storage. From equations (19) and (20), substituting for the length scale from equations (3), (13) and (14), and using $f_p$ from equation (18),

atmospheric tunnel. The Reynolds and Mach number envelope is shown in Figure 23 compared with the tandem section atmospheric tunnel.

The pressurized tunnel could accommodate the required 3 m diameter rotor but it could only be tested down to a speed of about 17 $ms^{-1}$ in the working section, and from about 10 $ms^{-1}$ to 13 $ms^{-1}$ in the settling chamber if a contraction ratio of 10 : 1 is assumed. This still leaves a gap in the low-speed test range although the higher speed range would be covered adequately. Provided the settling chamber could be used to cover the very low-speed test range from about 10 $ms^{-1}$ to 14 $ms^{-1}$, then a working section at least 5·5 m × 4·5 m would be needed to cover the complete test speed range for a relatively highly loaded rotor. CTOL aircraft models with the required span of 3 m could be tested in the 4·8 m × 4·0 m pressurized tunnel without undue difficulty. However, the capital cost of this tunnel would be at least twice the cost of the tandem working section atmospheric tunnel. If there is a requirement to accept 3 m models for commercial development work then the capital cost of building a pressurized tunnel in which to test them is very high and this would need to be carefully assessed against the benefits of an expanded $R_N$ test envelope and the ability to separate $M_N$ and $R_N$ effects.

## 6. CONCLUDING REMARKS

The merits and disadvantages of using a pressurized circuit instead of an atmospheric circuit for low-speed wind tunnel testing have been considered. The performance of tunnels designed to operate at atmospheric pressure, and at pressures between 2 and 5 atmospheres, have been compared on the basis of variable capital cost and power input. Both factors have a significant effect on the performance of any new wind tunnel because funds for its construction and operation will almost certainly be limited, and because economic considerations will generally require the most versatile tunnel with the best performance to be provided within given values of these constraints.

If the capital cost and power input for both types of tunnel are constant, then pressurization allows the maximum $R_N$ and $M_N$ to be increased significantly, but the working section is much smaller. For example, a tunnel with a design pressure of 3 atmospheres would only be about 0·55 of the linear size of the atmospheric tunnel, but the maximum $R_N$ and $M_N$ would be respectively 1·7 and 1·5 times their value in the atmospheric tunnel. Higher design pressures lead to higher maximum test Reynolds and Mach numbers but even smaller working sections. If the power input remains the same then increasing the capital cost of the pressurized tunnel by up to 100% increases the size of the working section by up to 60%, but the maximum $R_N$ remains about the same, provided the ratio of the mass of air to be stored to the mass of air in the tunnel and the time required to fill the air storage are constant. Reducing the power input by 50% leads to an increase in tunnel size of about 5% and decreases the maximum $R_N$ by nearly 25%.

An increase in test Reynolds number capability of the order of 100%, depending on the actual value attained, can be very important because the effects of scale-dependent local flows have become more significant in modern aircraft designs, particularly combat aircraft, and to simulate these complex flows with sufficient accuracy the models must be tested at a higher Reynolds number than previously accepted.

As well as an appreciably higher Reynolds number, tunnel pressurization also enables the Reynolds and Mach number effects to be investigated separately. This can be important when testing V/STOL models, and CTOL models in high-lift configurations, but there would be substantial extra testing costs involved in separating these effects.

Although models for the pressurized tunnel would be smaller and easier to handle they would be difficult and time-consuming to design and construct because of the higher dynamic pressures they must withstand. However, overall, they may be slightly less expensive due to their smaller size. If a maximum pressure of 3 to 4 atmospheres were specified it should not be too difficult to design a model with sufficient strength, although higher model distortion and sting interference may result.

The analysis for the relative performance of similar pressurized and atmospheric tunnels has been applied to a tandem section tunnel put forward for discussion as a possible configuration suitable for upgrading and extending low-speed aeronautic and aerospace test facilities in Australia. The proposed atmospheric tunnel has test section sizes of $4{\cdot}7\ m \times 3{\cdot}4\ m \times 10\ m$, and $6\ m \times 6\ m \times 13{\cdot}5\ m$, with maximum speeds of $135\ ms^{-1}$ and $60\ ms^{-1}$ respectively. On the basis of the same capital cost and power input a tunnel pressurized to 3 atmospheres would have sections $2{\cdot}6\ m \times 1{\cdot}9\ m \times 5{\cdot}5\ m$ and $3{\cdot}3\ m \times 3{\cdot}3\ m \times 7{\cdot}4\ m$. Unfortunately these smaller sections would not accommodate large enough V/STOL or CTOL models for commercial development work. In addition, the V/STOL low-speed test regime cannot be covered adequately and it would be difficult to carry out certain tests involving a large downwash or a high angle of attack, for example, during take-off and landing, or in combat manoeuvring. The ability to test a range of large or full scale components in both the aeronautical and non-aeronautical fields would also be compromised. However, the pressurized tunnel would meet many of the requirements for other types of aircraft work such as research and investigations of operational problems.

An alternative pressurized tunnel with a single section $4{\cdot}8\ m$ wide and $4{\cdot}0\ m$ high capable of operating at up to 3 atmospheres was considered. Although the maximum Reynolds number was twice its value in the atmospheric tunnel and the Mach number range was similar, the V/STOL test requirements could still not be completely satisfied particularly at low speeds. This tunnel was estimated to be at least twice as expensive as the atmospheric tunnel. Even larger sections would be better able to cope with the V/STOL test requirements but they would be prohibitively expensive. However, when considering costs of a major test facility it is wise to build-in at the outset more capability than current needs fully justify as an investment against greater needs in the future.[22]

## REFERENCES


1. Lemaire, D. A., Matheson, N., and Thompson, D. A. 'A projected large low-speed wind tunnel to meet Australian requirements'. Department of Defence, Defence Science and Technology Organization, Aeronautical Research Laboratories, Aerodynamics Note 410, March 1982.

2. 'Science and Technology in Australia 1977–78'. A report to the Prime Minister by the Australian Science and Technology Council (ASTEC), Volume 1B, January 1979.

3. Wilson, M. 'The RAE 5 m low-speed wind tunnel'. Flight International, March 1973.

4. Pope, A., and Harper, J. J. 'Low-speed Wind Tunnel Testing'. John Wiley and Sons, New York, 1966.

5. Trebble, W. J. G. 'Techniques for the aerodynamic testing of V/STOL models'. AGARDograph No. 126, May 1968.

6. Williams, J., and Holbech, A. 'Acoustic considerations for noise experiments at model scale in subsonic wind-tunnels'. AGARD report R-601, 1972, paper No. 8.

7. Carrara, J., and Masson, A. 'Three years of operation of the ONERA pressurized subsonic wind tunnel'. International Council of the Aeronautical Sciences, Proceedings of the 12th Congress, 1980.

8. Seidel, M., and Jaarsma, F. 'The German–Dutch low-speed wind tunnel DNW'. Aeronautical Journal, April 1978.

9. Spence, A., and Spee, B. M. 'Some considerations of future low-speed tunnels for Europe'. AGARD Report No. 600, paper No. 1, 1972.

10. Large wind tunnels working group. 'The need for large wind tunnels in Europe'. AGARD, AR 60, December 1972.

11. First report of the Mini LaWs working group. 'A review of current research aimed at the design and operation of large wind tunnels'. AGARD, AR 68, March 1974.

12. Second report of the Mini LaWs working group. 'A further review of current research aimed at the design and operation of large wind tunnels'. AGARD, AR 83, September 1975.

13. Simons, I. A., and Derschmidt, H. 'Wind tunnel requirements for helicopters'. AGARD Report No. 601, April 1973, paper No. 7.

14. Jeffery, R. W., Tuck, A. N., and Law, R. D. 'A system for the measurement of the attitude of wind tunnel models'. Proceedings of the 11th AIAA Aerodynamic Testing Conference, Colorado Springs, Colorado, March 18–20, 1980, paper 80-0465.

15. Ewald, B. 'Low-speed tunnels with tandem test sections, a contribution to some design problems'. AGARD Conference Proceedings No. 174, March 1976, paper No. 7.

16. Templin, R. J. 'The choice of working section size and shape for V/STOL wind tunnels'. Quarterly bulletin of the Division of Mechanical Engineering and the National Aeronautical Establishment of the National Research Council Canada, 1st October to 31st December, 1965.

17. Carbonaro, M. 'Interference problems in V/STOL testing at low speeds'. AGARD Conference Proceedings No. 174, March 1976, paper No. 40.

18. Sears, W. R., Vidal, R. J., Erickson, J. C., and Ritter, A. 'Interference free wind-tunnel flows by adaptive wall technology'. J. Aircraft, Vol. 14, No. 11, 1977.

19. Green, J. E. 'On the influence of free stream turbulence on a turbulent boundary layer, as it relates to wind tunnel testing at subsonic speeds'. AGARD Report No. 602, Fluid Motion Problems in Wind Tunnel Design, paper No. 4, 1973.

20. Bradshaw, P., and Pankhurst, R. C. 'The design of low-speed wind tunnels'. NPL Aero Report 1039, 1962.

21. Bernstein, S., and Joppa, R. G. 'Development of minimum-correction wind tunnels'. J. Aircraft, Vol. 13, No. 4, April 1976.

22. Baals, D. D., and Corliss, W. R. 'Wind Tunnels of NASA'. National Aeronautics and Space Administration, Washington, D.C., 1981.

## APPENDIX I

## TUNNEL COOLING

Part of the heat input to the air in the circuit is transmitted through the tunnel walls to the surrounding air and the remainder is extracted by the heat exchanger. However, the heat flow through the walls is limited by the natural connective heat transfer coefficient for the external surface, and in a conventional atmospheric tunnel operating under equilibrium conditions at a maximum airstream temperature of 45°C and speed of 130 m/sec the heat loss through the walls is only approximately 10% to 15% of the heat input. In a similar but smaller pressurized tunnel with the same power input the heat passing out through the walls is an even smaller proportion of the total heat input. Since the heat transmitted through the walls is only a small part of the total heat input it is neglected in the following brief considerations of the heat exchanger.

The heat transfer coefficient in the heat exchanger is governed by forced convection between the air in the tunnel and the external surface of the exchanger, and for circular cylinders with $1000 \leqslant R_d \leqslant 100\,000$, can be approximated by

$$N_u = 0{\cdot}26 R_d^{0{\cdot}6} P_n^{0{\cdot}3} \tag{1}$$

and the total heat extracted can be calculated from

$$Q = h A_d \theta_m. \tag{2}$$

Circular sections are assumed in the following discussion to illustrate certain aspects of tunnel cooling. In an actual installation non-circular sections with a minimum drag coefficient would be used.

Provided the mean temperature of the air in the tunnel and the coolant are not significantly different, then, from equations (1) and (2), the relative heat extracted from a pressurized and an atmospheric tunnel is:

$$(Q_p/Q_a)_E = [d_p/d_a]^{-1}[R_{d,p}/R_{d,a}]^{0{\cdot}6}[A_{d,p}/A_{d,a}][\theta_{m,p}/\theta_{m,a}] \tag{3}$$

where the subscripts $p$ and $a$ refer to a pressurized and an atmospheric tunnel respectively. For geometrically similar heat exchangers inside each tunnel, equation (3) simplifies to

$$(Q_p/Q_a)_E = [R_{Np}/R_{Na}]^{0{\cdot}6}[l_p/l_a][\theta_{m,p}/\theta_{m,a}] \tag{4}$$

The relative heat input to the circuit is proportional to the power required to circulate the air and is given by

$$(Q_p/Q_a)_I = (N_p/N_a)[(1-k_{1p}-k_{2p})/(1-k_{2a})] \tag{5}$$

The ratio of the heat extracted to the heat input for a pressurized tunnel compared with a given atmospheric tunnel is therefore

$$(Q_E/Q_I)_p/(Q_E/Q_I)_a = (R_{Np}/R_{Na})^{0{\cdot}6}(l_p/l_a)(\theta_{m,p}\theta/_{m,a})$$
$$(N_p/N_a)^{-1}[1-k_{1p}-k_{2p})/(1-k_{2a})]^{-1} \tag{6}$$

Table 1 shows values of $(Q_E/Q_I)_p/(Q_E/Q_I)_a$, calculated from equation (6), for tunnels operating at their maximum power input and various design and operating pressures, and selected capital cost and power input conditions (see Sections 3.1 and 3.2). The values in Table 1 were calculated after substituting equations (3), (10), (13) and (27) into equation (6) in this Appendix, with the constants given in Sections 2.4 to 2.7, and assuming the same mean temperature difference $\theta_{m,p} = \theta_{m,a}$. When $C_p = C_a$ and $N_p = N_a$ the pressurized tunnel operating at low pressures has only about half the cooling capacity of the atmospheric tunnel, but as the

operating pressure is increased to the design pressure the cooling capability is increased to about 80% due to the increased Reynolds number. To keep the air in each tunnel at a constant temperature, particularly when operating at low pressure ratios, either a relatively larger heat exchanger or an increased mean temperature difference would be needed. Possibly varying the mean temperature difference using a chiller or refrigeration plant would be the most suitable.

**TABLE 1**

**Relative Heat Extracted to Heat Input Ratios for Pressurized and Atmospheric Tunnels Operating at Maximum Power Input with Geometrically Similar Heat Exchangers and the same Mean Temperature Difference**

| (*a*) $C_p = C_a$, $N_p = N_a$ | | | (*b*) $C_p = C_a$, $N_p = 0{\cdot}5\,N_a$ | | |
|---|---|---|---|---|---|
| $(P_p/P_a)_D$ | $P_p/P_a$ | $(Q_E/Q_I)_p/(Q_E/Q_I)_a$ | $(P_p/P_a)_D$ | $P_p/P_a$ | $(Q_E/Q_I)_p/(Q_E/Q_I)_a$ |
| 5 | 5 | 0·82 | 5 | 5 | 1·76 |
| | 1 | 0·43 | | 1 | 0·92 |
| 4 | 4 | 0·83 | 4 | 4 | 1·76 |
| | 1 | 0·47 | | 1 | 1·01 |
| 3 | 3 | 0·82 | 3 | 3 | 1·74 |
| | 1 | 0·53 | | 1 | 1·12 |
| 2 | 2 | 0·79 | 2 | 2 | 1·65 |
| | 1 | 0·60 | | 1 | 1·26 |
| (*c*) $C_p = 1{\cdot}5\,C_a$, $N_p = N_a$ | | | (*d*) $C_p = 1{\cdot}5\,C_a$, $N_p = 0{\cdot}5\,N_a$ | | |
| $(P_p/P_a)_D$ | $P_p/P_a$ | $(Q_E/Q_I)_p/(Q_E/Q_I)_a$ | $(P_p/P_a)_D$ | $P_p/P_a$ | $(Q_E/{}_IQ)_p/(Q_E/Q_I)_a$ |
| 5 | 5 | 1·22 | 5 | 5 | 3·04 |
| | 1 | 0·64 | | 1 | 1·60 |
| 4 | 4 | 1·22 | 4 | 4 | 3·02 |
| | 1 | 0·70 | | 1 | 1·73 |
| 3 | 3 | 1·23 | 3 | 3 | 2·96 |
| | 1 | 0·79 | | 1 | 1·91 |
| 2 | 2 | 1·16 | 2 | 2 | 2·73 |
| | 1 | 0·88 | | 1 | 2·08 |
| (*e*) $C_p = 2\,C_a$, $N_p = N_a$ | | | (*f*) $C_p = 2{\cdot}0\,C_a$, $N_p = 0{\cdot}5\,N_a$ | | |
| $(P_p/P_a)_D$ | $P_p/P_a$ | $(Q_E/Q_I)_p/(Q_E/Q_I)_a$ | $(P_p/P_a)_D$ | $P_p/P_a$ | $(Q_E/Q)_p/(Q_E/Q_I)_a$ |
| 5 | 5 | 1·73 | 5 | 5 | 6·21 |
| | 1 | 0·91 | | 1 | 3·52 |
| 4 | 4 | 1·73 | 4 | 4 | 6·49 |
| | 1 | 0·99 | | 1 | 3·73 |
| 3 | 3 | 1·69 | 3 | 3 | 5·93 |
| | 1 | 1·09 | | 1 | 3·82 |
| 2 | 2 | 1·59 | 2 | 2 | 4·92 |
| | 1 | 1·21 | | 1 | 3·73 |

As the capital cost is increased the pressurized tunnel becomes relatively larger and for the same power input an increasing proportion of the power is required to pressurize the circuit and air storage in a given time ($\lambda = 4$ hours). The heat input is therefore proportionately smaller, and since the Reynolds number ratio does not change significantly, a geometrically similar heat exchanger is better able to cope with the cooling requirements as shown in Table 1, (*a*) (*c*) and (*e*).

Decreasing the power input to the pressurized tunnel to $N_p = 0{\cdot}5\,N_a$ leads to a much smaller heat input and a slightly larger tunnel for the three capital cost conditions considered, so that a geometrically similar heat exchanger can provide the required cooling as shown in Table 1 (*b*), (*d*) and (*f*). It therefore seems that for most of the cases considered the atmospheric and pressurized tunnels could be operated with similar circuit air temperatures for similar periods of time.

## APPENDIX II

## RELATIVE STRESSES, FORCES AND MOMENTS ON MODELS IN PRESSURIZED AND ATMOSPHERIC WIND TUNNELS

Consider a model of a simple aircraft mounted on a sting or single strut in a wind tunnel as shown in Figure 17. Assuming that the drag, $D$, lift, $L$, and pitching moment, $M_z$, are the only aerodynamic forces and moments acting on the wing at the $\frac{1}{4}$ chord as shown, then the force components along the $x$, $y$ and $z$ axis at a section of the wing are

$$F_{x,y,z} \propto q.l_m^2 \tag{1}$$

and the moment components along the same axes are

$$M_{x,y,z} \propto q.l_m^3 \tag{2}$$

The ratio of the stresses at corresponding locations on geometrically similar models tested in pressurized and atmospheric tunnels under similar conditions and at the same temperature can then be written as:

$$\tau_{Fx,p}/\tau_{Fx,a} = (q_p/q_a)(l_{m,p}/l_{m,a})^2(A_{\tau,a}/A_{\tau,p}) \tag{3}$$

$$\tau_{Fy,p}/\tau_{Fy,a} = (q_p/q_a)(l_{m,p}/l_{m,a})^2(A_{\tau,a}/A_{\tau,p}) \tag{4}$$

$$\tau_{Mz,p}/\tau_{Mz,a} = (q_p/q_a)(l_{m,p}/l_{m,a})^3(Z_{mz,a}/Z_{mz,p}) \tag{5}$$

$$\sigma_{Fz,p}/\sigma_{Fz,a} = (q_p/q_a)(l_{m,p}/l_{m,a})^2(A_{\sigma,a}/A_{\sigma,p}) \tag{6}$$

$$\sigma_{Mx,p}/\sigma_{Mx,a} = (q_p/q_a)(l_{m,p}/l_{m,a})^3(Z_{x,a}/Z_{x,p}) \tag{7}$$

$$\sigma_{My,p}/\sigma_{My,a} = (q_p/q_a)(l_{m,p}/l_{m,a})^3(Z_{y,a}/Z_{y,p}) \tag{8}$$

These equations can be used in a stress analysis to estimate the relative design stresses required for a given load member, or to give the relative section modulus and area for a given design stress.

Normally, and particularly at small angles of incidence, the stresses due to the drag, the force along the $z$ axis, and the pitching moment are all small with respect to the stress caused by the lift so that, in most cases, the stresses and the dimensions of the load carrying members in the models can be compared using equations (4) and (7). If the models are not tested under similar conditions, for example, if the drag, lift and pitching moment coefficients are influenced significantly by testing at different Mach or Reynolds numbers, then these changes should be taken into account.

## APPENDIX III

## RELATIVE MODEL AND STING DEFLECTIONS IN PRESSURIZED AND ATMOSPHERIC WIND TUNNELS

To illustrate the effects of model deflection in a pressurized tunnel compared with an atmospheric tunnel consider the wing of the aircraft referred to in Appendix II. Only the twist of the wing, $\phi_z$, due to the pitching moment, and the deflection at right angles to the chord in the $y$–$z$ plane, $\theta_y$, due to the lift are considered, and are given by

$$\phi_z \propto l_m/GJ_{Mz}) \tag{1}$$

and

$$\theta_y/l_m \propto l_m{}^4\, q/(E\, I_x) \tag{2}$$

For geometrically similar models tested in pressurized and atmospheric tunnels the relative twist and deflection are therefore

$$\phi_{z,p}/\phi_{z,a} = (q_p/q_a)(l_p/l_a)^4(G_a/G_p)(J_{Mz,a}/J_{Mz,p}) \tag{3}$$

and

$$(\theta_{y,p}/l_{m,p})/(\theta_{y,a}/l_{m,a}) = (q_p/q_a)(l_{m,p}/l_{m,a})^4(E_a/E_p)(I_{x,a}/I_{x,p}) \tag{4}$$

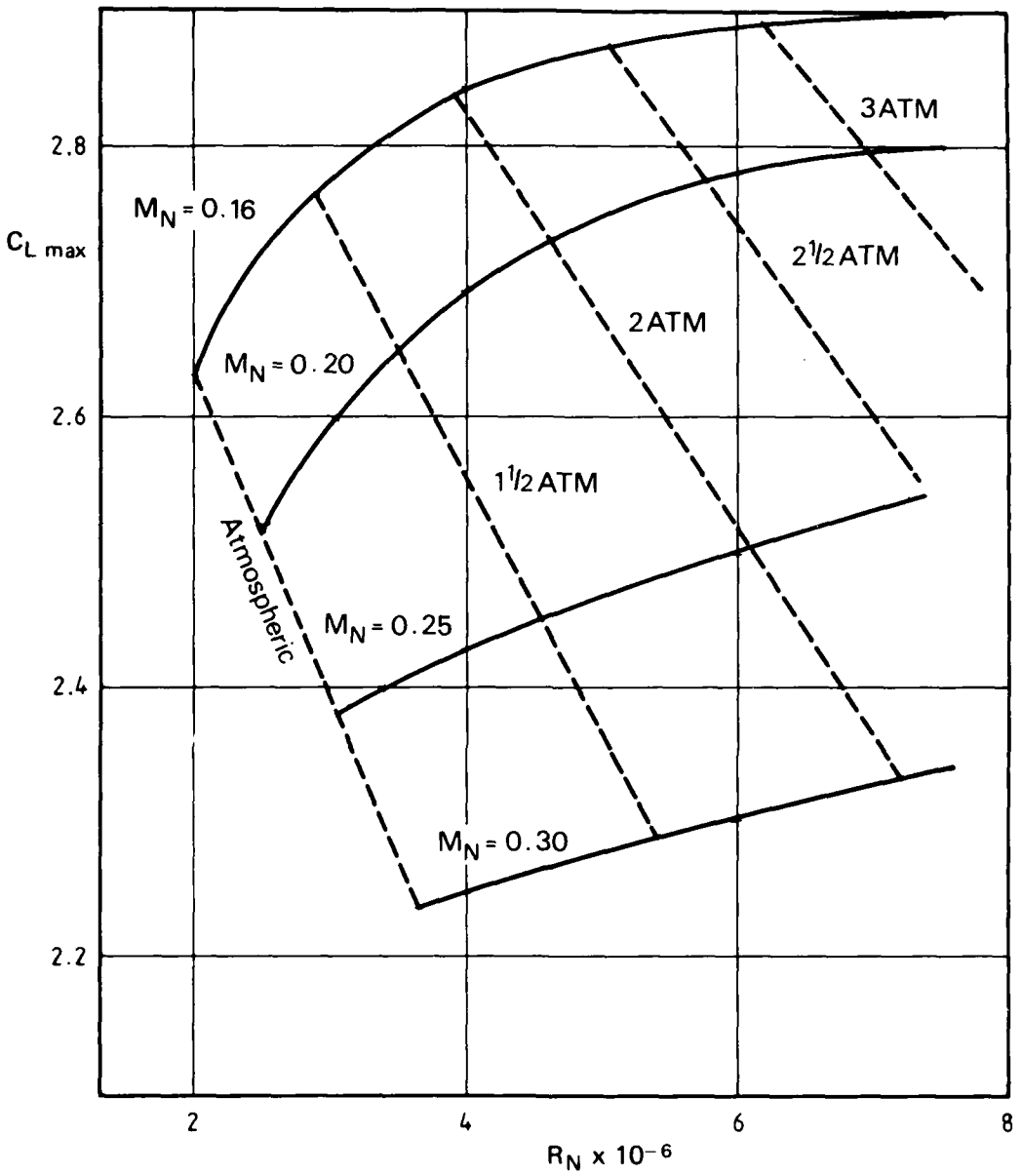


Fig. 1 Effect of Mach number and Reynolds number on the maximum lift coefficient of a Wing[3]

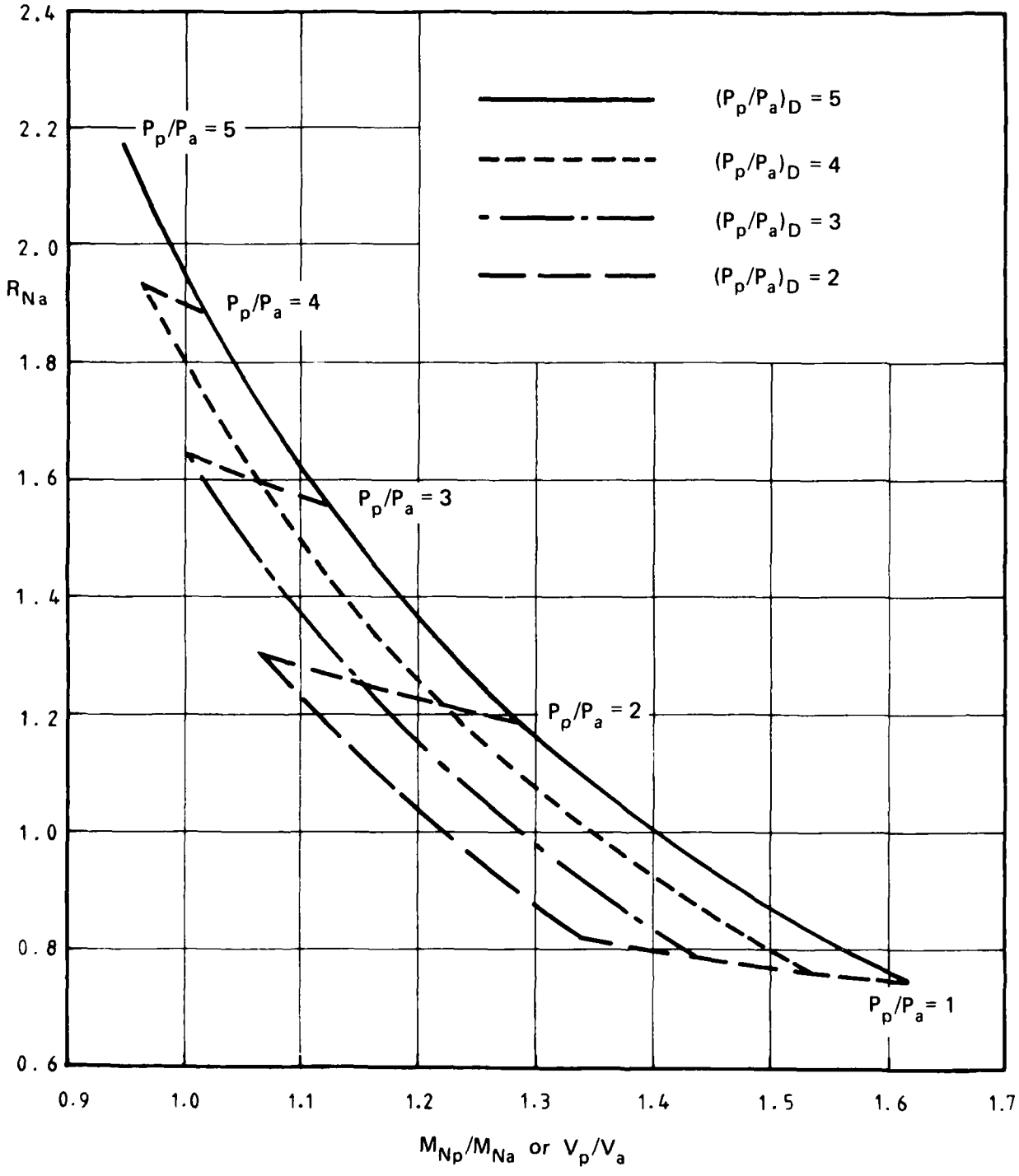


Fig. 2 Reynolds number, Mach number and velocity ratios for tunnels with $C_p = C_a$, $N_p = N_a$, and design pressures of 2, 3. 4 and 5 atmospheres.

(a) b = 2.0, e = 0.7

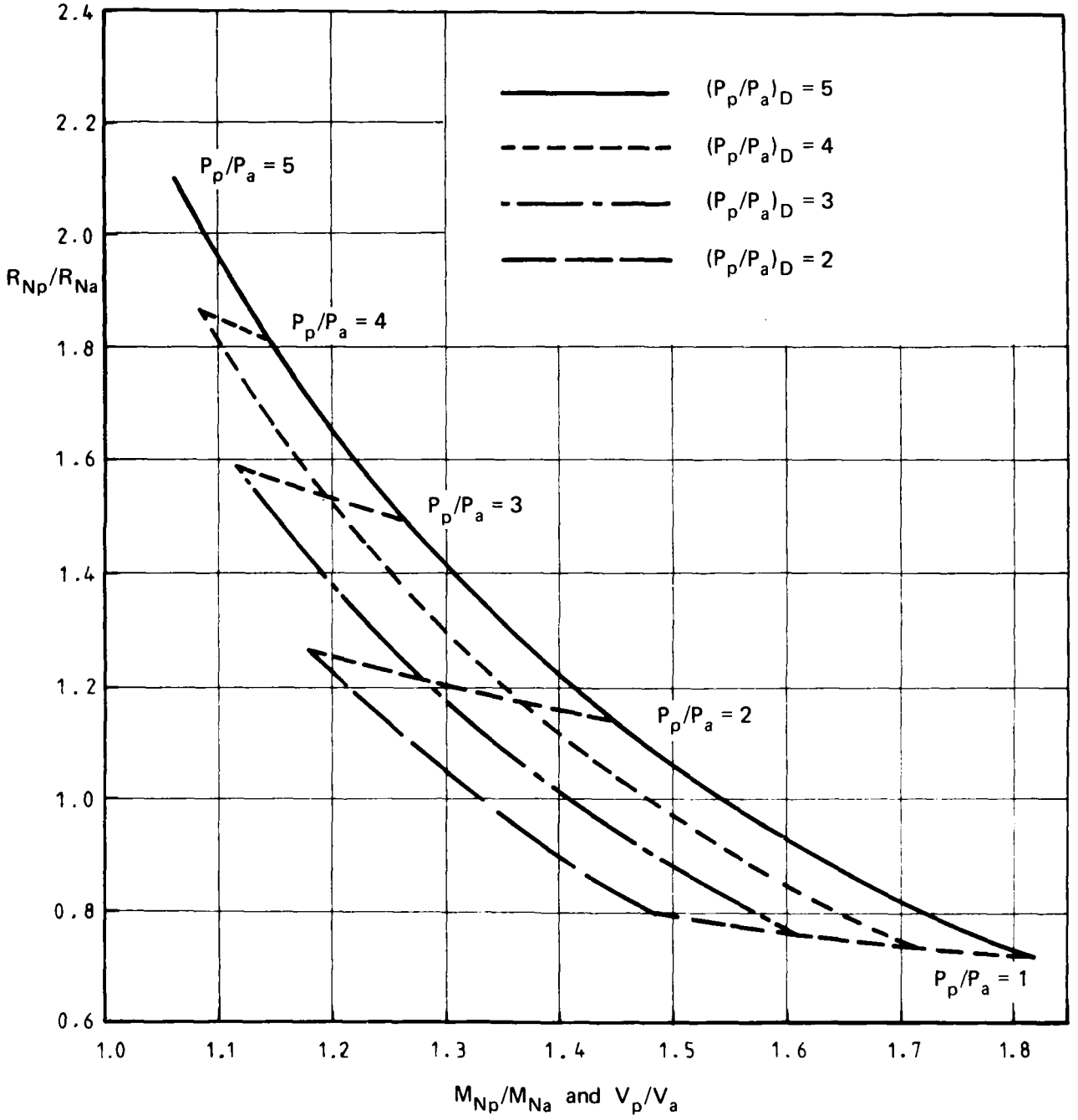


Fig. 2 (Cont.)

(b) b = 2.5, e = 1.0

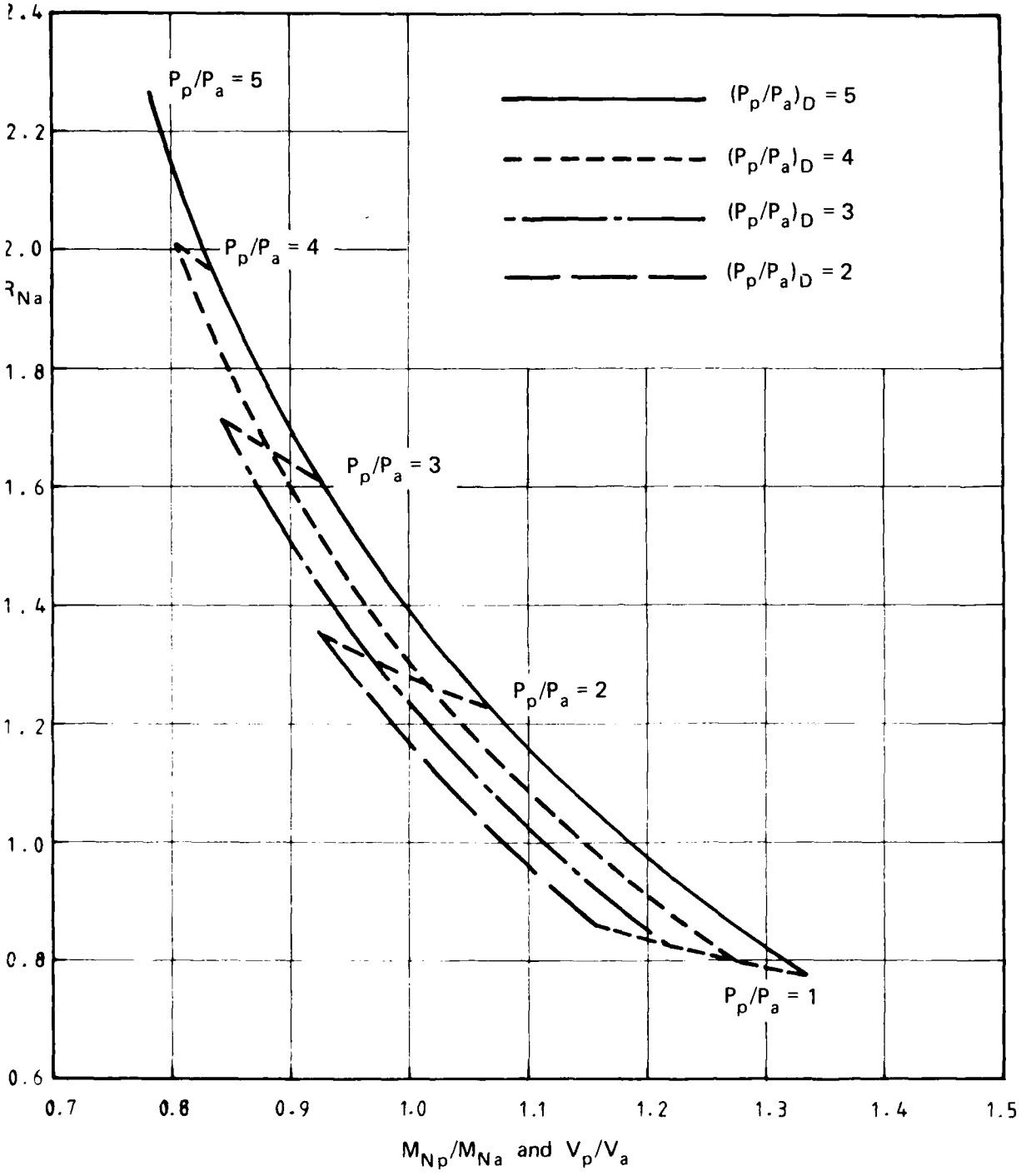


Fig. 2 (cont.)

(c) b = 1.5, e = 0.4

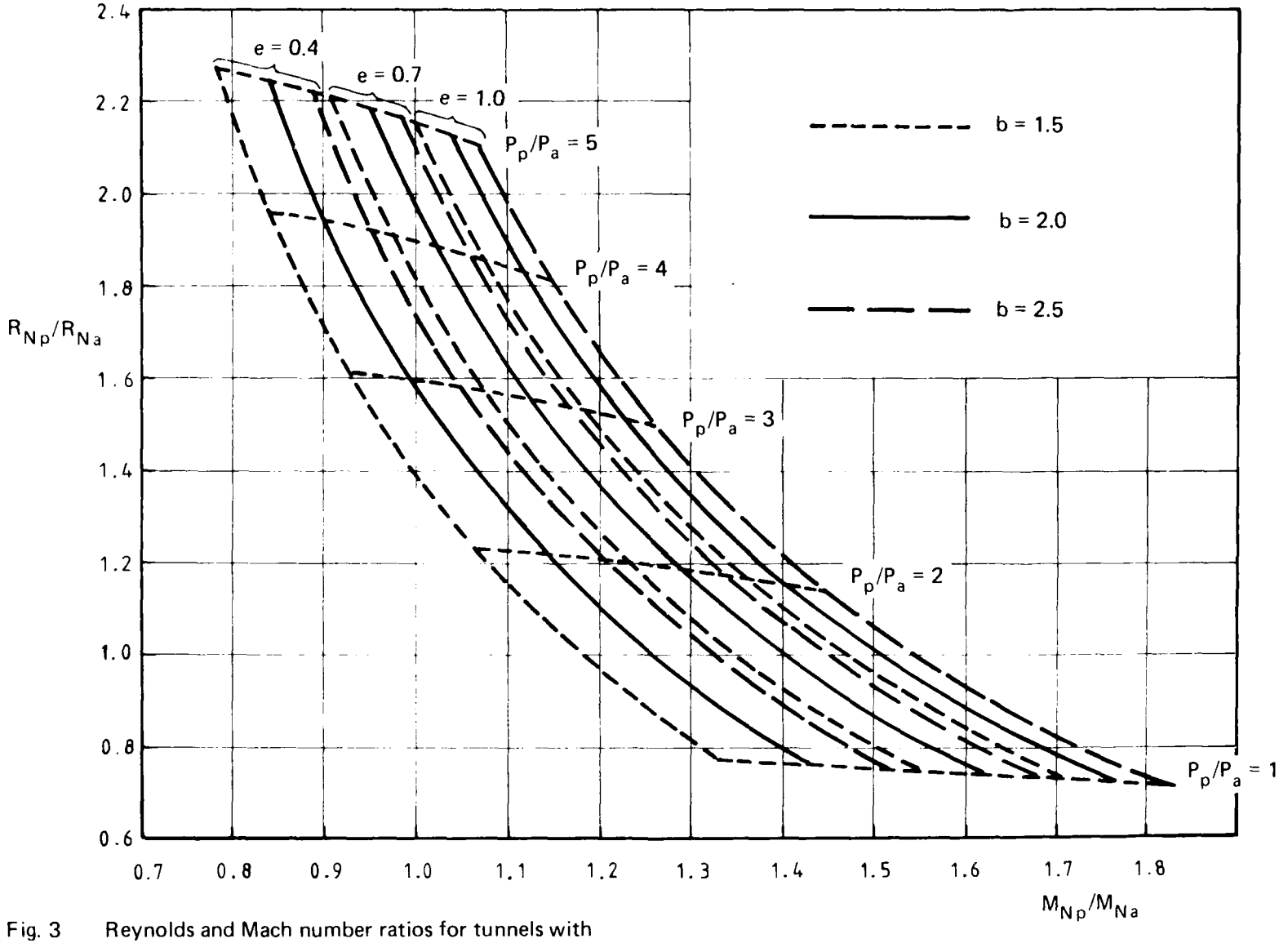


Fig. 3 Reynolds and Mach number ratios for tunnels with $C_p = C_a$, $N_p = N_a$, and various cost factors

(a) $(P_p/P_a)_D = 5$

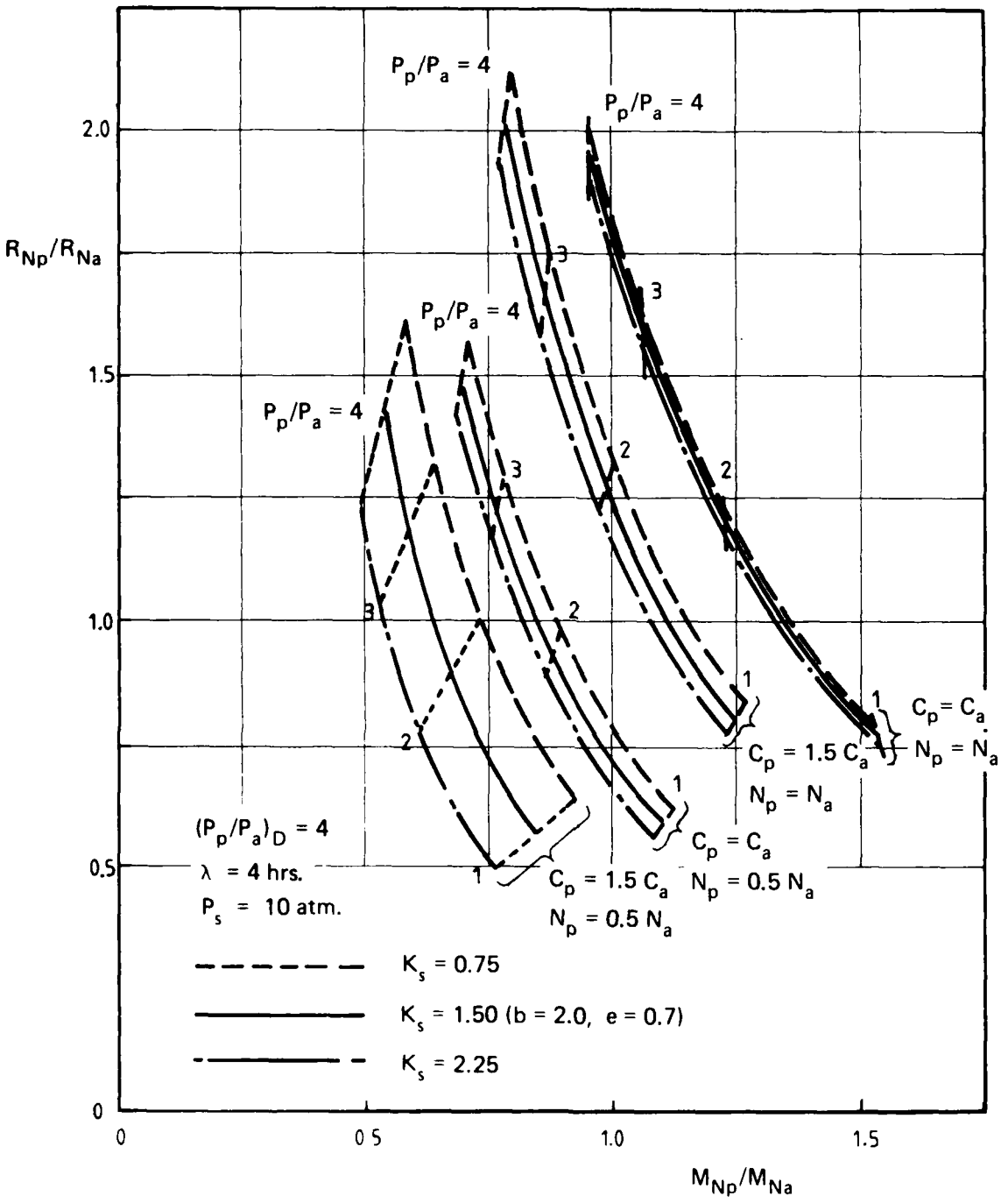


Fig. 13 Effect of changing relative stored air mass on Reynolds and Mach number ratios when $(P_p/P_a)_D = 4$, $P_s = 10$ atmosphere and $\lambda = 4$ hrs.

(a) $C_p = C_a$, and $C_p = 1.5\ C_a$

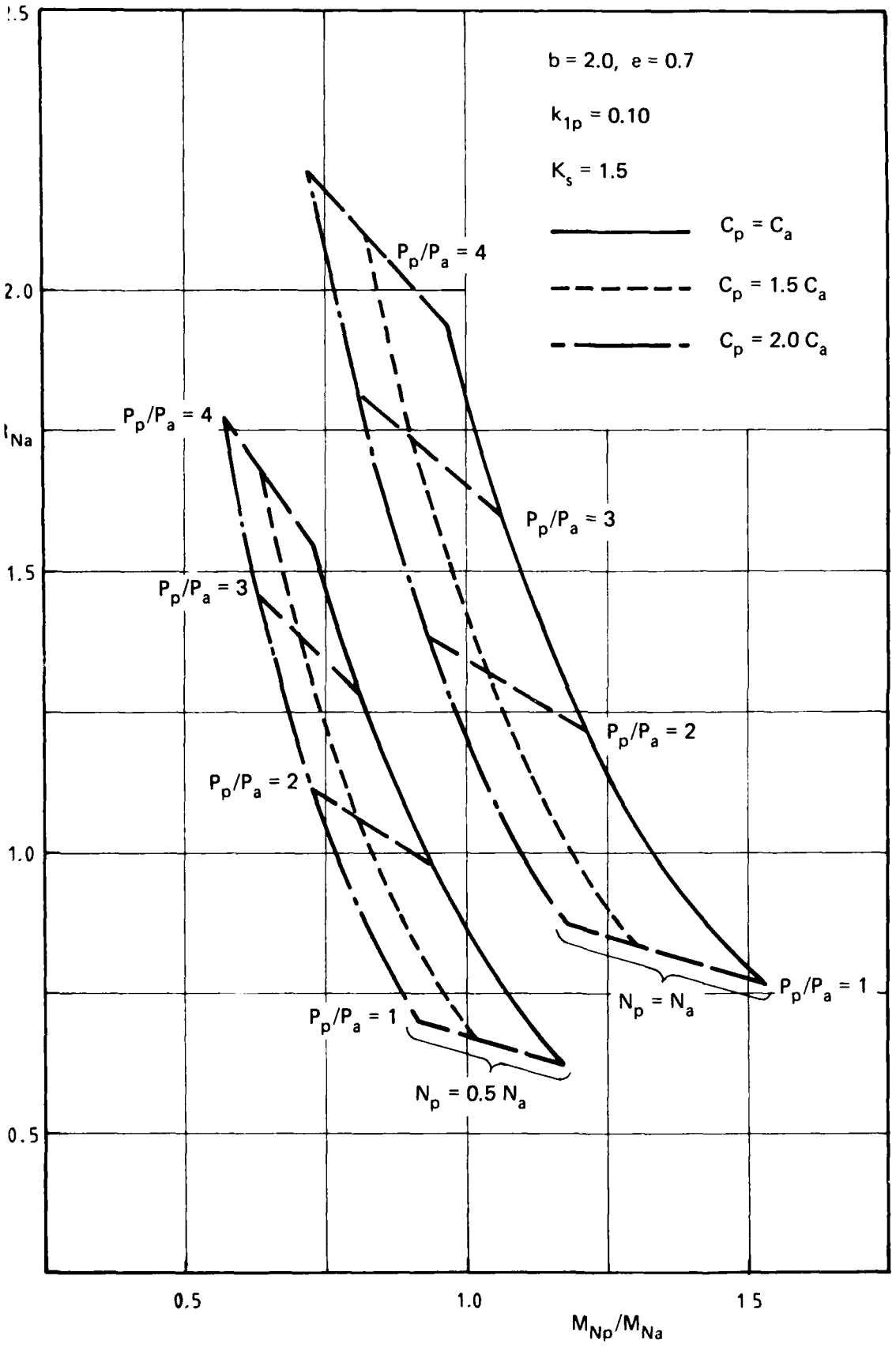


Fig. 12 Reynolds and Mach number ratios for various capital cost and power input ratios when $(P_p/P_a)_D = 4$ and $k_{1p} = 0.10$

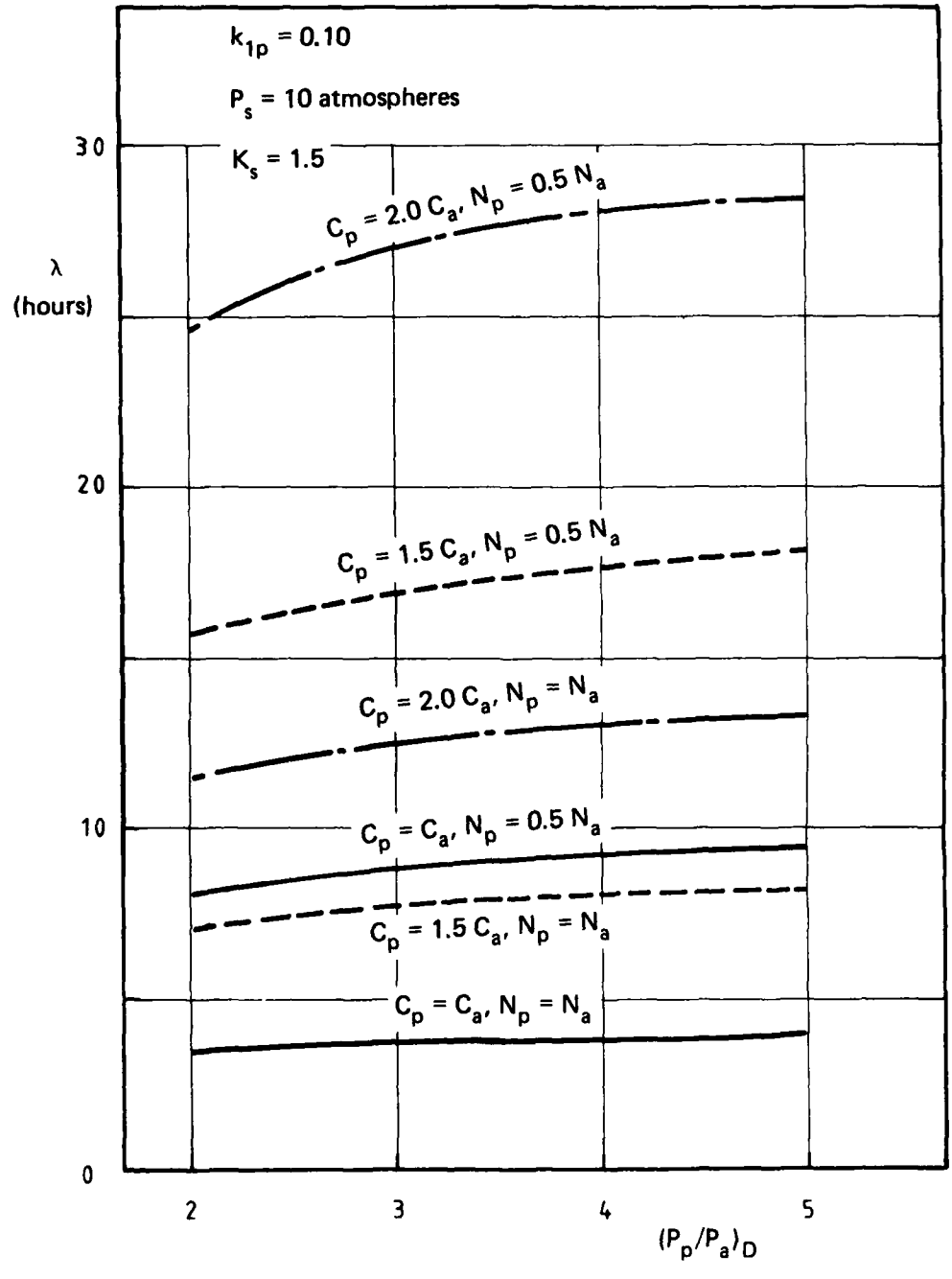


Fig. 11 Pressurisation time as a function of design pressure ratio for various cost and power input ratios when $k_{1p}$ = 0.10

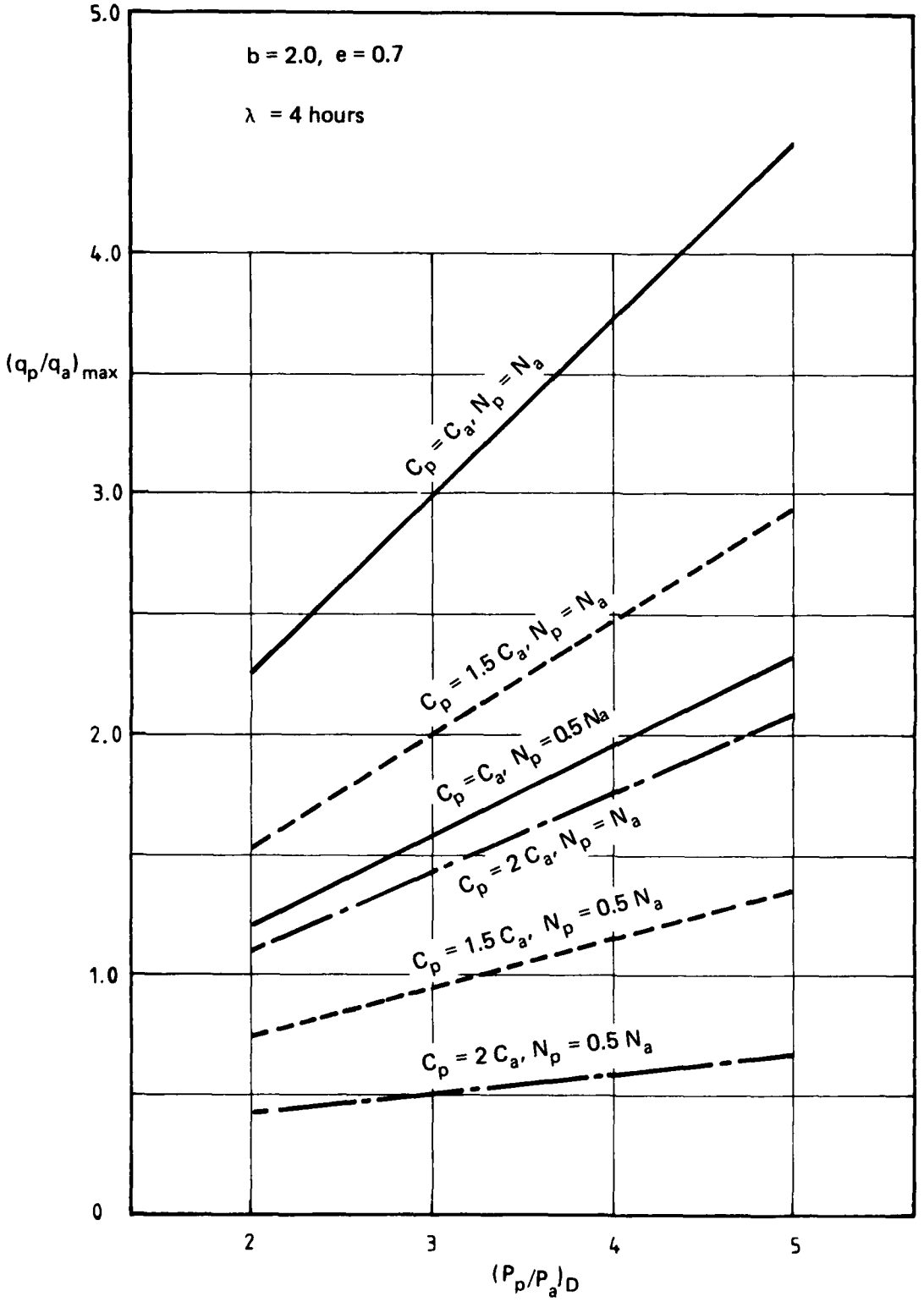


Fig. 10 Maximum dynamic pressure ratio as a function of tunnel design pressure ratio for various capital cost and power input ratios and a pressurisation time of 4 hours.

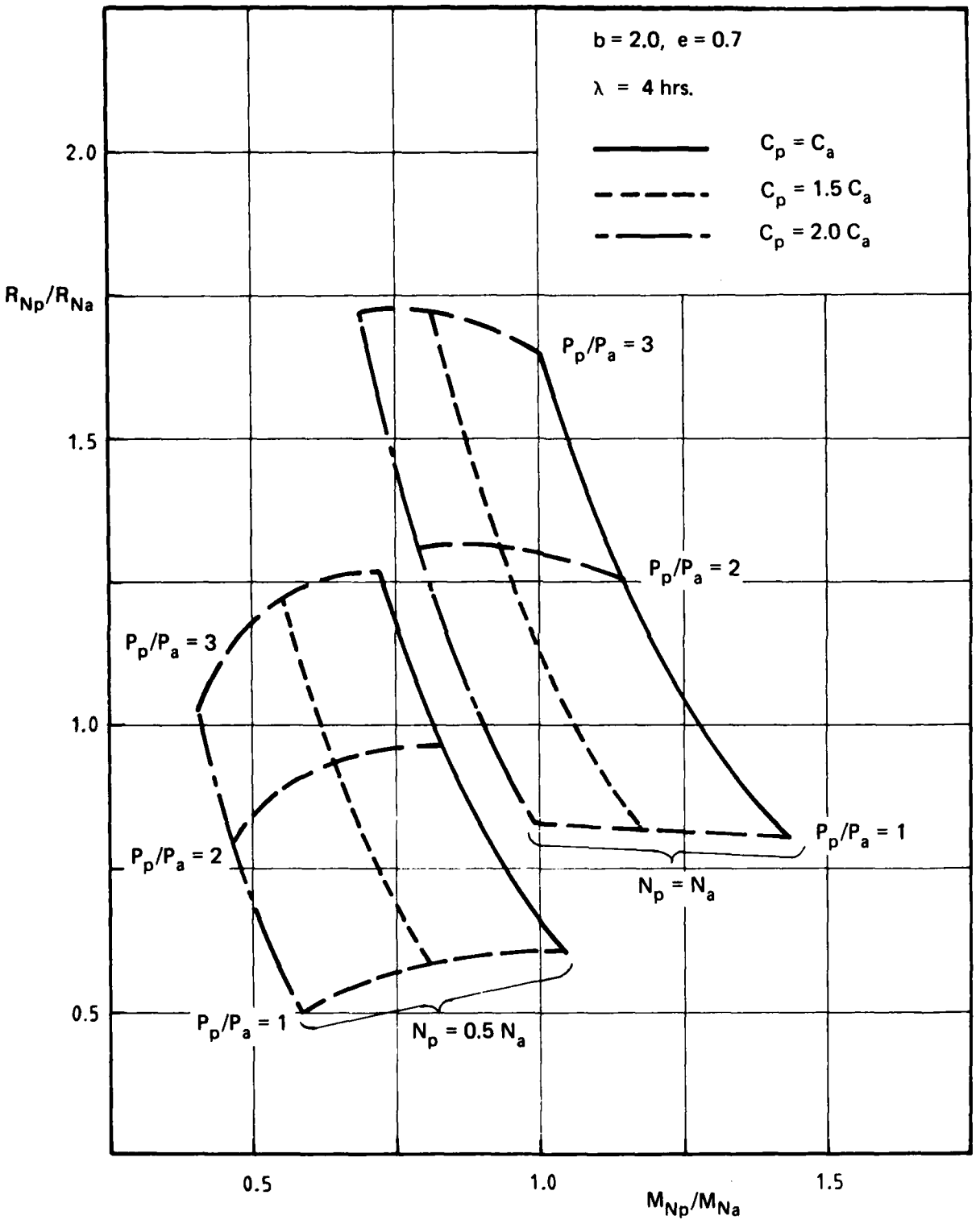


Fig. 9 (cont.)

(c) $(P_p/P_a)_D = 3$

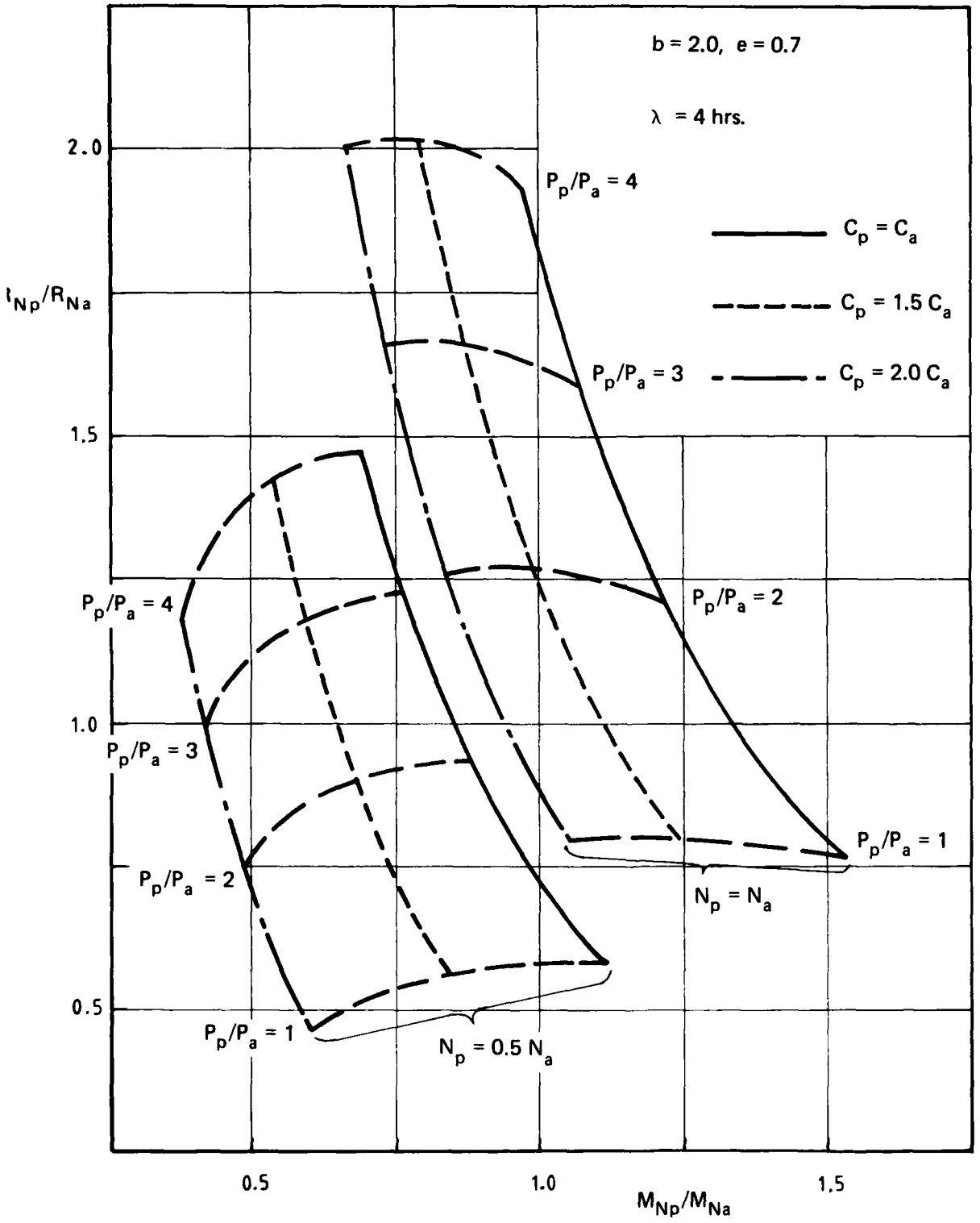


Fig. 9 (cont.)

(b) $(P_p/P_a)_D = 4$

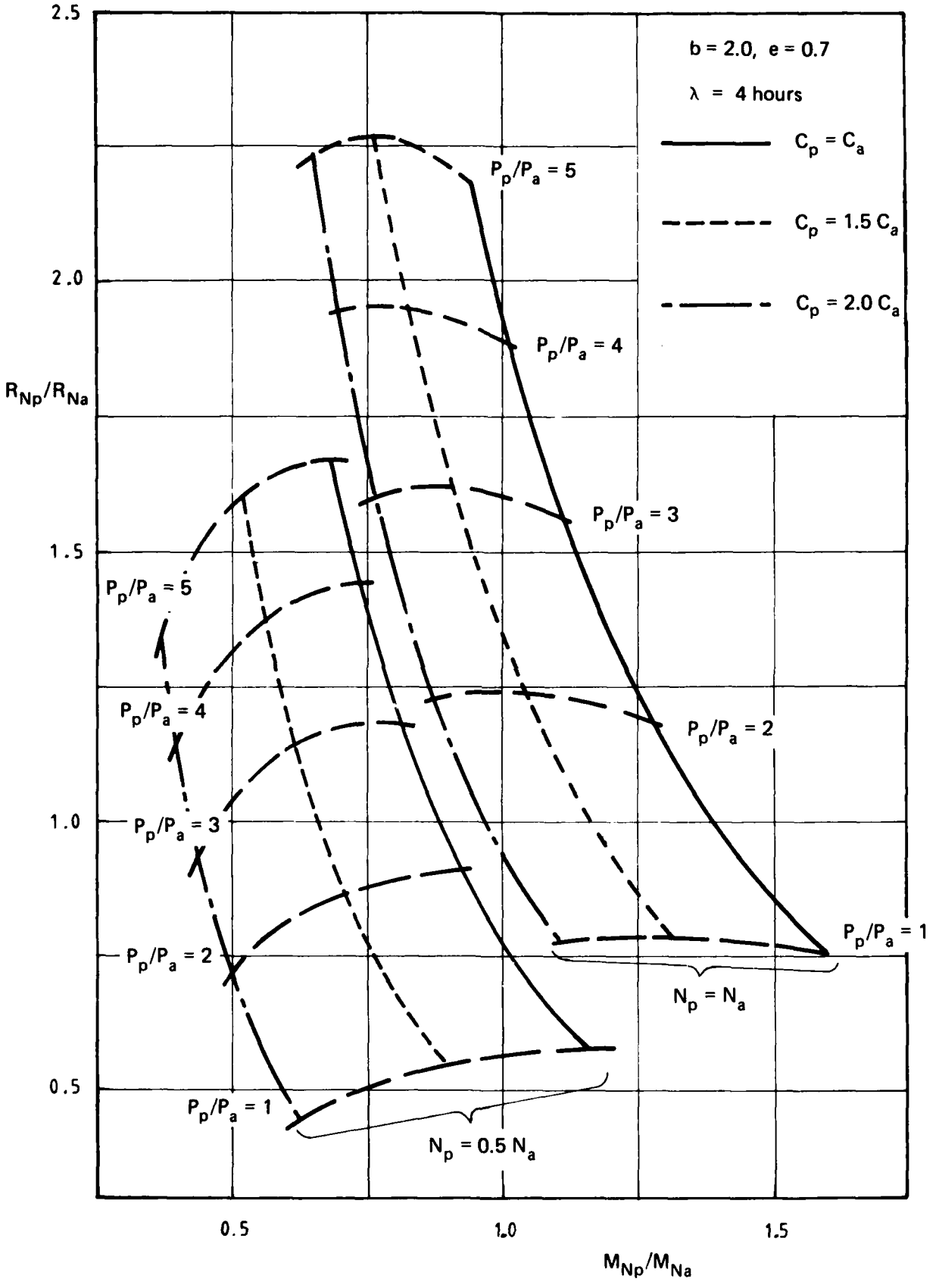


Fig. 9 Reynolds and Mach number ratios for various capital cost and power input ratios, and a pressurisation time of 4 hours.

(a) $(P_p/P_a)_D = 5$

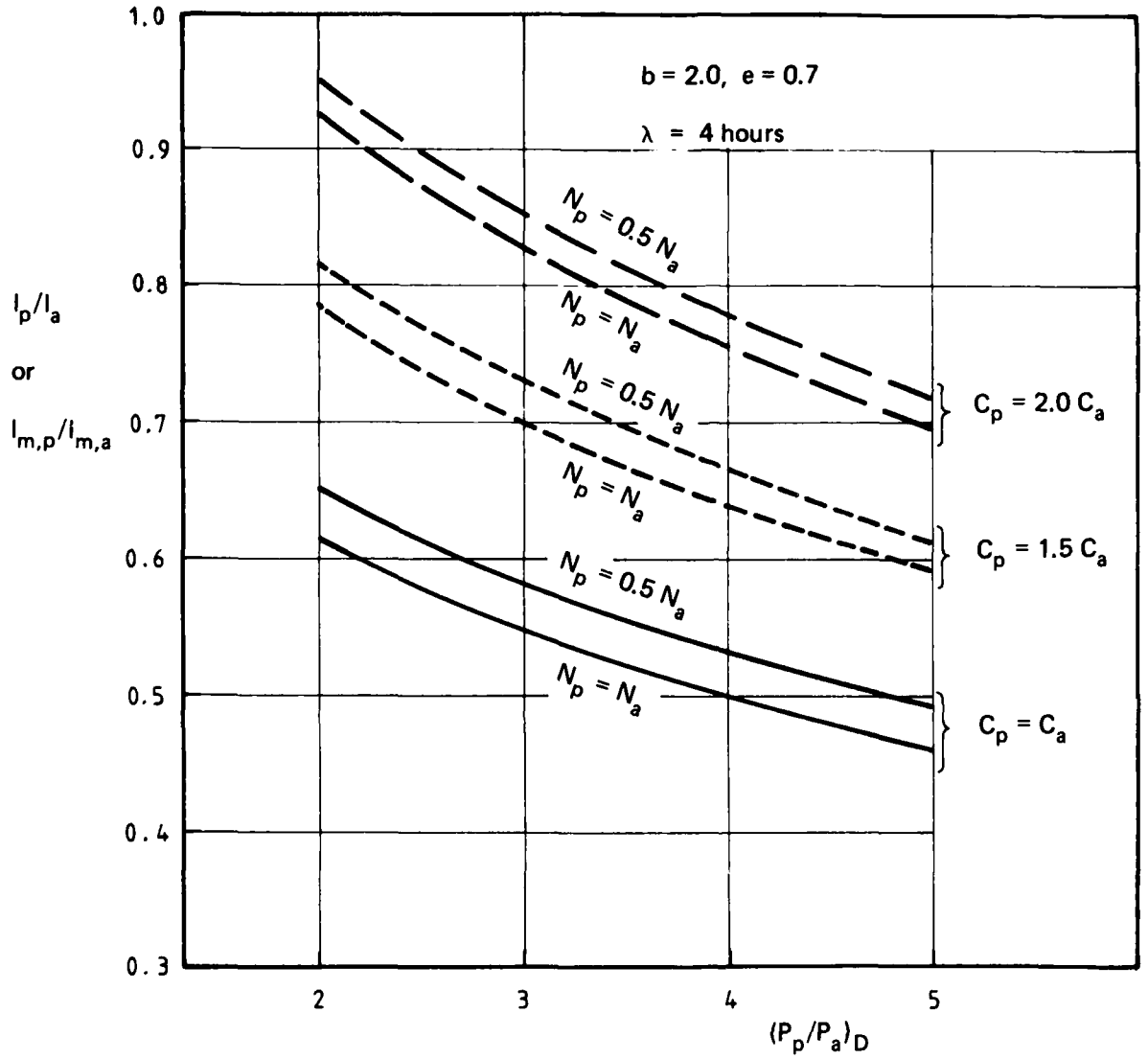


Fig. 8 Working section and model size ratios as a function of design pressure ratio for various capital cost and power input ratios.

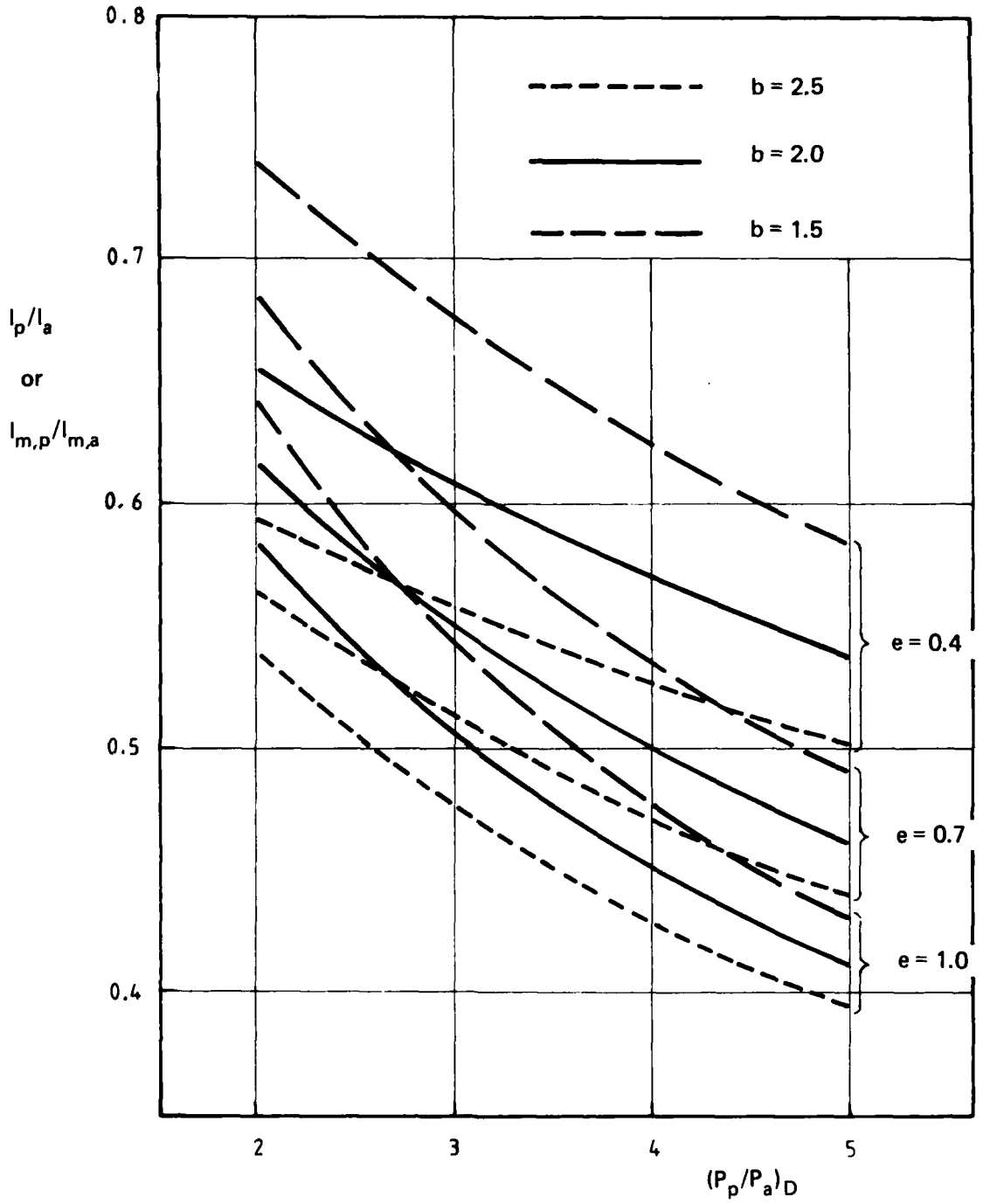


Fig. 7 Working section and model size ratios as a function of design pressure ratio for tunnels with various cost factors and $C_p = C_a$, and $N_p = N_a$.

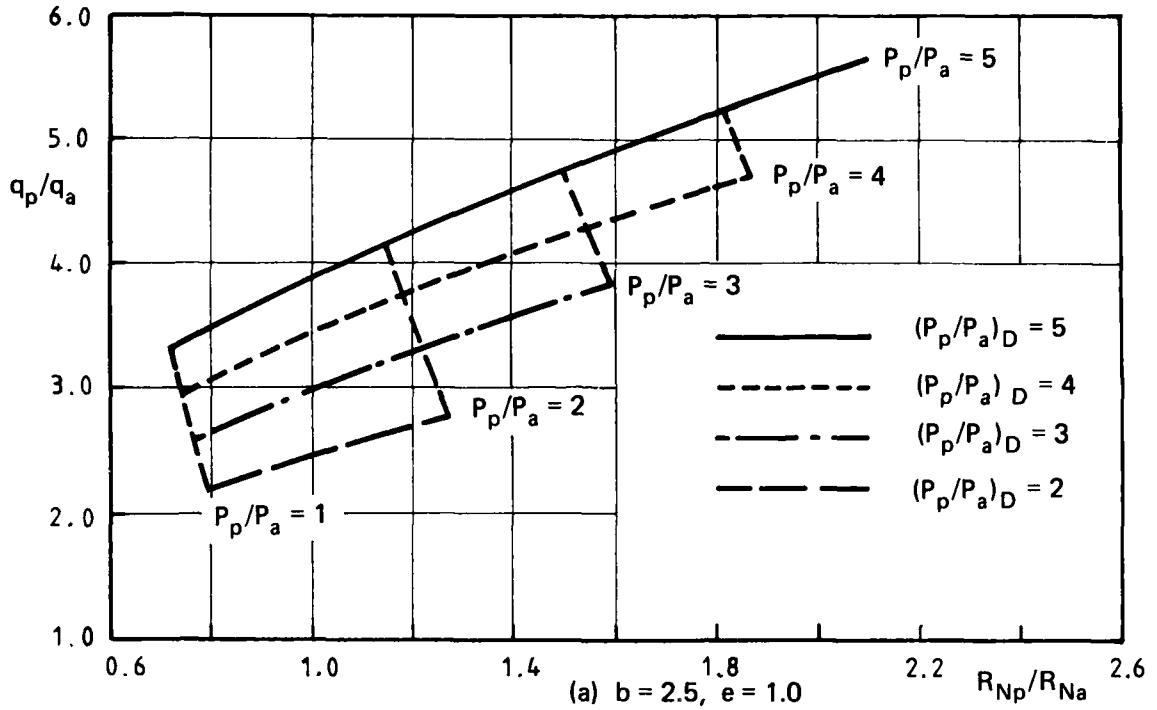


(a) b = 2.5, e = 1.0

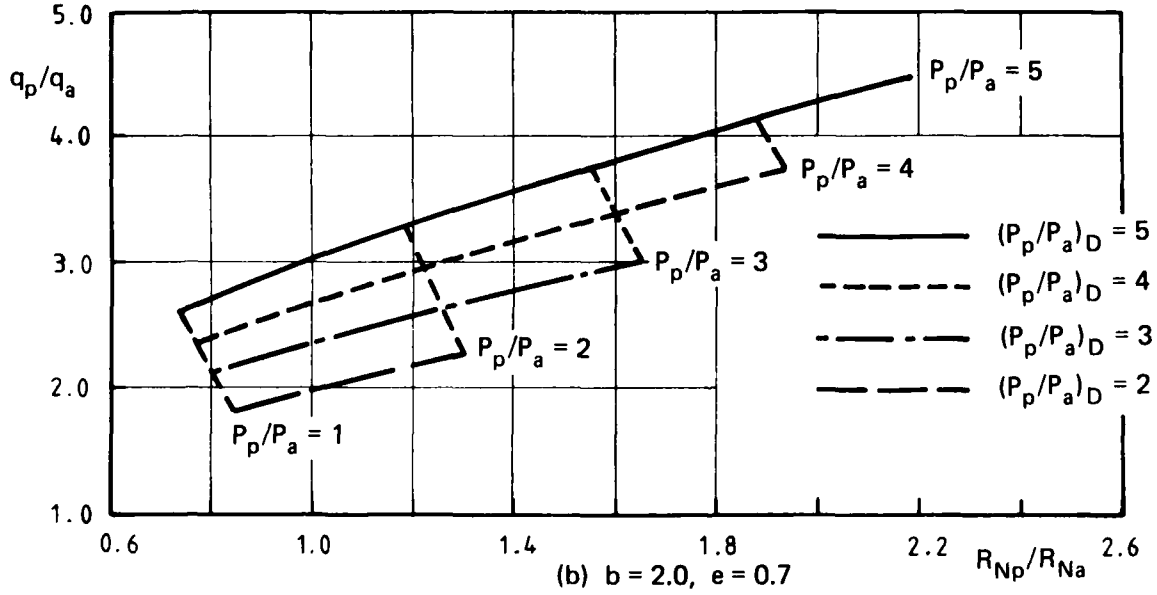


(b) b = 2.0, e = 0.7

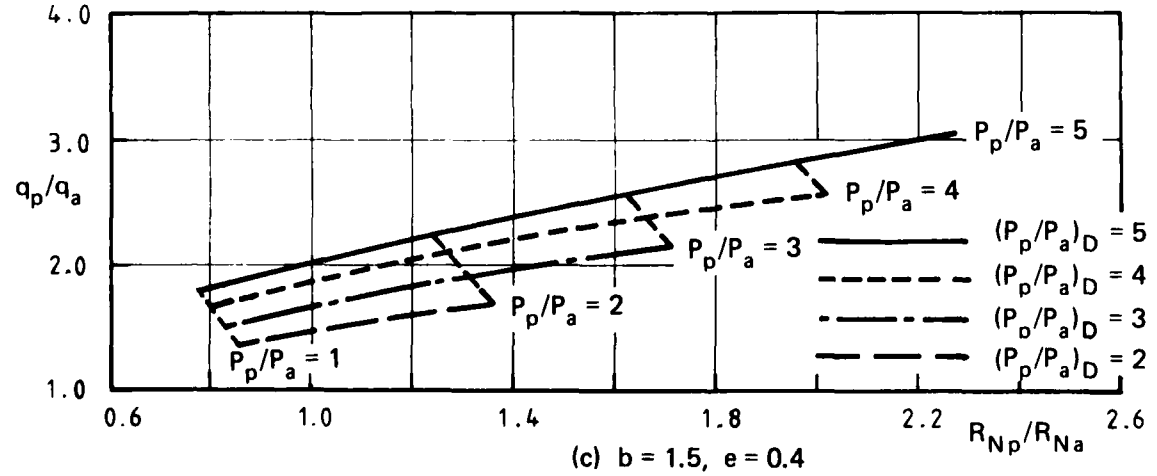


(c) b = 1.5, e = 0.4

Fig. 6 Dynamic pressure ratio as a function of Reynolds number ratio for tunnels with $C_p = C_a$, $N_p = N_a$, and design pressures of 2, 3, 4 and 5 atmospheres.

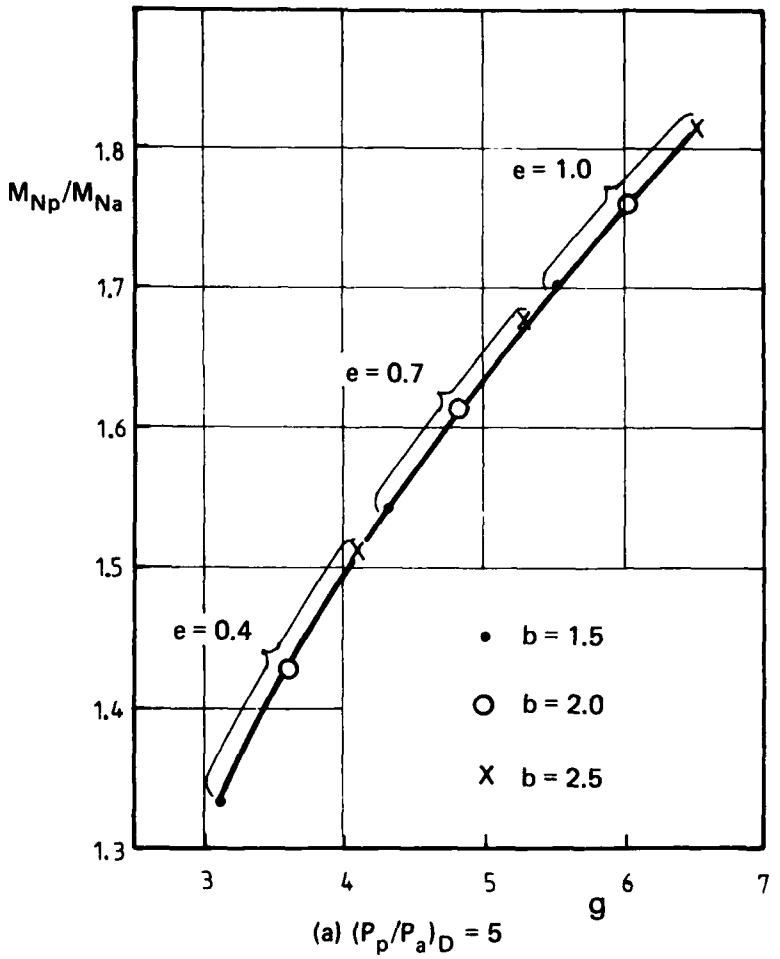


(a) $(P_p/P_a)_D = 5$

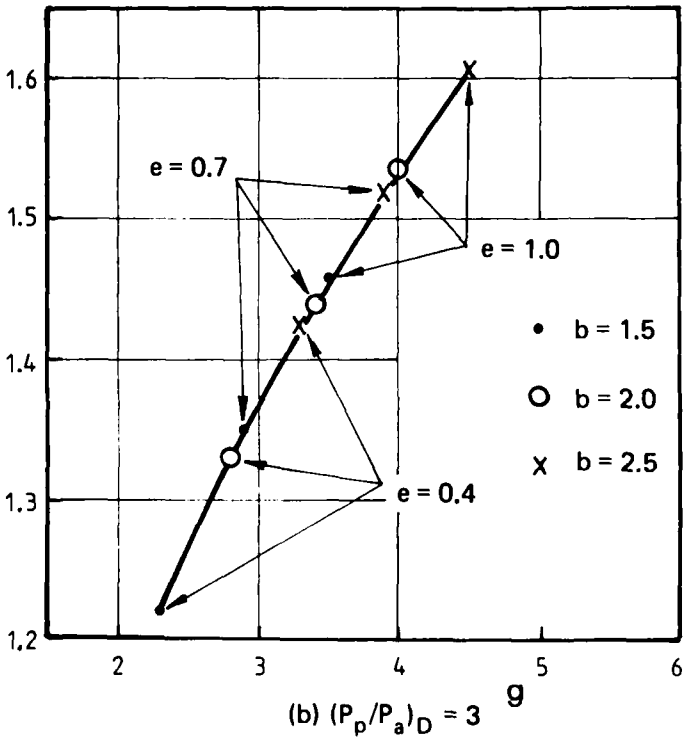


(b) $(P_p/P_a)_D = 3$

Fig. 5 Maximum Mach number ratio as a function of cost factor for tunnels with $C_p = C_a$, $N_p = N_a$, and design pressures of 2, 3, 4 and 5 atmospheres.

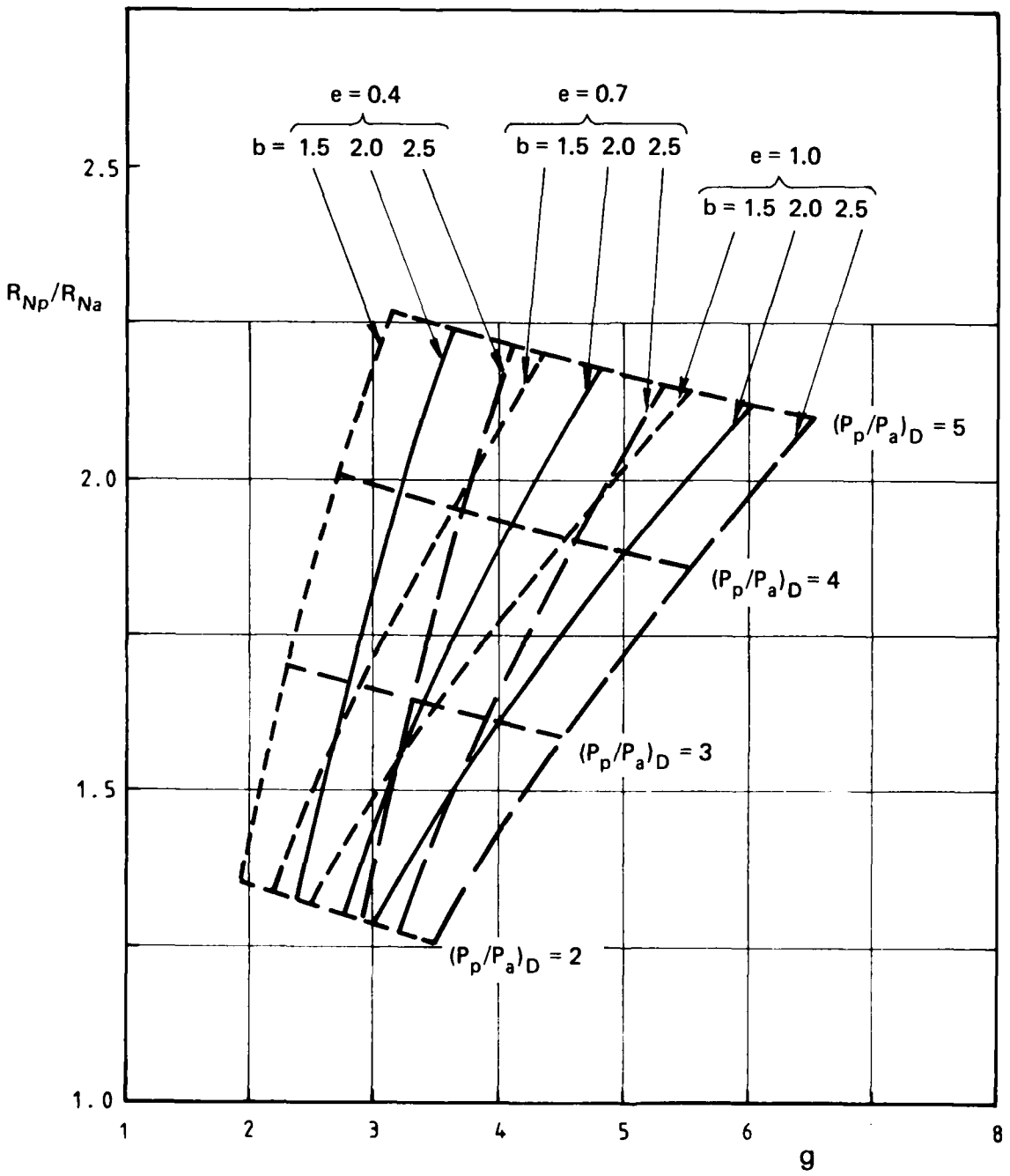


Fig. 4 Maximum Reynolds number ratio as a function of cost factor for tunnels with $C_p = C_a$, $N_p = N_a$, and design pressures of 2, 3, 4 and 5 atmospheres.

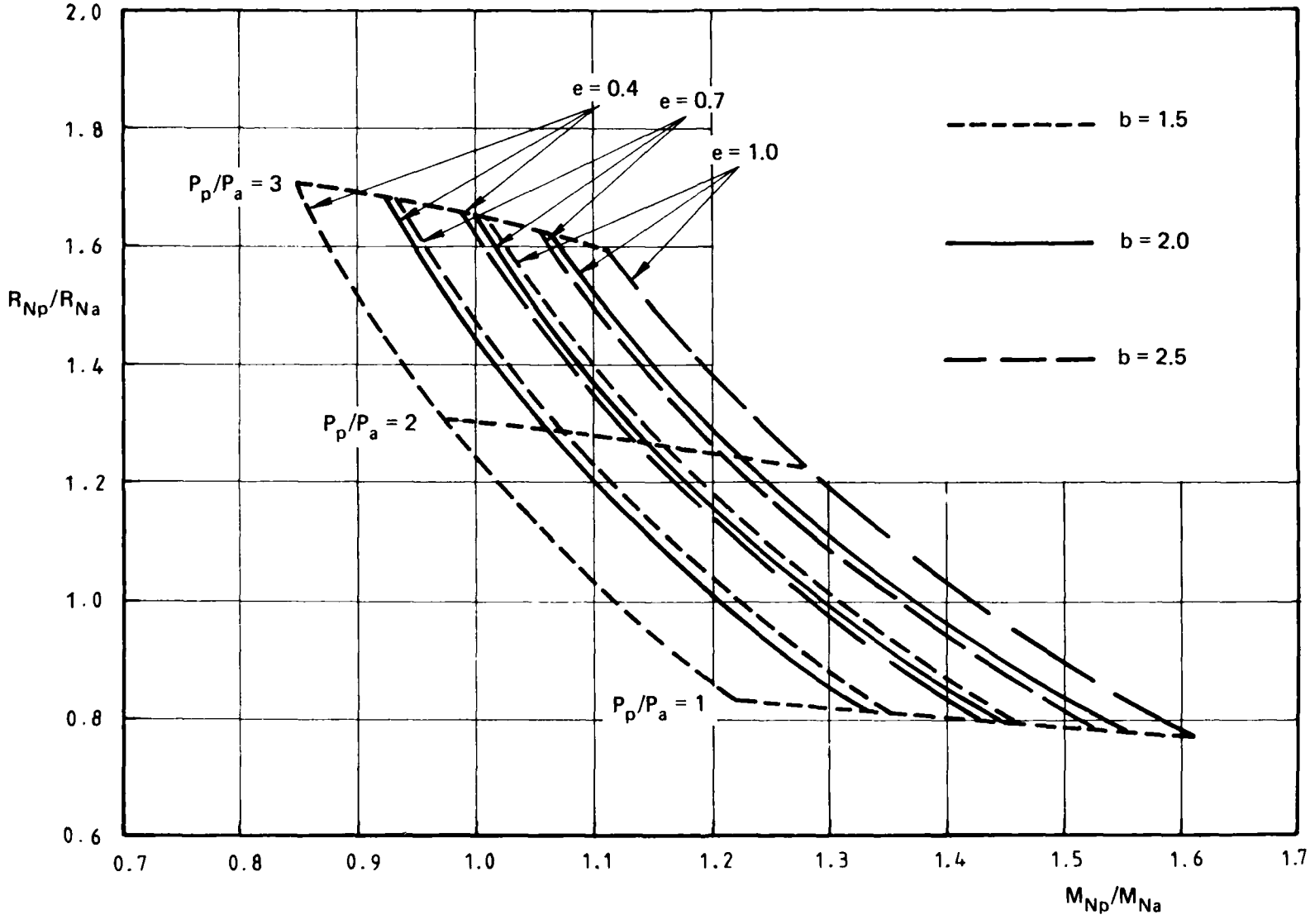


Fig. 3 (cont.)

(c) $(P_p/P_a)_D = 3$

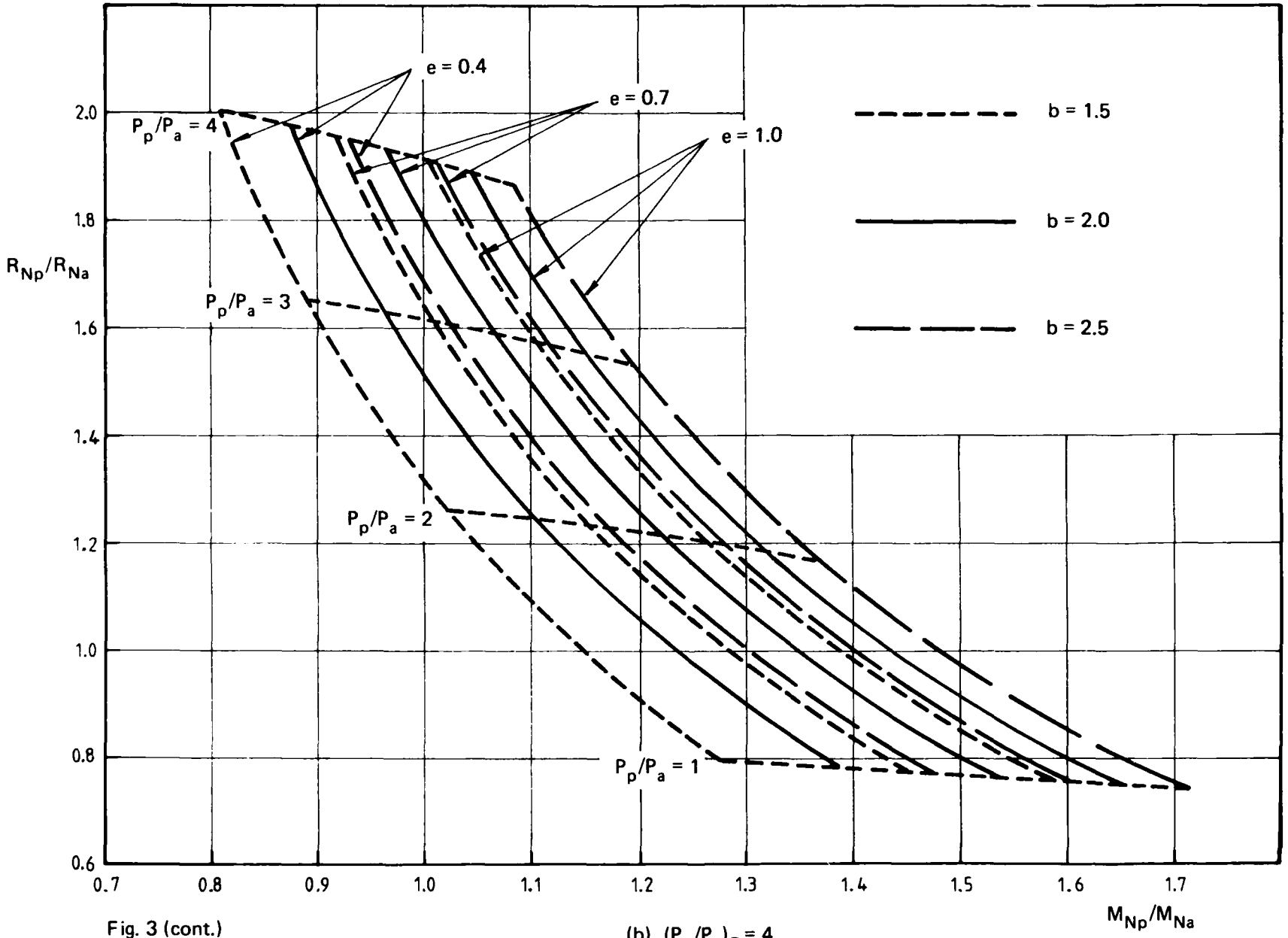


Fig. 3 (cont.)

(b) $(P_p/P_a)_D = 4$

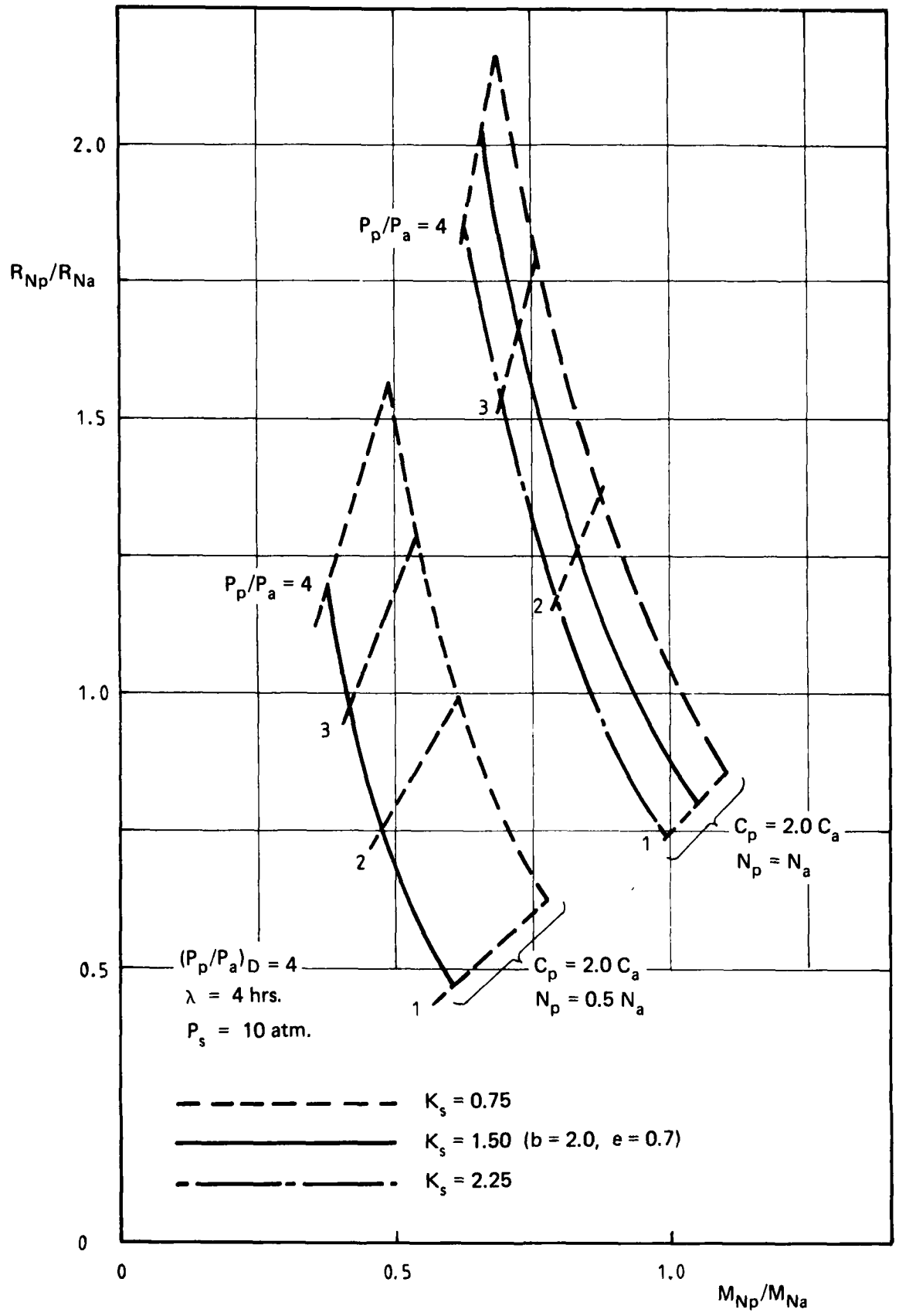


Fig. 13 (cont.)

(b) $C_p = 2.0\ C_a$

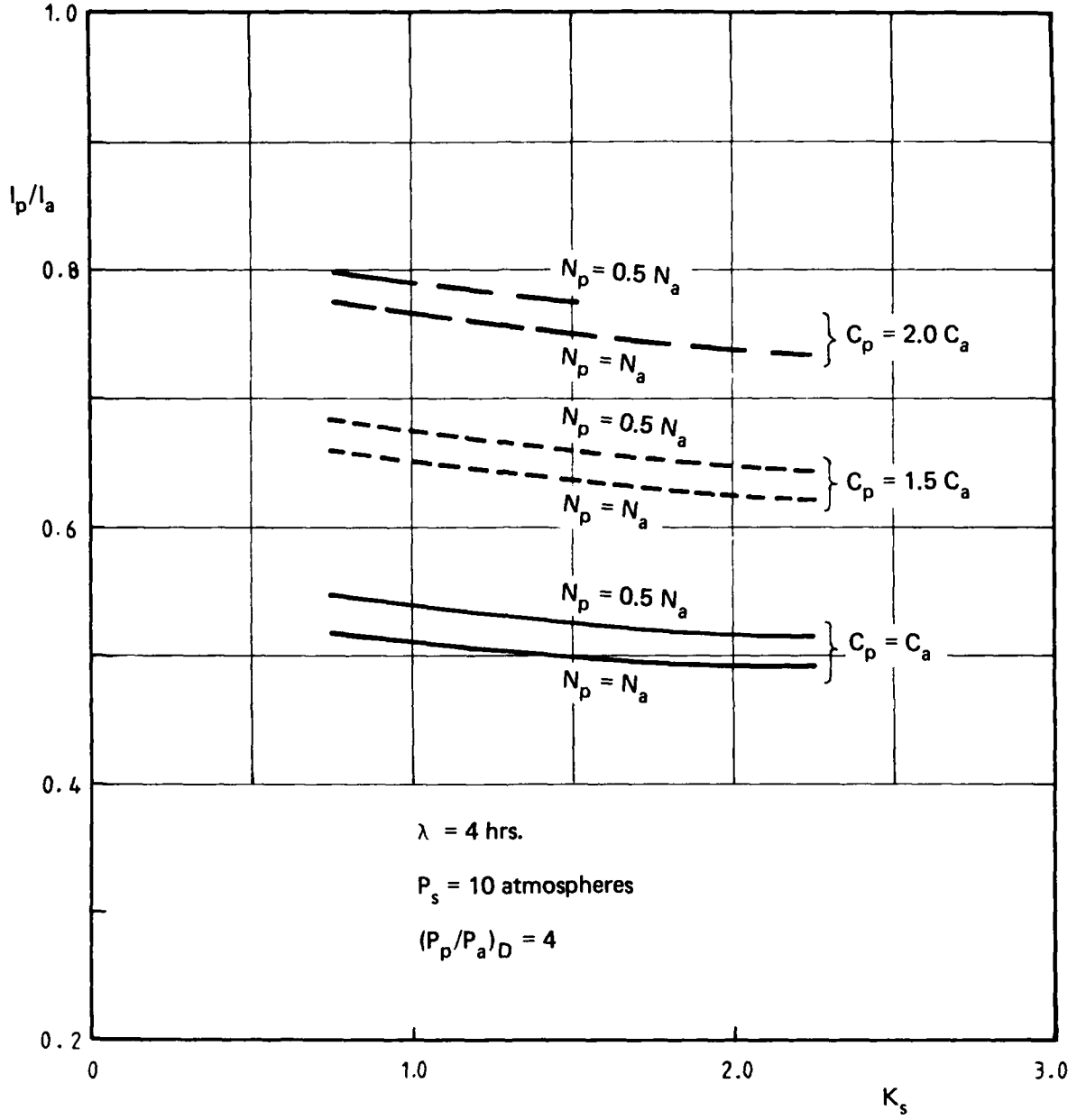


Fig. 14 Effect of changing relative stored air mass on tunnel size when $(P_p/P_a)_D = 4$, $P_s = 10$ atmospheres, and $\lambda = 4$ hours.

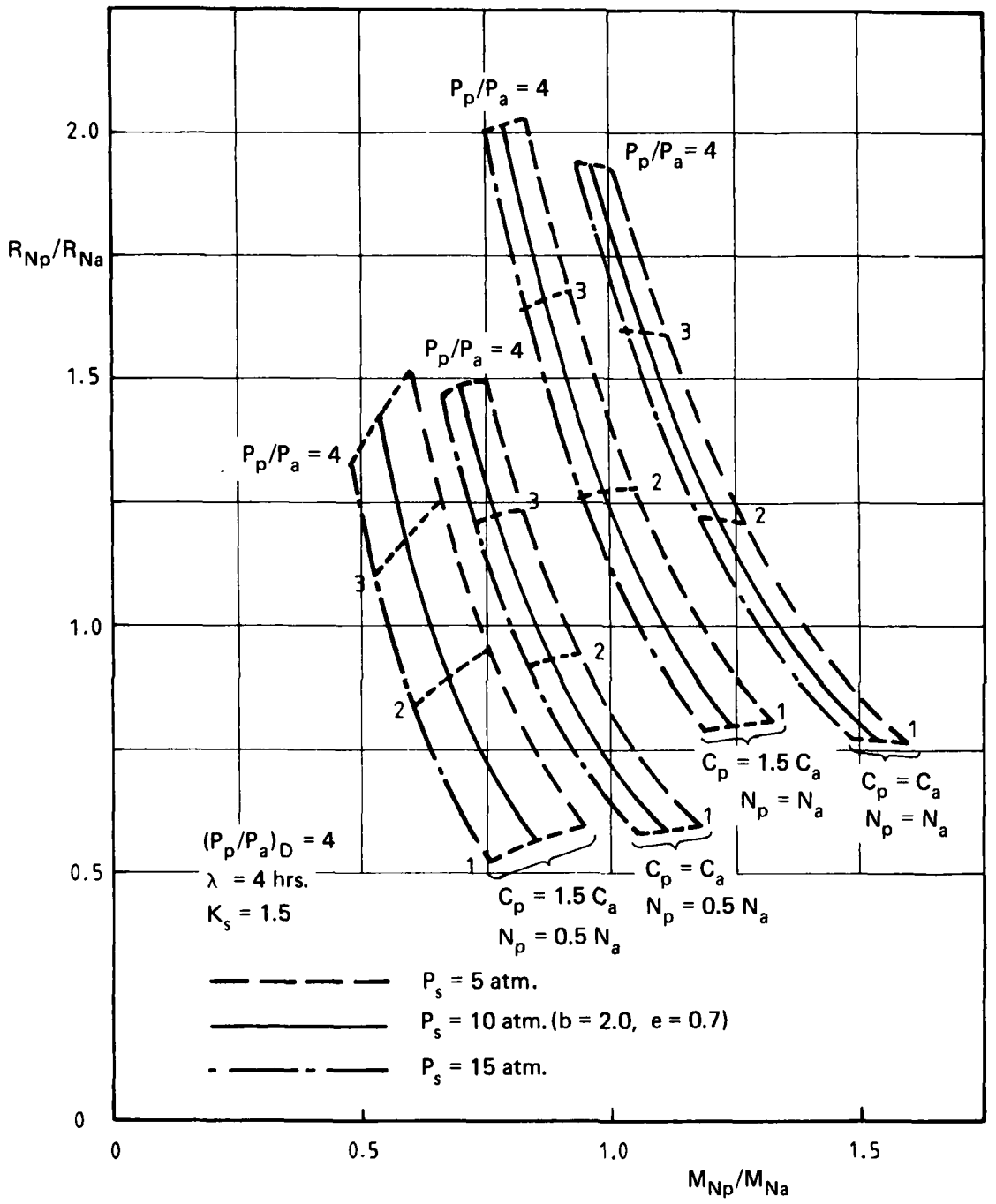


Fig. 15 Effect of changing air storage pressure on Reynolds and Mach number ratios when $(P_p/P_a)_D = 4$, $K_s = 1.5$ and $\lambda = 4$ hrs.

(a) $C_p = C_a$, and $C_p = 1.5\ C_a$

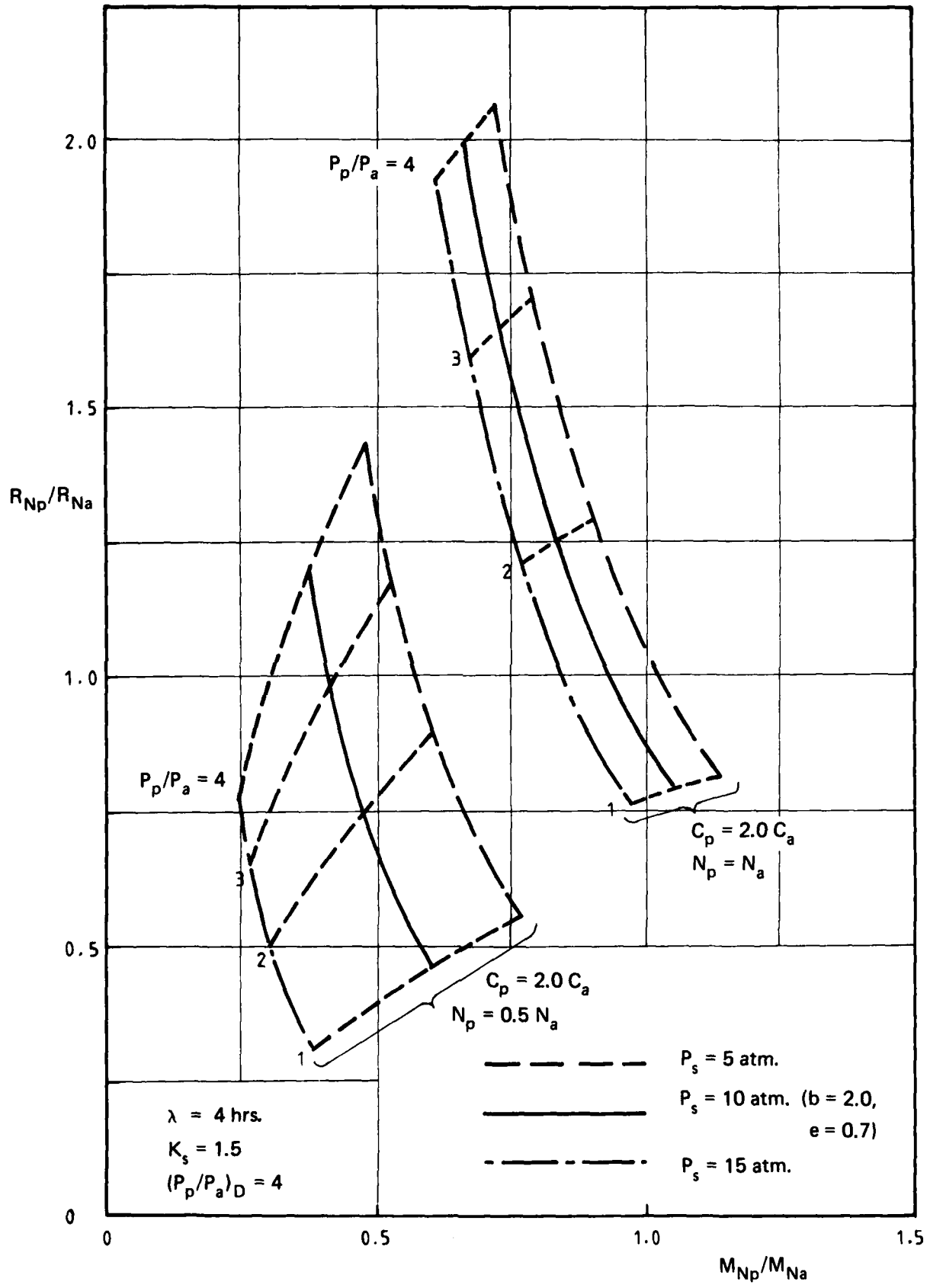


Fig. 15 (cont.)

(b) $C_p = 2.0\ C_a$

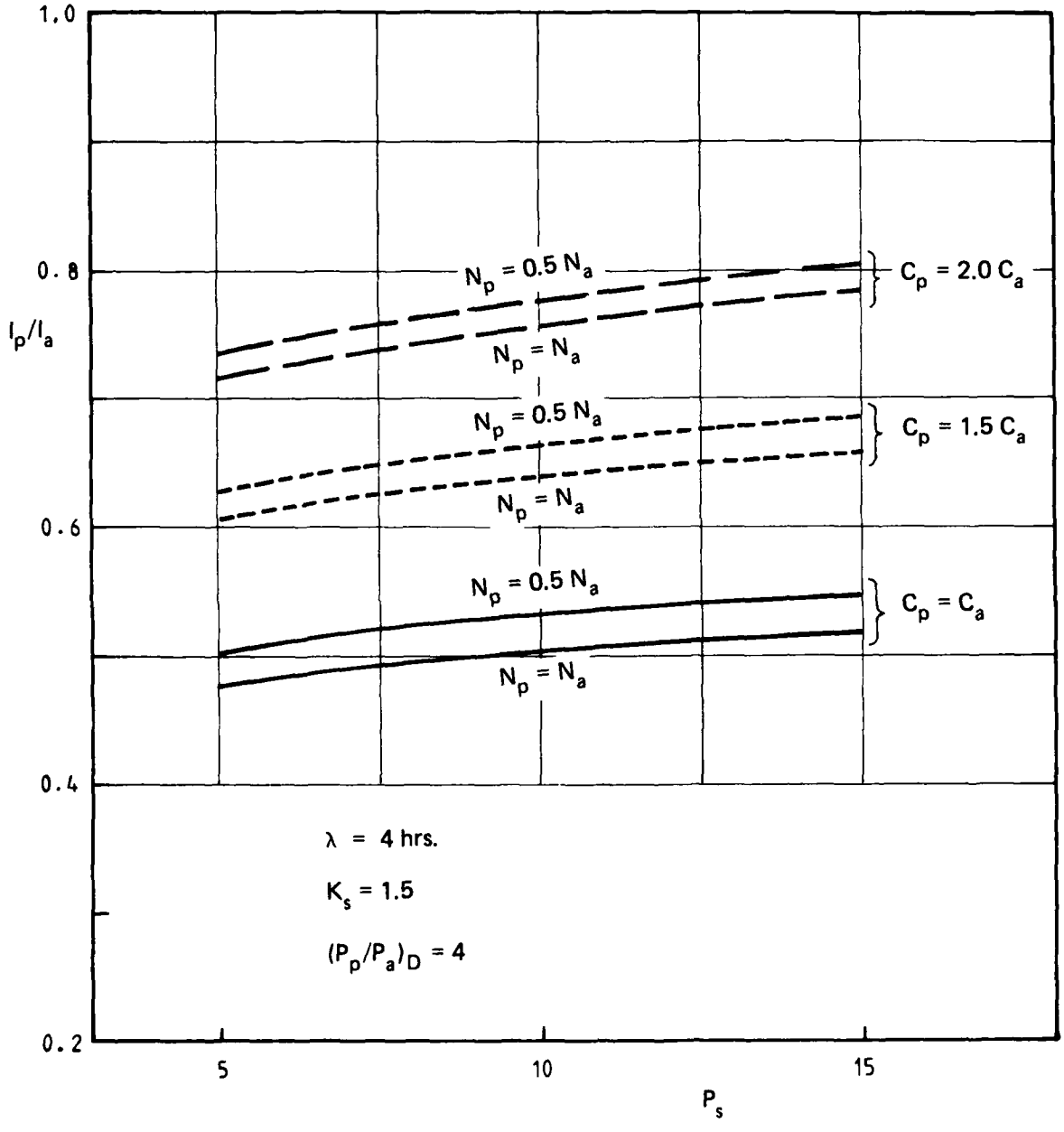


Fig. 16 Effect of changing air storage pressure on tunnel size when $(P_p/P_a)_D = 4$, $P_s = 10$ atmospheres, and $\lambda = 4$ hours.

(a) Single strut mount

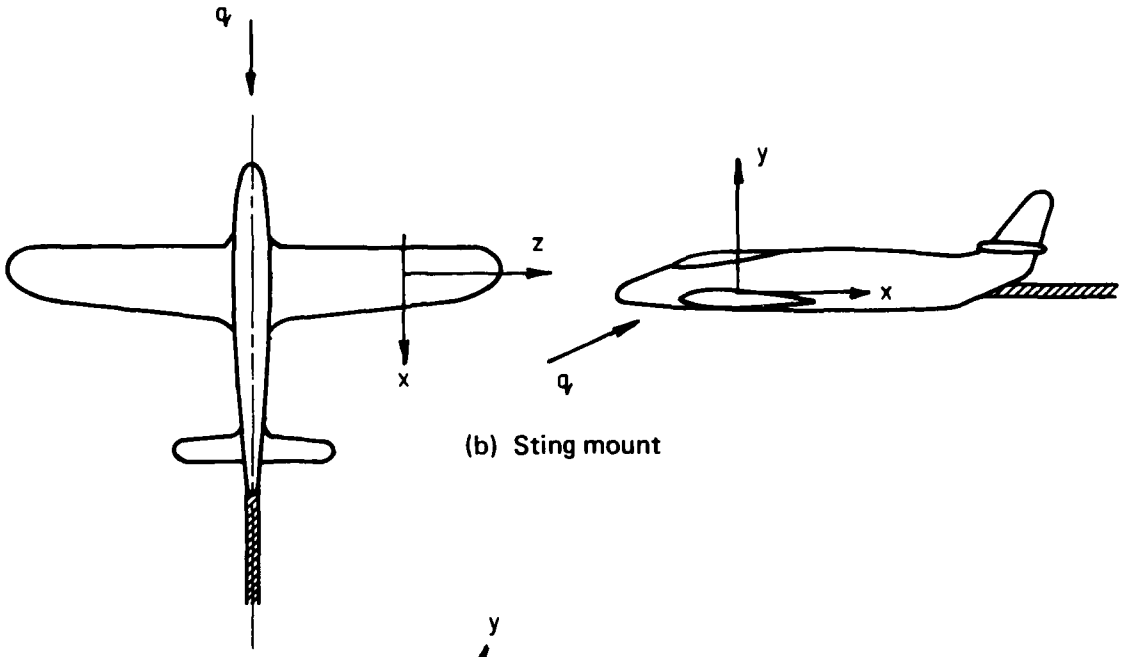


(b) Sting mount

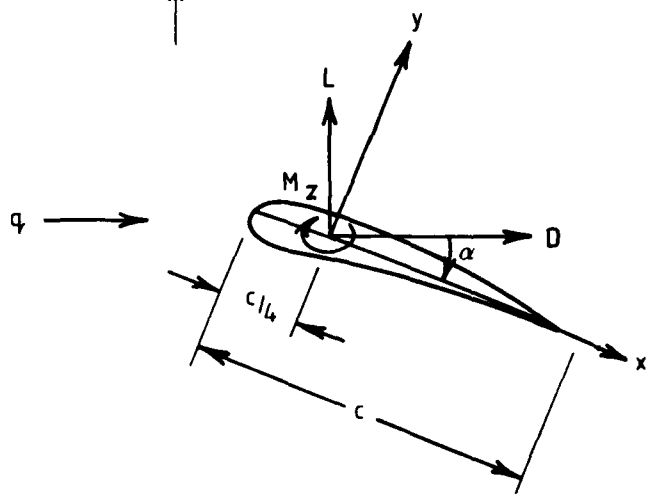


(c) Forces and moments acting at wing section in x–y plane

Fig. 17 Forces and moments acting at a section of a wing of an aircraft model mounted on either a single strut or a sting.

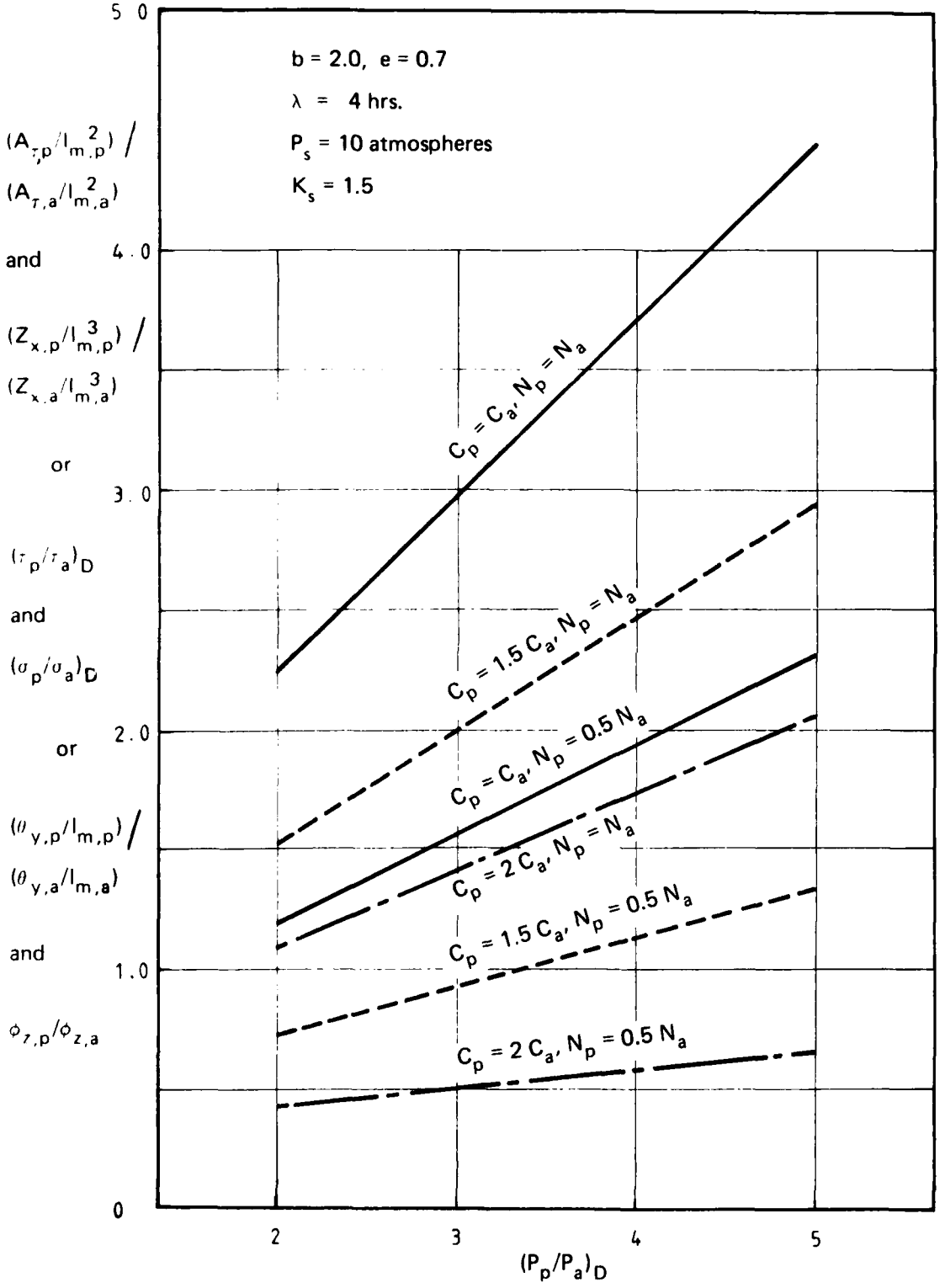


Fig. 18 Relative section area, section modulus, stress, and deflection of a model tested in an atmospheric and pressurised wind tunnel.

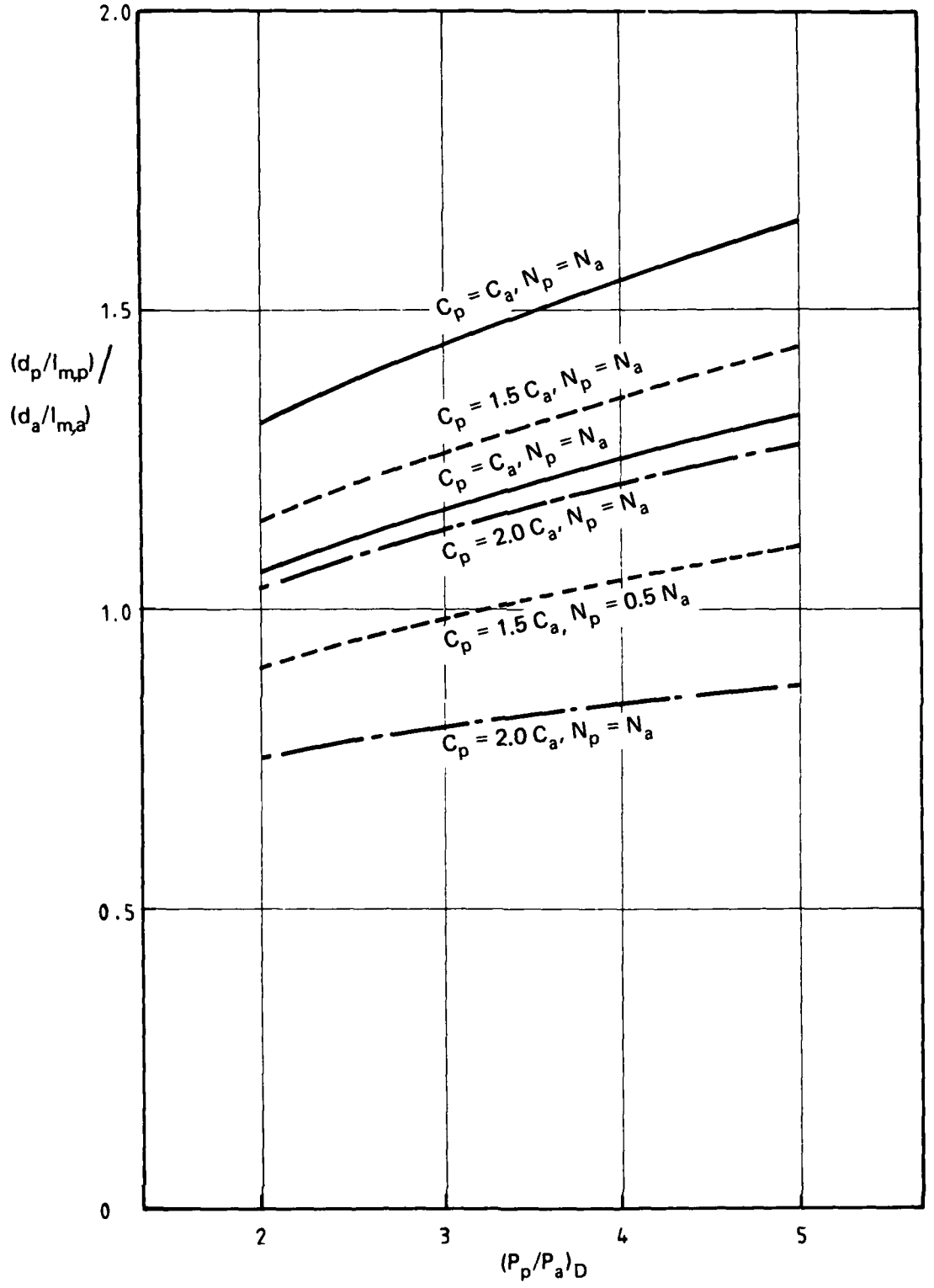


Fig. 19 Relative diameter of model mounting stings made from materials with the same design stress.

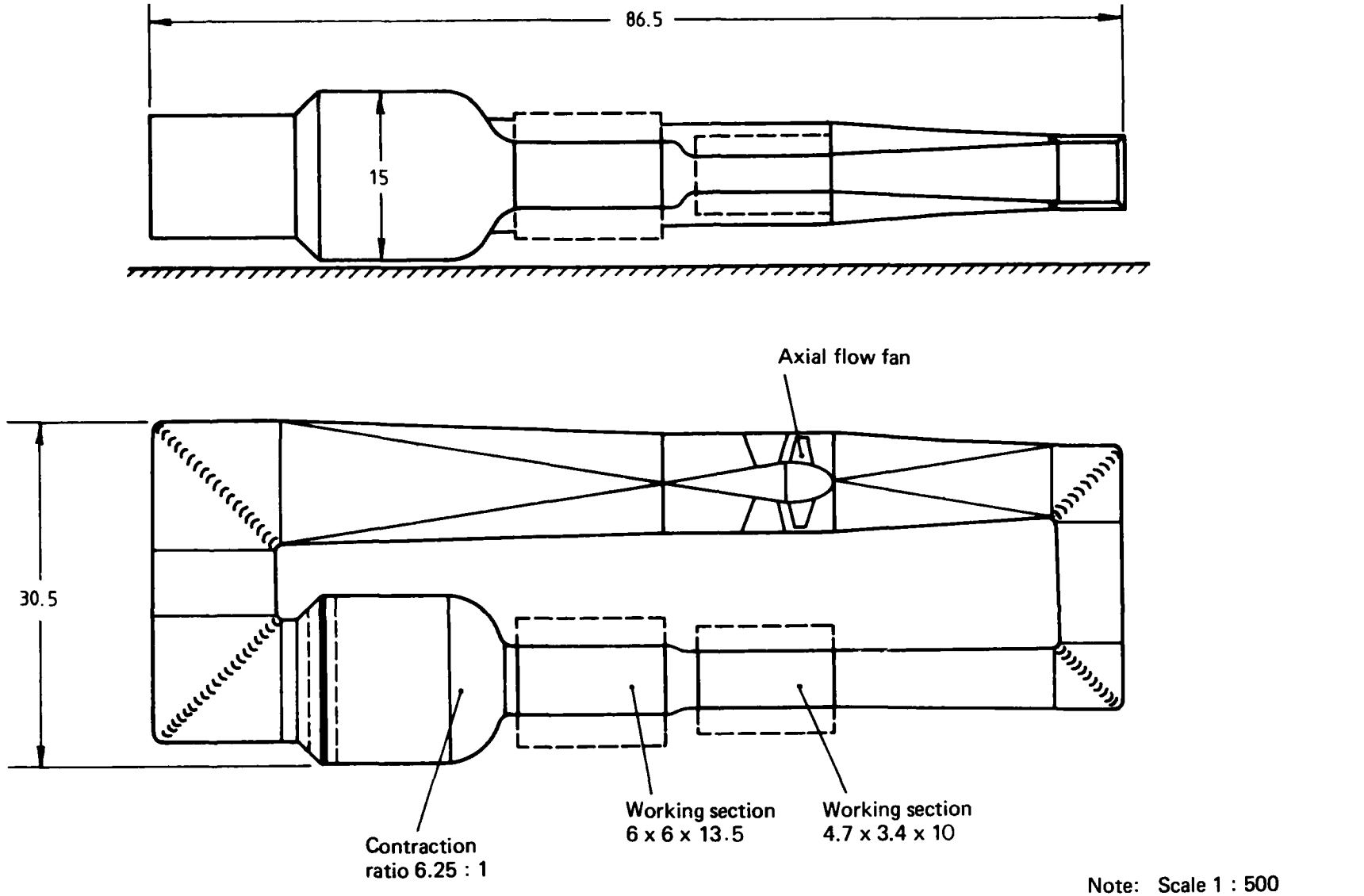


Note: Scale 1 : 500
Dimensions in metres

Fig. 20 Projected ARL atmospheric pressure low speed wind tunnel (ref. 1)

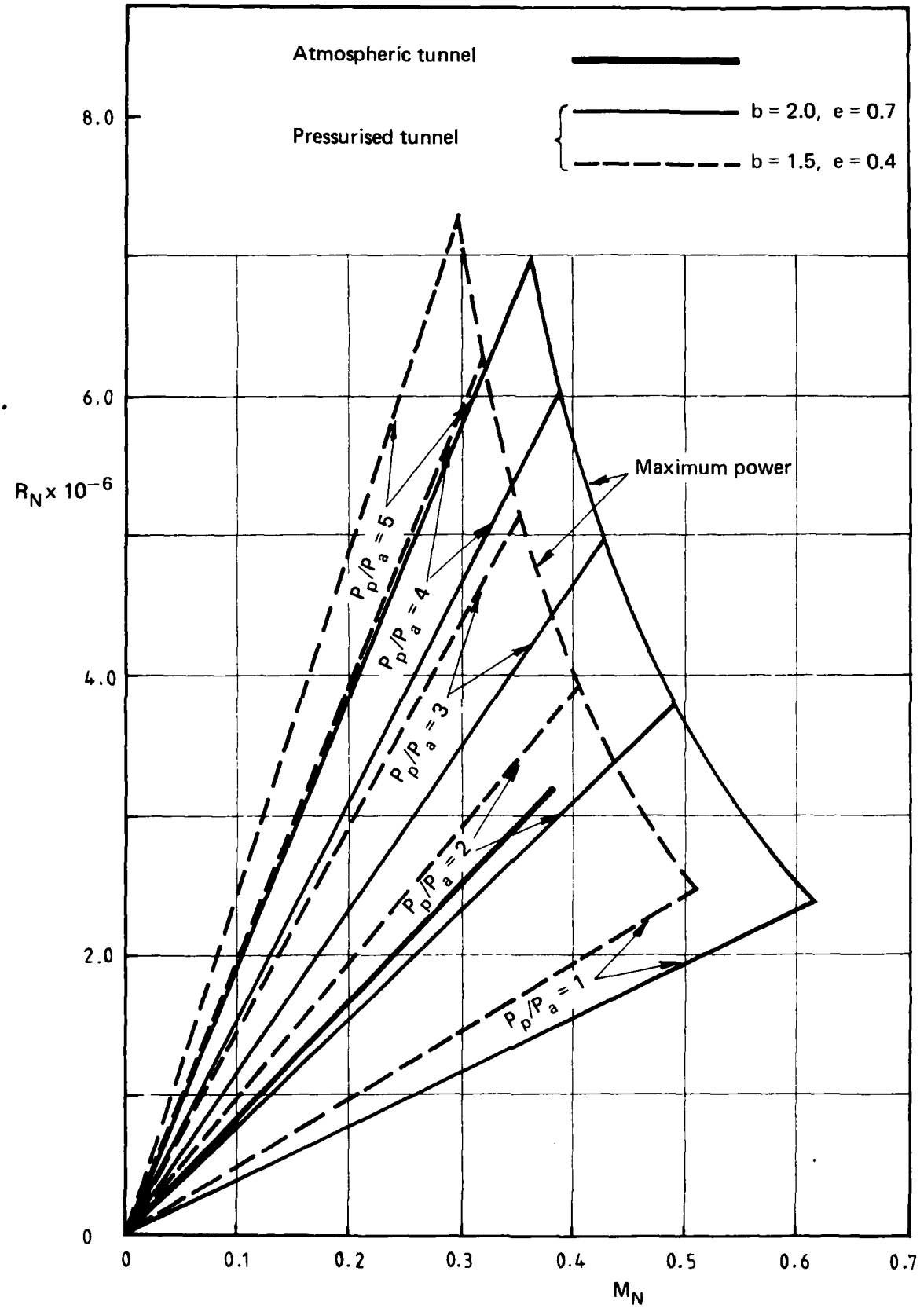


Fig. 21 Reynolds and Mach number test envelope based on a length scale of $0.1\,(A)^{1/2}$ for the 4.7m x 3.4m atmospheric tunnel and for similar pressurised tunnels with $C_p = C_a$, $N_p = N_a$, and design pressures of 2, 3, 4 and 5 atmospheres.

(a) $(P_p/P_a)_D = 5$

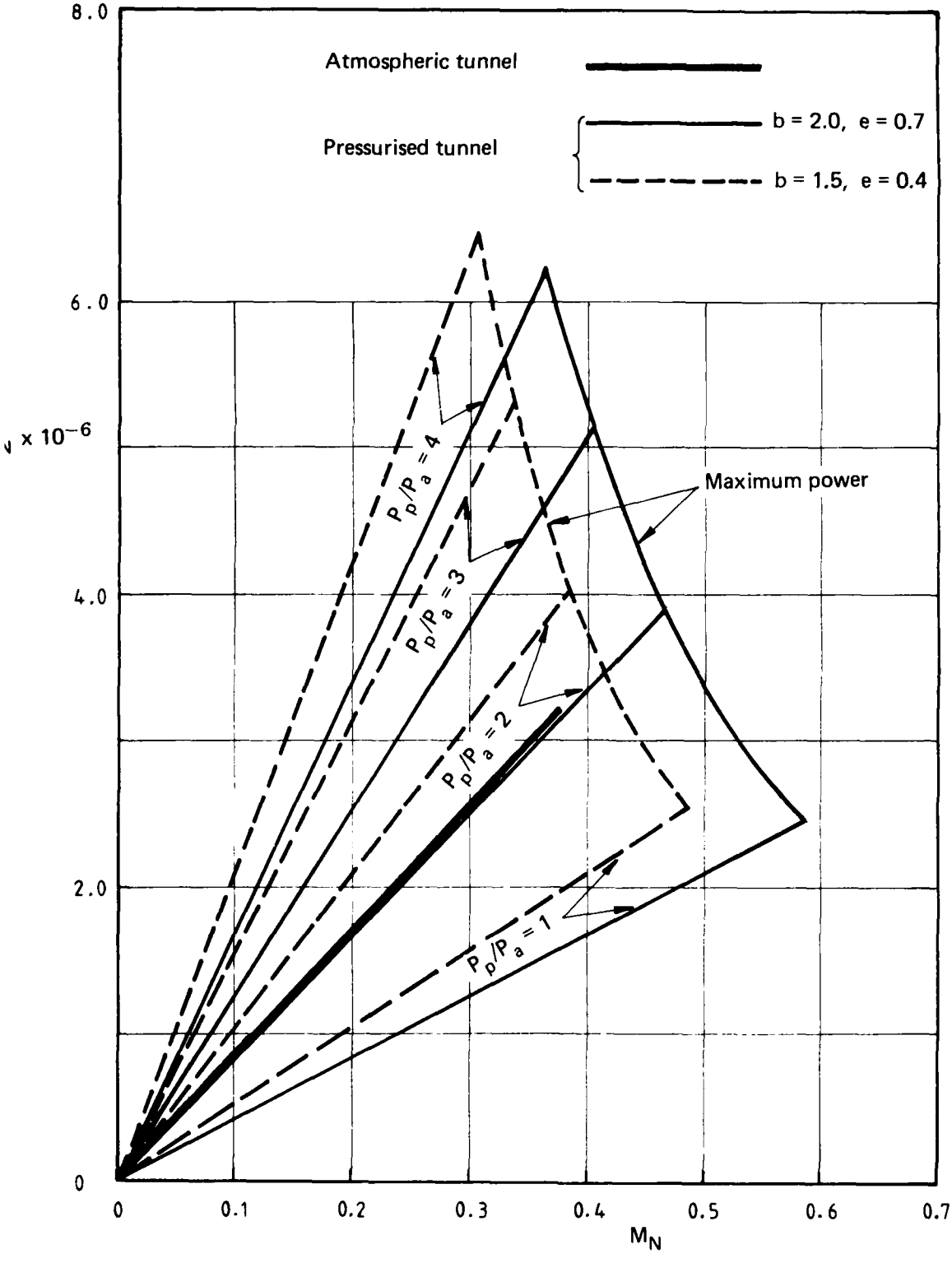


Fig. 21 (cont.)

(b) $(P_p/P_a)_D = 4$

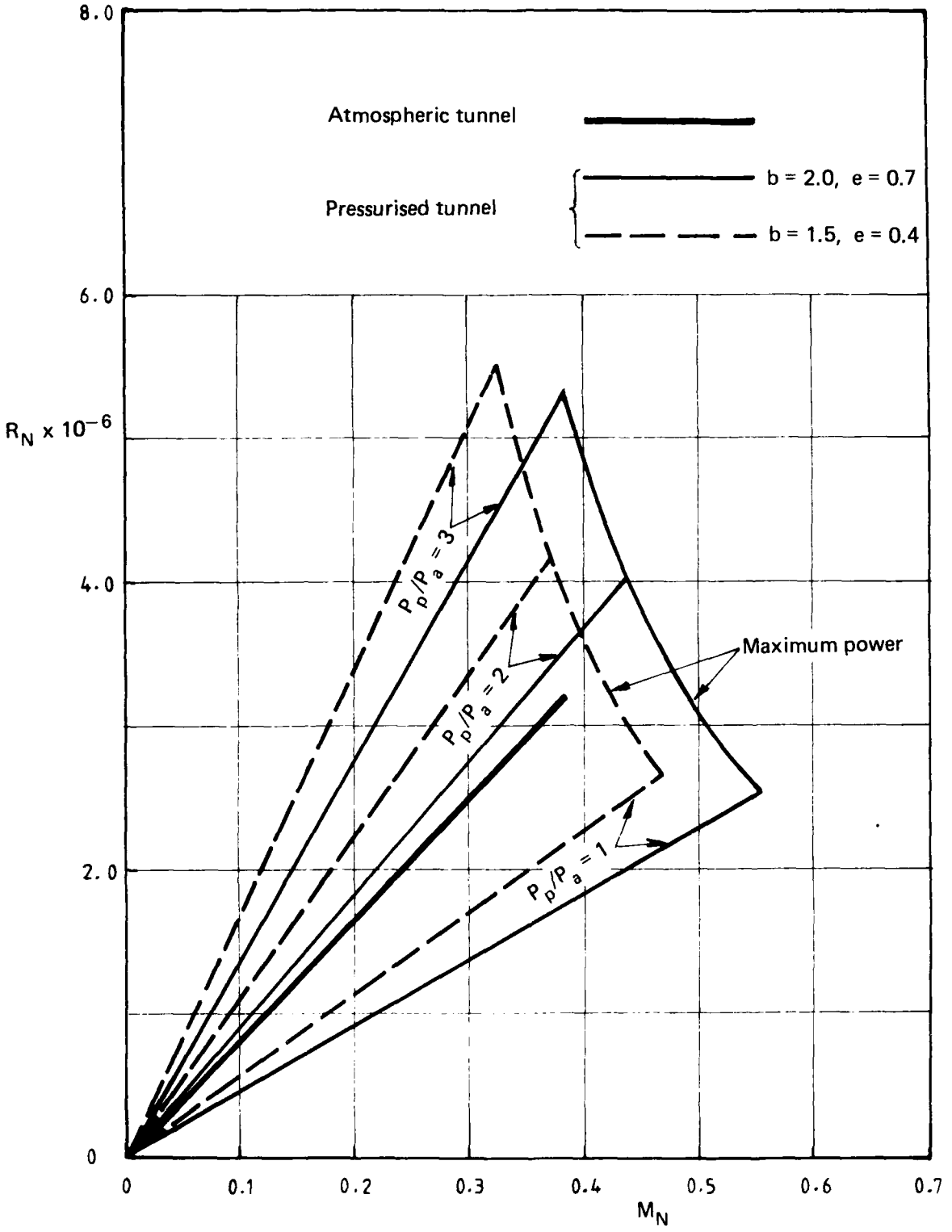


Fig. 21 (cont.)

(c) $(P_p/P_a)_D = 3$

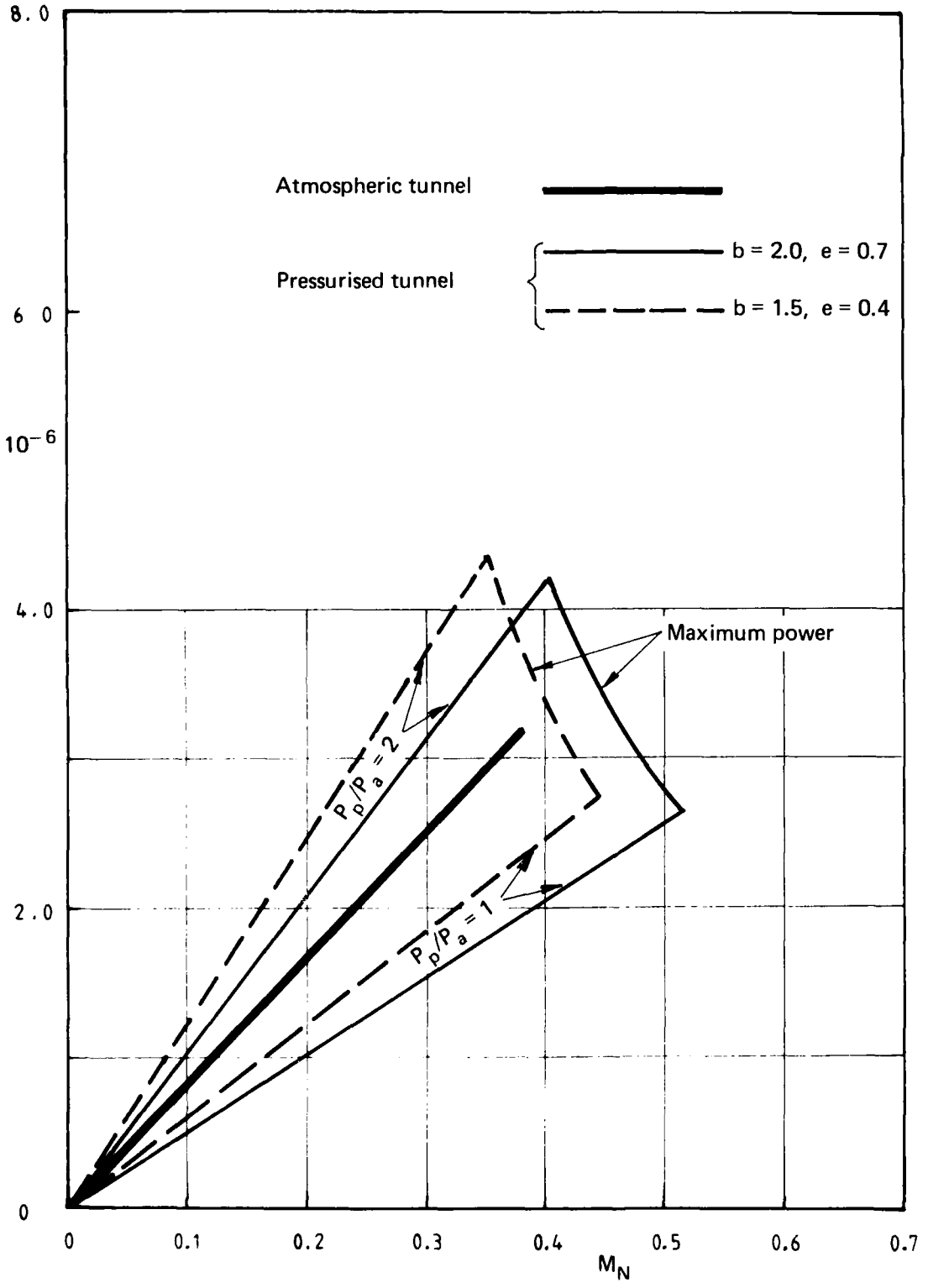


Fig. 21 (cont.)

(d) $(P_p/P_a)_D = 2$

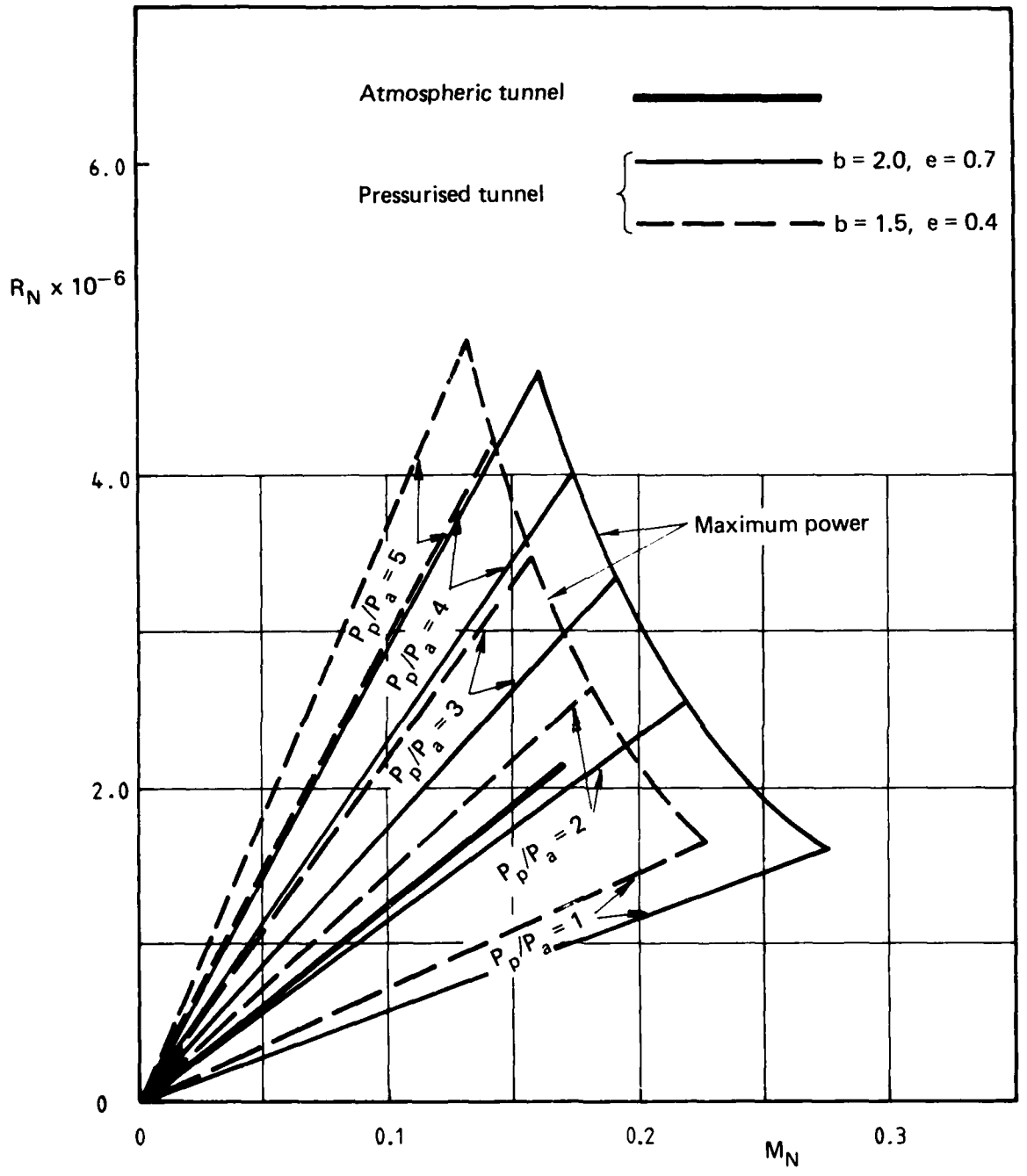


Fig. 22 Reynolds and Mach number test envelope based on a length scale of 0.1 $(A)^{1/2}$ for the 6.0m x 6.0m atmospheric tunnel and for similar pressurised tunnels with $C_p = C_a$, $N_p = N_a$, and design pressures of 2, 3, 4 and 5 atmospheres.

(a) $(P_p/P_a)_D = 5$

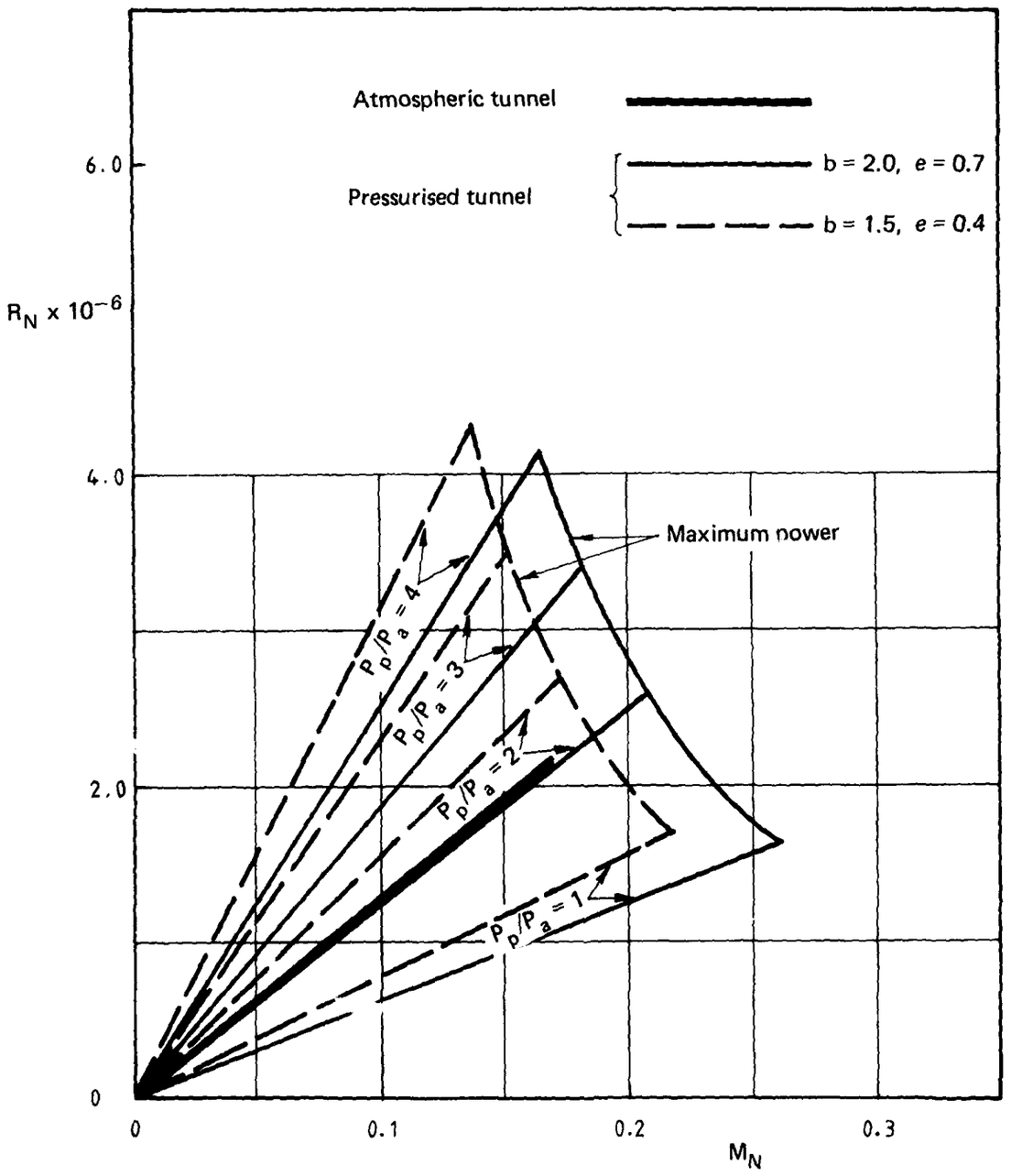


Fig. 22 (cont.)

(b) $(P_p/P_a)_D = 4$

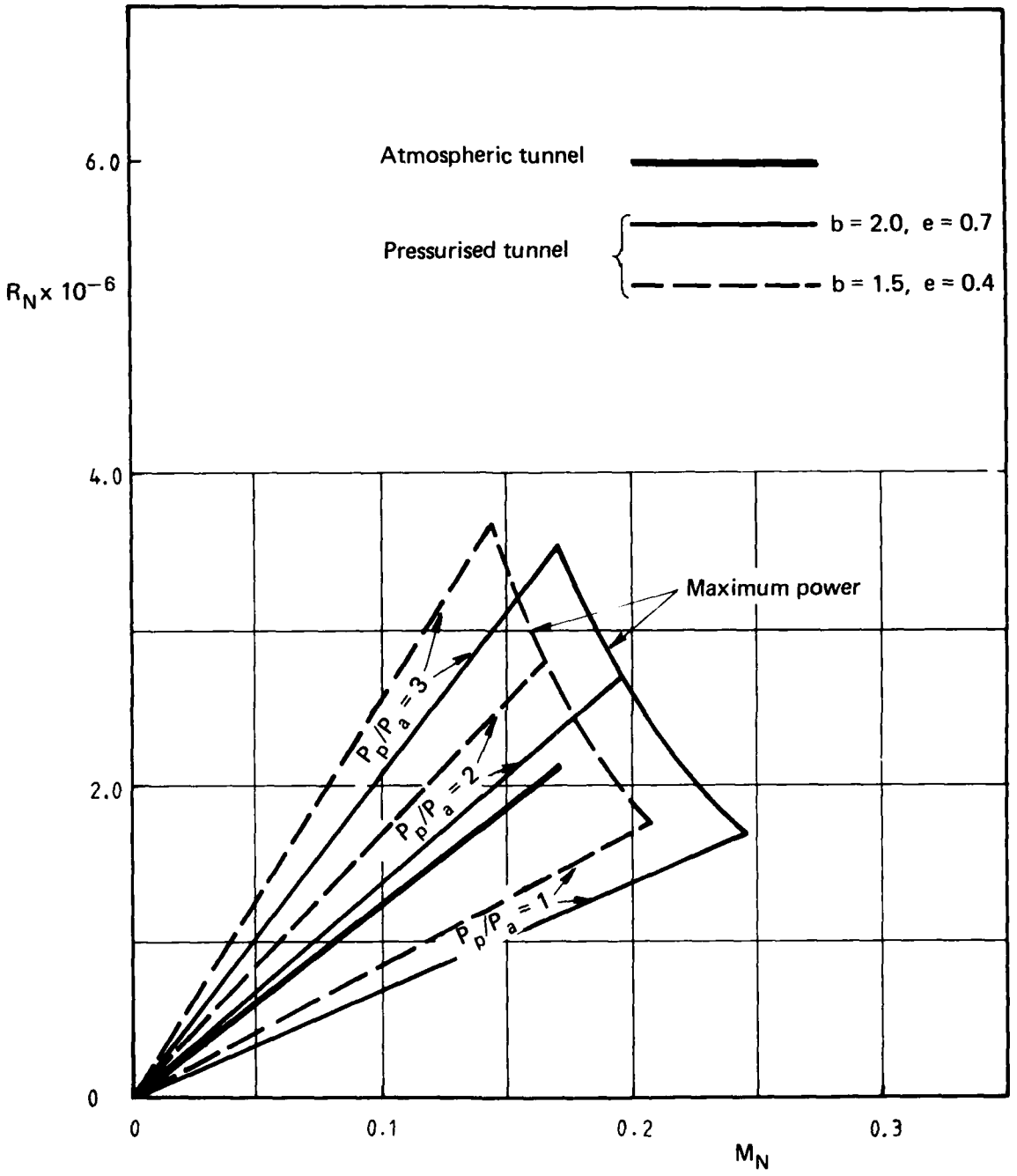


Fig. 22 (cont.)

(c) $(P_p/P_a)_D = 3$

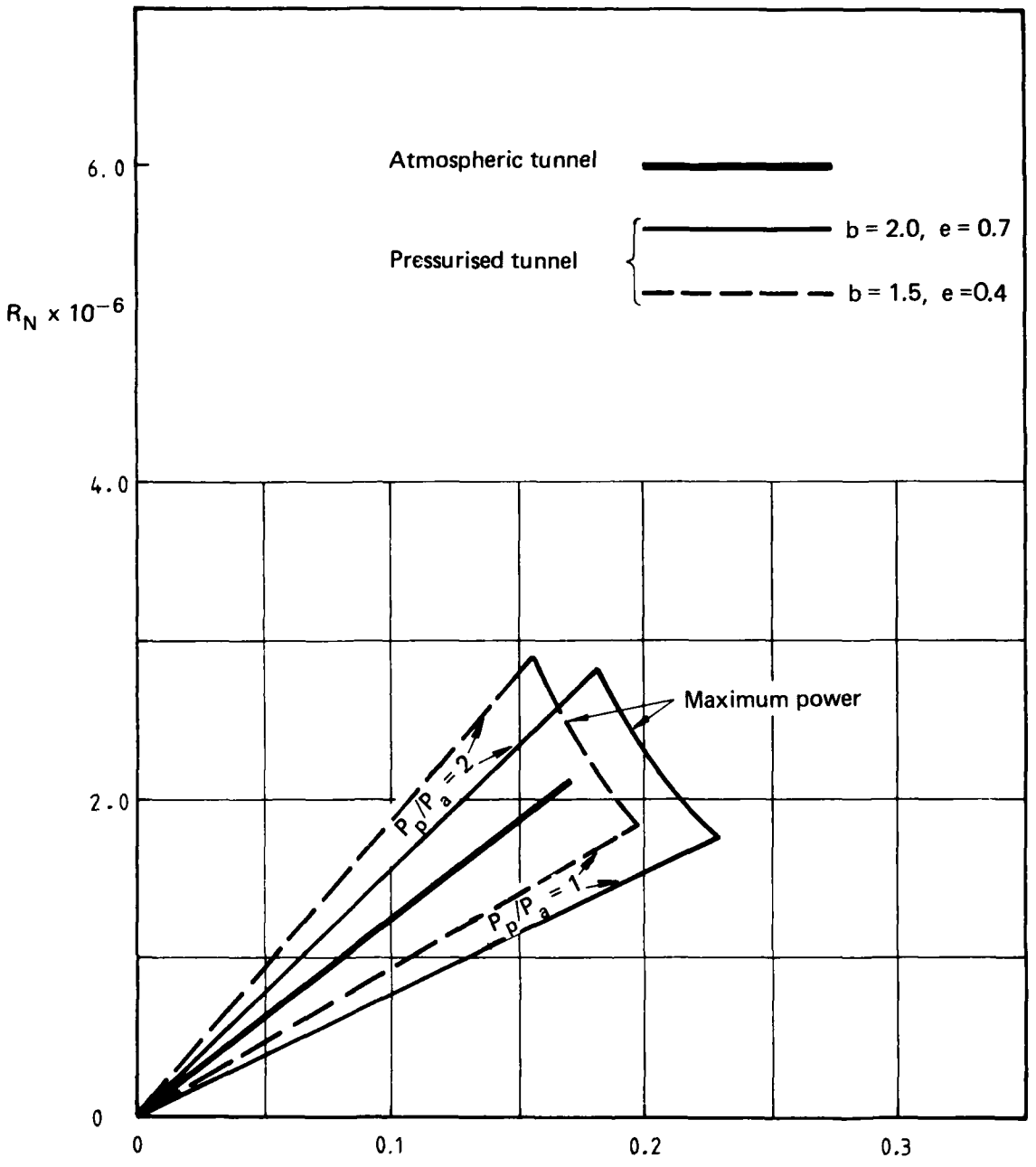


Fig. 22 (cont.)

(d) $(P_p/P_a)_D = 2$

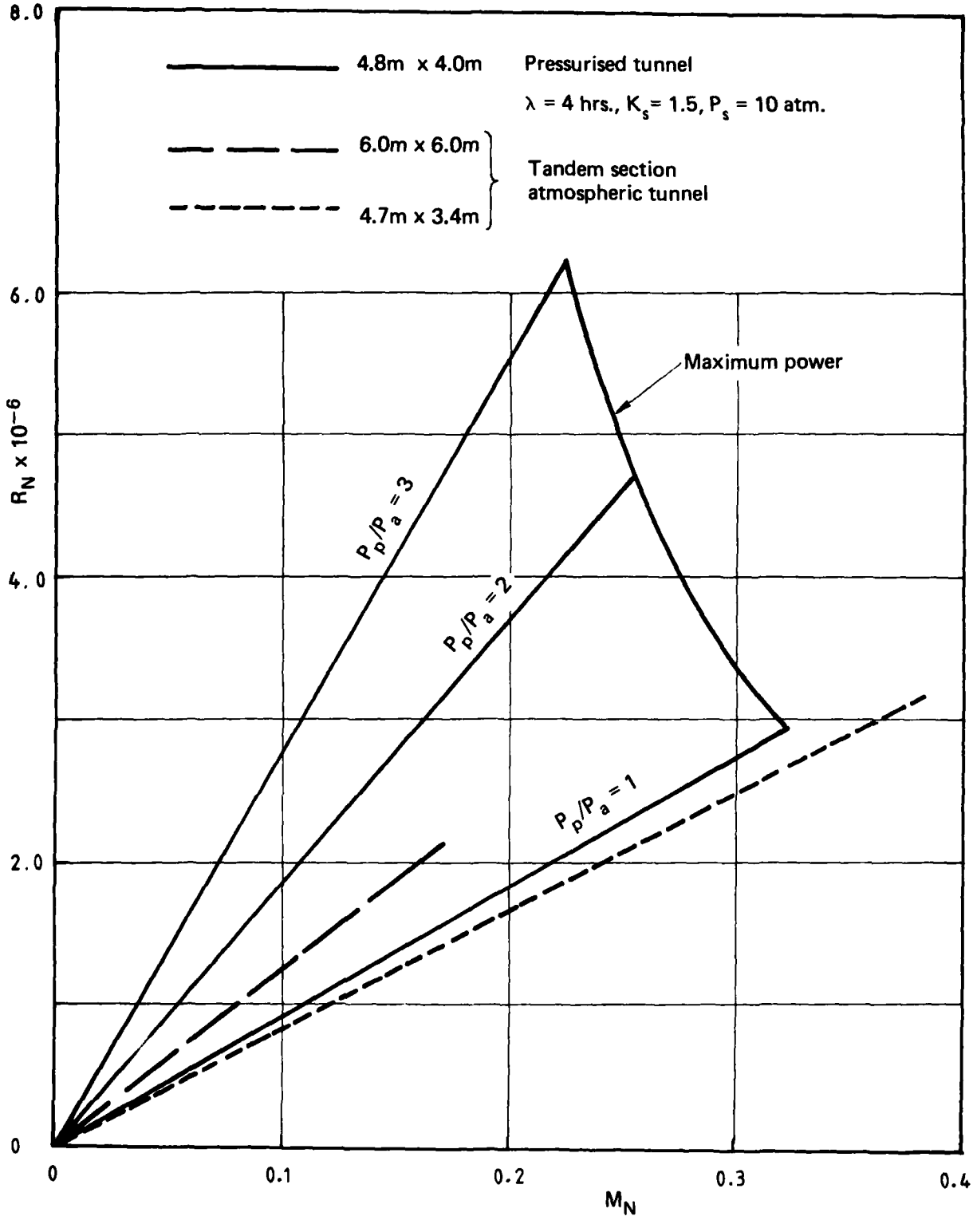


Fig. 23 Reynolds and Mach number test envelope based on a length scale of $0.1(A)^{½}$ for a 4.8m x 4.0m tunnel pressurised to 3 atmospheres compared with the tandem section atmospheric tunnel[1].

## DISTRIBUTION

### AUSTRALIA

### DEPARTMENT OF DEFENCE

**Central Office**
Chief Defence Scientist
Deputy Chief Defence Scientist
Superintendent, Science and Program Administration
Controller, External Relations, Projects and Analytical Studies
(1 copy)
Defence Science Adviser (U.K.) (Doc. Data sheet only)
Counsellor, Defence Science (U.S.A.) (Doc. Data sheet only)
Defence Central Library
Document Exchange Centre, D.I.S.B. (18 copies)
Joint Intelligence Organisation
Librarian H Block, Victoria Barracks, Melbourne
Director General—Army Development (NSO) (4 copies)

**Aeronautical Research Laboratories**
Director
Library
Superintendent—Aerodynamics
Divisional File—Aerodynamics
Author: N. Matheson
D. A. Lemaire
N. Pollock
M. K. Glaister

**Materials Research Laboratories**
Director/Library

**Defence Research Centre**
Library

**Navy Office**
Navy Scientific Adviser
Directorate of Naval Aviation Policy

**Army Office**
Army Scientific Adviser
Engineering Development Establishment, Library

**Air Force Office**
Air Force Scientific Adviser
Aircraft Research and Development Unit
Library
Technical Division Library

Director General Aircraft Engineering—Air Force
Director General Operational Requirements—Air Force
RAAF Academy, Point Cook

**Central Studies Establishment**
Information Centre

## DEPARTMENT OF DEFENCE SUPPORT

**Government Aircraft Factories**
Library

## DEPARTMENT OF AVIATION

Library
Flying Operations and Airworthiness Division

## STATUTORY AND STATE AUTHORITIES AND INDUSTRY

Commonwealth Aircraft Corporation, Library
Hawker de Havilland Aust. Pty. Ltd., Bankstown, Library

## UNIVERSITIES AND COLLEGES

| | |
|---|---|
| Adelaide | Barr Smith Library |
| Flinders | Library |
| Latrobe | Library |
| Melbourne | Engineering Library |
| Monash | Hargrave Library |
| Newcastle | Library |
| Sydney | Engineering Library |
| N.S.W. | Physical Sciences Library |
| Queensland | Library |
| Tasmania | Engineering Library |
| Western Australia | Library |
| R.M.I.T. | Library |

## CANADA

DSMA International Inc., W. J. Rainbird
NRC, Aeronautical & Mechanical Engineering Library

**Universities and Colleges**

| | |
|---|---|
| Toronto | Institute for Aerospace Studies |

## FRANCE

ONERA, Library

**INDIA**

Defence Ministry, Aero Development Establishment, Library
National Aeronautical Laboratory, Information Centre

**JAPAN**

Institute of Space and Astronautical Science, Library

**NETHERLANDS**

National Aerospace Laboratory (NLR), Library

**NEW ZEALAND**

Defence Scientific Establishment, Library

**SWEDEN**

Aeronautical Research Institute, Library
Swedish National Defence Research Institute (FOA)

**UNITED KINGDOM**

CAARC, Secretary
Royal Aircraft Establishment
  Bedford, Library
  Farnborough, Library
British Library, Lending Division
Aircraft Research Association, Library
British Ship Research Association
Rolls-Royce Ltd.
  Aero Division Bristol, Library
Welding Institute, Library
British Aerospace
  Kingston-upon-Thames, Library
  Hatfield-Chester Division, Library

**Universities and Colleges**

| | |
|---|---|
| Cambridge | Library, Engineering Department |
| London | Aero Engineering Library |
| Manchester | Library |
| Southampton | Library |
| Liverpool | Library |
| Cranfield Inst. of Technology | Library |
| Imperial College | Aeronautics Library |

**UNITED STATES OF AMERICA**

NASA Scientific and Technical Information Facility
Applied Mechanics Reviews
Lockheed-California Company
Lockheed Missiles and Space Company

Lockheed Georgia
McDonnell Aircraft Company, Library
Sverdrup Technology Inc., S. R. Pate

**Universities and Colleges**

| | |
|---|---|
| John Hopkins | Engineering Library |
| Princeton | Engineering Library |
| Massachusetts Inst. of Technology | M.I.T. Libraries |
| California Inst. of Technology | Aeronautical Labs. Library |

SPARES (10 copies)

TOTAL (113 copies)

Department of Defence

# DOCUMENT CONTROL DATA

| 1. a. AR No. | 1. b. Establishment No. | 2. Document Date | 3. Task No. |
|---|---|---|---|
| AR-003-027 | ARL-AERO-R-160 | May 1984 | DST 82/029 |

| 4. Title | 5. Security | 6. No. Pages |
|---|---|---|
| ATMOSPHERIC AND PRESSURIZED LOW-SPEED WIND TUNNEL PERFORMANCE AND COST COMPARISONS | a. document: Unclassified<br>b. title: U. c. abstract: U. | 34<br>7. No. Refs: 22 |

| 8. Author(s) | 9. Downgrading Instructions |
|---|---|
| N. Matheson | |

| 10. Corporate Author and Address | 11. Authority (*as appropriate*) |
|---|---|
| Aeronautical Research Laboratories, G.P.O. Box 4331, Melbourne, Vic. 3001. | a. Sponsor c. Downgrading<br>b. Security d. Approval<br>— |

12. Secondary Distribution (*of this document*)

Approved for public release

Overseas enquirers outside stated limitations should be referred through ASDIS, Defence Information Services Branch, Department of Defence, Campbell Park, CANBERRA, ACT, 2601.

13. a. This document may be ANNOUNCED in catalogues and awareness services available to . . .

No limitations

13. b. Citation for other purposes (*i.e. casual announcement*) may be (*select*) unrestricted (*or*) as for 13 a.

| 14. Descriptors | 15. COSATI Group |
|---|---|
| Wind tunnels | 01010 |
| Test facilities | 14020 |
| Subsonic wind tunnels | |
| Model tests | |

16. Abstract

*The performance of a series of low-speed wind tunnels designed to operate at various maximum pressures ranging from 2 to 5 atmospheres is estimated and compared with the performance of a similar atmospheric tunnel on the basis of capital cost and power input. The choice of the design of a new tunnel is usually influenced by cost and power considerations and it is important to provide the most capable design and to maximize performance within given limits of these variables.*

*Pressurization offers a major advantage in allowing $R_N$ and $M_N$ effects to be investigated separately. This can be particularly important for tests of modern aircraft configurations operating at high lift. For the same capital cost and power consumption, pressurization allows the maximum $R_N$ and $M_N$ to be increased substantially, but the working section is much smaller. This may*

**This page is to be used to record information which is required by the Establishment for its own use but which will not be added to the DISTIS data base unless specifically requested.**

16. Abstract (*Contd*)

*make it difficult to satisfy some test requirements particularly for V/STOL aircraft. Models for a pressurized tunnel are also more complex and may be more costly because they must withstand much higher aerodynamic loads.*

*To illustrate the effects of tunnel pressurization the analysis is applied to a tandem section low-speed tunnel previously suggested as suitable for future Australian test requirements.*[1,2]

17. Imprint

Aeronautical Research Laboratories, Melbourne

| 18. Document Series and Number | 19. Cost Code | 20. Type of Report and Period Covered |
|---|---|---|
| Aerodynamics Report 160 | 536090 | |

21. Computer Programs Used

—

22. Establishment File Ref(s)

# END

# FILMED

4-85

# DTIC